Shear Resisting Mechanisms in Composite Steel-Concrete Beams

Floriana Petrone
Rome, December 2012

SAPIENZA
UNIVERSITÀ DI ROMA

Sapienza University of Rome

Department of Structural
and Geotechnical Engineering

Abstract

The lack of a formulation in National and International Codes for the evaluation of shear resistance in Composite Steel-Concrete Beams (CSCB) led to a comparative study between reinforced concrete beams' shear mechanisms and CSCB' ones in order to propose a design and verification method consistent with those currently adopted. The analysis of the theoretical approach of the National Code, based on the Lower bound Theorem within the framework of Plasticity Theory, brought out some critical aspects mainly related to the non-fulfillment of the "equilibrium condition" and of the requirement of pseudo-ductile shear behavior. To overcome these limits, a new simplified mechanical model has been introduced, capable of predicting the yield of shear steel bars and the corresponding stress in concrete elements. The proposed model stems for a variational approach (Principle of Minimum Potential Energy), able to meet both the compatibility and the equilibrium conditions. In order to verify the validity of the results of the simplified mechanical model with a complete one, a parametric stiffness matrix of a CSCB has been developed, embedded in a worksheet able to evaluate stresses and strains of the whole beam, the collapse load and the pseudo-ductile or brittle behavior of the structural element. Afterwards, experimental tests on full-scale beams have been conceived, in order to verify the validity of the proposed theoretical approach. The comparison between the experimental evidence and the results of simplified and complete mechanical models showed a significant agreement, since the mechanical models are able to predict the collapse load and the structural behavior. On the basis of the validation of these models, an optimization procedure of beams' shape has been proposed, able to guarantee a pseudo-ductile shear behavior, the maximum contribution of concrete in the resistance system and the minimum amount of material. The proposed mechanical models and design procedure are much more reliable than the ones proposed by Codes. In fact they are able to always guarantee the pseudo-ductile shear behavior of structures since the yield of steel becomes the base condition of design and optimization.

Acknowledgement

First and foremost I want to thank my supervisor prof. Giorgio Monti. I'm grateful for all his contributions of time and ideas to make my Ph.D. experience fruitful and stimulating. I treasure the dedication and enthusiasm he has for research that was motivational for me, even during tough times of my Ph.D.

Furthermore I would like to acknowledge prof. Sashi Kunnath of UCDavis, who I worked with during the last months of my Ph.D., for all the useful advices he gave me during the last hectic research activities.

My sincere thanks also goes to all they who helped and supported me during the experimental tests, expecially prof. Beppe Marano, the laboratory team of Sapienza and the staff of Metal.Ri. snc.

My time during my Ph.D. was made enjoyable also thanks to many friends I met and I spent time with: Wang Hao, Hao Ji, Giada, Giovanna, Silvia, Daniela, Adel, Ehsan, Roberto, Gheorghe, Christian, Archak, Danielle and Claire.

And I really want to thank Vincenzo, who gives me his unconditional support, needful for me, with no distance and no time.
Lastly I would like to thank my parents and my brothers, because their pride encourages me more than they can deem.

Summary

Chapter 2

Resistance to vertical shear in RC structures

Chapter 3

Simplified model

Chapter 4

Complete model

Chapter 5

Experimental tests

Chapter 1
State of the art

1.1. Introduction

The aim of this section is to outline the origins and the historical evolution of a special type of partially prefabricate structures, made up of precast steel trusses embedded in cast in place concrete. In spite of the wide use of such structures since about forty years, nowadays neither National nor International Codes or a reliable bibliography provide proper mechanical models or design formulations.

From a technological standpoint, such systems are made up of columns, beams and joints. Referring to "beam elements", unlike traditional reinforced concrete beams, prefabricated steel trusses can bear their own weight and the weight of concrete and slabs without any provisional support. The Code EN 1994-1-1:2004 [12] labels such constructions as "un-propped structures". This stage is called "the first dry assembly stage". Afterwards, the hardening of concrete marks the changeover to "the second stage", when the composite behavior occurs.

Referring to the constructive stages, all the steel components are made up in the assembly shops and then are moved toward the building site and are placed between couples of columns. In these conditions, structures behave like classical steel structures and the mechanical model to adopt for design purpose is a beam constrained with sliding supports at the ends.
To ensure the structural continuity during the 2nd stage, additional reinforcing steel bars are placed over the beam-columns joints, on both upper and lower sides. So, after the hardening of concrete, structural joints behave like "composite joints".
The Italian Code (Decreto Ministeriale of January 14th, 2008, at paragraph 4.6 [5]) mentions this special kind of structures stating that for their use it is necessary to require an official authorization to the Servizio Tecnico Centrale on the judgment of the Superior Council of Public Works.

In the following, the origins of these structures will be retraced in order to identify all the critical aspects of classical structures that furthered the research of new constructive solutions. Among all the requirements that pushed the development of constructions, the most influent was the industrialization of the building process.

1.2. Historical framework

Partially prefabricate structures have a beginning as a technological evolution of classical reinforced concrete (RC) structures.
Nowadays RC structures are the most common in national countrywide for both the slowness to innovation of technology in civil constructions and technical reasons, which meanly deal with the knowledge of mechanical models and design formulations, supported by several laboratory tests and practical experience. This is the main reason why, about one hundred years away their introduction, RC structures are still used and made up following the same construction steps, although they present many critical issues related to all the design prescriptions that must be enforced.

Classical RC structures are usually made up by casting fluid concrete in formworks, where steel rods have been previously placed. After the hardening of concrete, the mechanical behavior of structures depends on many factors. Among all of them the most important are: the characteristics of materials, the geometrical and mechanical percentage of reinforcement and the quality of detailing design.
Several efforts have been made to renew the building process of classical RC structures, especially in order to make the process faster, less expensive and to reduce the uncertainties, typical of building sites. The last issue refers both to the lowering of risks and injuries for workers and to the lowering of the uncertainties related to the accurate application of design provisions: in fact, building site hand labors deal with the use of formworks, the disposal of props and the assembling of steel rods as reinforcement.

Steel and concrete composite structures are made up by assembling cold-formed steel elements and by casting in place concrete. Steel and concrete components are connected by means of shear connection in order to limit

the longitudinal slip between concrete and steel [12]. Nowadays both National and International Codes provide mechanical models and design formulations for these structures.

Referring to the industrialization of building process, an important step forward has been accomplished thanks to the introduction of prefabrication techniques. Briefly, they consist in the dry assembling of structural elements - beams and columns - made up in assembly shops and tested by random sampling. Then, these structural components are moved towards building sites where they are connected by means of different kinds of structural joints. Even if this technology allows reducing building time length and lowering building site uncertainties, it presents several issues related to the structural behavior. Such structures, in fact, are usually statically determinate and this characteristic limits their use just to a few building typologies, as single-storey industrial buildings or bridges. Moreover, the structural continuity, achieved by statically indeterminate structures, is a prerequisite to build multilevel constructions and dissipative structures, able to dissipate energy during earthquakes by means of plastic hinges.

In this overall framework, the new type of composite steel and concrete beams (CSCB) seems to be an interesting balance solution between statically indeterminate structures wholly realized in building sites and statically determinate structures made up in the assembly shops: in fact on one hand steel truss beams coming from the assembly shops are tested like every industrial product and it allows guarantying a high control of the quality of products and on the other hand casting in place of concrete allows the structures being statically indeterminate, without in situ weldings or connections by means of tightening torques.

1.3. The origins and the development of CSCB

This section deals with the analysis of the development of CSCB typologies. As stated in the previous, nowadays there is not a reliable bibliography which presents an official historical evolution of CSCB and shows the date and the patent's author of the first composite steel and concrete beams. Therefore the historical evolution, presented in the following, has been outlined gathering some official documents and patents. Moreover it has been often necessary referring to the history of some national companies and to their brands that, in collaboration with engineers and professors, furthered the introduction of new models and new constructive solutions.

1964 Mr Prassede Savoia submitted the request for patent to the Ministry of Industry of Torino for the industrial invention n. 16687/64 of July 27th, 1964, whose title was "Self-bearing reinforcement for reinforced concrete slabs". The patent n. 735007 was issued on 1996. The structural model covered by patent consisted of a self-bearing steel truss beam made up of a steel rod as upper chord, a steel truss as shear reinforcement and a steel plate as lower chord. All these elements, put together by welding, formed the steel component of the beam, completed by the cast in place concrete. The shape and the structural behavior of such elements were similar to the CSCB, but with an area of applicability limited to the slabs.

1967 Eng. Salvatore Leone submitted the request for patent entitled "steel beam for slabs and vaulted ceilings, which can bear the weight of other structural elements and embedded in cast in place concrete". The patent was registered on July 28th 1967. This

structural model marked the beginning of the use of truss beams as structural elements able to bear the weight of slabs. The first brand of such beams was SEP (Strutture Edili Prefabbricate), originated from the name of the fist company that produced and put to national market these elements.
In detail, these beams were characterized by: a steel plate as lower chord, one steel truss as shear reinforcement, the same depth of the slabs that they had to carry and, if necessary, a lateritium layer to cover the lower plate.

1972 The model proposed by Eng. Leone was improved by introducing two steel trusses as shear reinforcement and two supports at the ends of the beam able to avoid the slip of the beam during the 1st stage. Starting from these improvements, patents 966-663 and 966-664 were issued for these new models, which allowed the use of such beams, called REP that stands for Rapida Economica Pratica, for complex structures like long span bridges.

1978 The CSP Prefabbricati company introduced a new model of beams, whose lower chord was made up of reinforced concrete. Afterwards other models were proposed, whose main innovation dealt with different tilt angles of tensile and compressive bars. At that time, Fornaci Patricelli of Pescara and SEP put in the national market structural finished products. After the bankruptcy of SEP, the most widespread brand was REP and new kinds of products were conceived and patented: the most significant innovations dealt with the use of beams characterized by different depths, according to the depth of slabs. Moreover, they had more than two series of bent bars as shear reinforcement and three or more steel bars as upper chord.

In the late 70's was conceived a hybrid model of beam called "beam-slab", especially useful for long span bridges, in which the weight of the fluid concrete is the main load for the 1st stage.

1986 This date marks the beginning of research activities at RDB Laboratory, Pontenure (PC) thanks to an agreement among all the national REP companies.

1987-88 New models of beams were conceived and patented: beams with two separate series of bent bars as shear reinforcement (S.C.A:V.) and beams with bent bars placed on the left or right side of the cross section (Reato snc).

1996 The research activities increased and many new models of beam were covered by patent. Among all of them, it is useful to mention the steel truss beam which can be placed across structural joints (EDIS s.r.l.) and the beam with the upper chord shorted than the lower one (CSP).

Thanks to all these improvements, the use of this kind of beams spread and many new brands were born.

1.3.1. The idea and the patent

The authorship of the CSCB is commonly ascribed to Eng. Leone, who conceived the first models of beams like so they are produced still now.
This is the reason why a brief biography and all the official documents of his patents and structural models will be presented in the following.
Salvatore Leone was born in Cosenza in 1922. He graduated in 1954 at the Engineering Faculty of Naples, defending the thesis "Research about the

plastic strain and the shrinkage of reinforced concrete". From 1945 to 1950 he was Assistant Professor and he teamed up with Prof. Adriano Galli. He worked as a freelancer engineer in Naples, Milan and Pescara with E. Giangreco and V. Franciosi.

In 1967 he conceived and patented the first CSCB, called REP. In 1968 he developed the formulation for the structural design of such structures and in 1980, together with his wife Paola Pezzi, he founded the EDIS society for the management of patents for beams, columns, slabs and structural joints.

The idea originated from the necessity to minimize the time length of building site actions and to optimize the use of materials: starting from the existing steel and concrete composite structures, Eng. Leone tried to outline new structural details.

In the first model the web of the beam, that was usually made up of a steel plate in the classical steel and concrete composite structures, was replaced with a plate shaped as shown in Figure 1, the upper flange with a single steel rod and the lower flange with a steel plate.

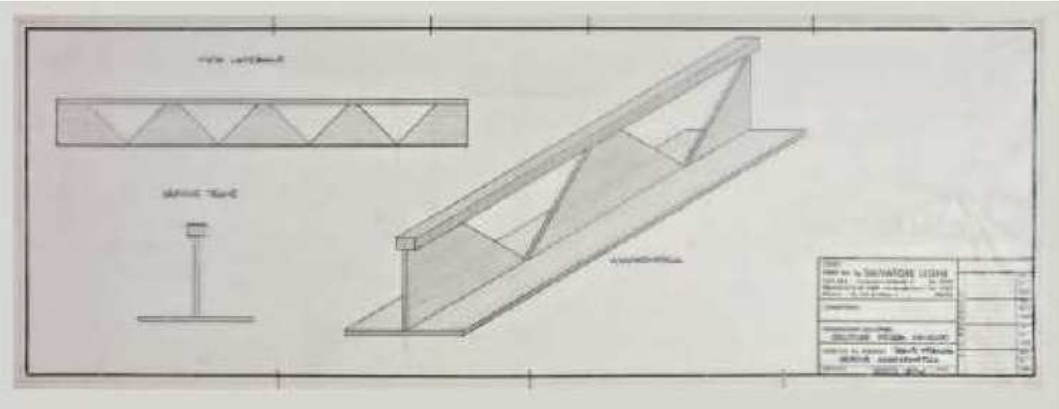

Figure 1. First model of CSCB

In the next models, the lower chord was made up of steel plate and one or more series of steel bending bars, see Figure 2.

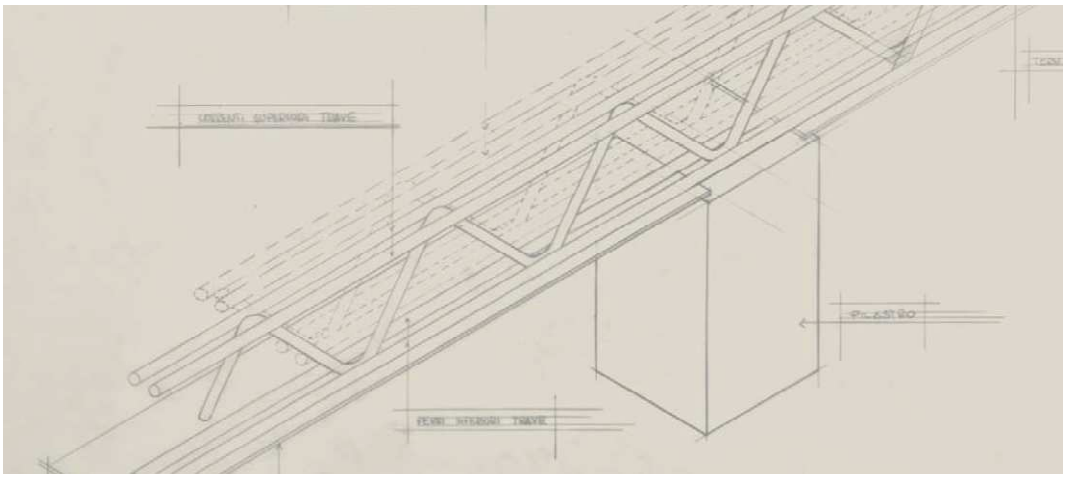

Figure 2. Next models of CSCB

All these devices allowed obtaining prefabricated reinforcements, mass-produced in the assembly shops. From a technological point of view, the new solution made the positioning of slabs faster and safer, since they can be placed on the lower plate of the beam, avoiding the use of props and formworks.

The patent n.805383 of July 28th, Figure 3, 1967 dealt with steel (Fe 510C UNI 7870) truss beams, in which the bent bars of the web were welded to the upper longitudinal bars and to the lower plate.

Figure 3. Patent n. n.805383 of July 28th, 1967

1.4. The technology

CSCBs can be defined as structural elements subjected to bending moment and shear, made up of a steel truss as shear reinforcement, welded to the upper chord, usually made up of steel rods, and to the lower chord, made up of a steel plate or a reinforced concrete plate.
Therefore, referring to Figure 4, the steel component of the CSCB is made up of:

- upper chord
- lower chord
- web
- other additional elements

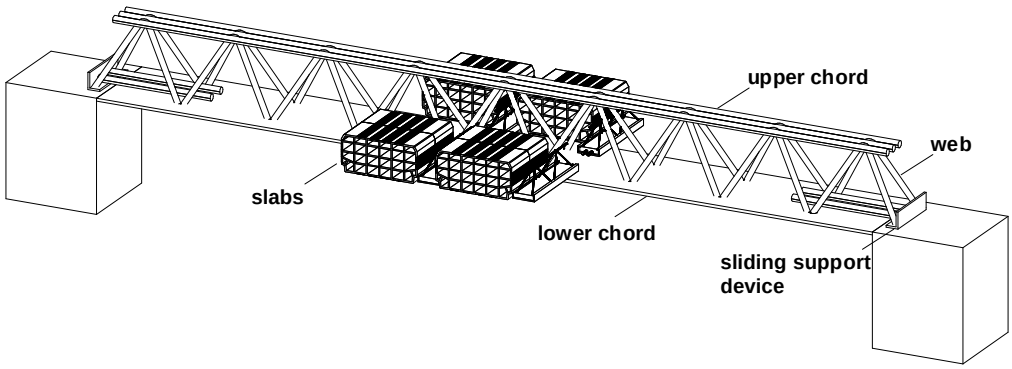

Figure 4. Main components of RCTB

The upper chord is usually made up of longitudinal bars – circular or square cross section – welded to the upper nodes of the web and symmetrically placed in the cross section. For common beams, the number of bars varies, 2 by 2, from a minimum of 1 to a maximum of 5.
The lower chord is usually made up of a steel plate or a reinforced/prestressed concrete bottom plate. The steel plate has usually

the same thickness along the span and in order to satisfy the design requirements, additional longitudinal bars can be welded on it.
Moreover, if the slabs have the same depth of the beam, the lower chord is usually designed in order that the bottom plate should be a support for slabs. In case of deep beams, the lower chord can be a C steel section. In both cases, the lower plate accomplishes all the tasks of the formworks.
The web is made up of one or more steel – high bond or smooth bars - trusses, whose nodes are welded to the lower and upper chords. The diameter of the bent web bars is usually constant.

The characterization of the web can be conducted on the basis of several parameters.
Referring to the cross section, it can be spatial, when the tilt angle of tensile and compressive bars is less than 90°, single-plane or multiple-plane, when the tilt angle is equal to 90°.

As for the longitudinal section, the webs of the beam can be aligned or staggered, the longitudinal axes can be curved or broker line and the depth can change along the span.

Moreover, referring to the position of the constrains, the sliding supports can be placed both at the ends, or one at the end and the other along the span or the web can be constrained with more than two sliding supports.

The bent bars of the web can be shaped so that they are both at the same angle on the horizontal axis or not.

The most common additional element typical of CSCB is the sliding support device, which is usually made up of transversal bars whose

purpose is to steady the steel beam during the placing. As structural components of the beam, they have to be designed to resist to all the loads – shear, tensile and compressive stresses – of the 1st and 2nd stage.
All the others additional elements are proper of each beam and depend on its depth and on the mutual position with the slabs. Other typical additional elements are: structural cross bracings, additional mid-depth supports for the slabs or additional longitudinal bars welded to the lower steel plate.

As stated in the previous, to ensure the structural continuity during the 2nd stage, additional reinforcing steel bars are located over beam-columns joints, on both upper and lower sides. As an alternative, additional steel trusses can be placed across the joints or reinforcing bars can be welded to both lower and upper chord of the beams.

Referring to the confinement of the concrete, the stirrups are usually welded at the ends of the beams and along the span, according to the design requirements.

1.5. 1st and 2nd stage: structural behavior

The service life of CSCB can be divided into 3 stages, in detail:

- **Stage 0**: it deals with the production, transportation and positioning of the steel trusses. During this stage the beams have to be inspected and tested like industrial prefabricated products, according to the requirements of proper Codes;
- **1st stage**: it starts from the positioning of steel elements on columns until the hardening of concrete. During this stage CSCB

behave like steel structures which can bear their own weight and the weight of slabs and concrete, with or without provisional supports, depending on the design requirements. They have to be designed according to the provisions of Codes about steel structures and referring to the model of beams constrained by sliding supports at the ends.

- **2nd stage**: it starts from the hardening of concrete until the end of structure's design service life. CSCB' behavior is outlined between reinforced concrete structures and composite steel concrete ones, since it has some peculiar characteristics of both of them, but of fact is different from them. In fact, during the 2nd stage, the steel truss beam is a prestressed structure embedded in the concrete and subjected to all the live and dead loads specific of this stage. Moreover, since the hardening of concrete marks the changeover of the structural model, from sliding supports to fixed end-supports, the design of the structure during the 2nd stage have to be conducted referring to continuous beam model.

1.6. Advantages

Nowadays the interest for this technology is growing up in Europe, mainly because of many advantages it provides with respect to the traditional reinforced concrete beams. Among all of them, referring mainly to the structural safety, the most important ones are the lowering of risk due to the manufacturing of beam reinforcement in the assembly shop rather than in the construction site and the possibility to build structures by assembling all members according to simple construction instructions. In addition to these advantages there are some others dealing with technological and economical aspects: for instance the prefabrication of the steel reinforcement speeds up the construction activities and since the

steel truss is self-carrying, it does not require any type of supports. Moreover, the reduction of the number of props reduces significantly the number of obstacles, which are the most important sources of risk and injury in building sites. Typically, all these positive features lead to a sensible reduction of management costs in comparison to traditional reinforced concrete structures.

1.7. Structural analysis methods

The analysis of a reinforced concrete structure can be conducted according to several models based on the three fundamental principles of mechanics of materials: the stress equilibrium condition, the strain compatibility condition and the constitutive laws of concrete and steel. Hsu and Mo [36] provided for the first time a unified theory made up of six models each of which is characterized by the fundamental principles employed and the degree of adherence to the rigorous principle of mechanics of materials. The six models are: (1) the struts and ties model, (2) the equilibrium (plasticity) truss model, (3) the Bernoulli compatibility truss model, (4) the Mohr compatibility truss model, (5) the softened truss model and (6) the softened membrane model.

Some of them may be particularly suitable for the analysis of discontinuity (or local) regions and others for continuity regions (also called beam or main regions). Moreover, some of them are intended for the service load stage or the ultimate load stage. In detail:

- **Struts and ties Model**
  Principles: Equilibrium condition only
  Applications: Design of local regions;
- **Equilibrium (Plasticity) Truss Model**
  Principles: Equilibrium condition and the theory of plasticity
  Applications: Analysis and design of M, N, V and T in the main regions at the ultimate load stage;
- **Bernoulli Compatibility Truss Model**
  Principles: 1-D Equilibrium condition, Bernoulli compatibility condition and 1-D or uniaxial constitutive law for concrete and reinforcement. The constitutive laws may be linear or nonlinear
  Applications: Analysis and design of M and N in the main regions at both the serviceability and the ultimate load stages;

- **Mohr Compatibility Truss Model**
  Principles: 2-D Equilibrium condition, Mohr's compatibility condition and 1-D or uniaxial constitutive law (Hook's Law is preferred) for both concrete and reinforcement
  Applications: Analysis and design of V and T in the main regions at both the serviceability load stage;
- **Softened Truss Model**
  Principles: 2-D Equilibrium condition, Mohr's compatibility condition and the 2-D softened constitutive law for concrete. The constitutive law of reinforcement may be linear or nonlinear
  Applications: Analysis and design of V and T in the main regions at both the serviceability and the ultimate load stages
- **Softened Membrane Model**
  Principles: 2-D Equilibrium condition, Mohr's compatibility condition and the 2-D softened constitutive law for concrete. The constitutive law of reinforcement may be linear or nonlinear. The Poisson effect is included in the analysis
  Applications: Analysis and design of V and T in the main regions at both the serviceability and the ultimate load stages.

1.8. Equilibrium (Plasticity) Truss Model

For the purpose of the analyses proposed in this work, the concept of the Equilibrium (Plasticity) Truss Model will be deepened in the following, especially referring to its application to the shear theory.
The use of limit analysis methods has been growing up in the last sixty years for the solution of engineering problems, as widely grounded by

Prager [34] and Chen [35], especially starting from 1950s, when the theory of plasticity was completely developed.

Before then all the structural analysis methods were based on the theory of elasticity, which starts from the well known assumption of zero residual stresses. Actually, referring to real structures, significant residual states of stress occur also for "elastic structures" and it is usually difficult to estimate them. Moreover, since ultimate loads of sufficiently ductile structures are independent of residual stresses, limit analysis methods can be a useful basis for strength design, especially for real complex structures. In addition, closed form solutions for ultimate load can be derived and usually the resulting expressions reflect the influence of the main parameters and the geometry of the problem, giving a clear idea about the load carrying behavior and the possible collapse mechanisms of the structure [33].

In the *struts and ties models* concrete compression struts and the tension steel ties outline a truss able to bear applied loads [37, 38]. This kind of model is usually adopted for the analysis of D-regions, where the classical De Saint Venant theory is not applicable [13, 44]. When the struts and ties models are employed for main regions' analysis (also well known as B-regions) they are called *Truss models* and are able to perform analysis of bending and axial loads and shear and torsion. The first application of truss theory to the shear design dates back to W. Ritter (1899) and E. Mörsch (1902): in their view a reinforced concrete beam acts like a parallel-stringer truss to resist bending and shear [36]. This model fits at best to describe the behavior of beams after the first 45° inclined cracks occur [45]. In fact these failures separate the concrete into a series of diagonal struts that, together with the transverse steel bars, are able to guarantee the equilibrium condition of external forces, by resisting respectively to compressive and tensile forces. Later, Rausch (1929), see [13, Vol. I], extended the concept of plane truss model for beam subjected to shear and flexure to members subjected to torsion. The weakness of this

truss model is that the concrete struts and the steel ties are treated like lines without cross-sectional dimensions and so it does not allow evaluating the stresses and the strains in the beam.
Such model was improved in the 1960's, when the dimensionless elements were replaced with more realistic 2-D elements. Starting from this new model, Nielsen (1967), [22, 48], and Lampert and Thurlimann (1968, 1969) derived three equilibrium equations, where the steel and concrete stresses should satisfy the Mohr stress circle.

1.8.1. Main hypotheses

Three main hypotheses underpin the equilibrium (plasticity) truss model.
Stress of materials: under the hypothesis that the yield of the steel occurs before the crushing of concrete struts, it is possible to use the three equilibrium equations to evaluate the stresses in the steel bars and in concrete struts at the ultimate load stage. This method of analysis is called *equilibrium (plasticity) truss model.*
Strain compatibility: the strain compatibility condition is irrelevant under the plasticity condition. So the equilibrium truss model can be applied for all type of actions (bending, axial loads, shear and torsion) and their interactions. Elfgren (1972) provided a complete interactive relationship of bending, shear and torsion.
Constitutive laws: the constitutive laws are not taken into account.

1.8.2. Limitations

The weakness of ignoring the strain compatibility and the constitutive laws of materials entails that the equilibrium (plasticity) truss model cannot be

used to derive the load deformation relationship of reinforced concrete beams subjected to shear and torsion. More sophisticated theories will have to be developed for shear and torsion that takes into account all the three principle of the mechanics of materials [36].

1.9. Shear theory

In the following is briefly introduced the evolution of the shear theory, mostly drawn from Hsu and Mo's work [36][1].
As stated in the previous, Nielson, Lampert and Thurlimann derived three equilibrium equations for the 2-D elements of the truss. Afterwards the three strain compatibility equations were derived by Baumann (1972) and Collins (1973), according to the Mohr's strain circle for both steel and concrete.
So, referring to linear analysis, the 2-D equilibrium equations, Mohr's compatibility equations and Hooke's law allow developing a linear shear theory, called Mohr compatibility truss model. It could be applied in the elastic range up to the service load stage. Nonlinear shear theory is required to describe the behavior of 2-D shear elements up to the ultimate load stage.
Shear in reinforced concrete membrane elements origins biaxial states of stress: if the shear stress can be solved referring to the principal tensile stress and the principal compressive stress in the 45° direction, on the other hand the biaxial constitutive relationship of a 2-D element was not easy to estimate since the stresses and strains in two directions affect each other. Robinson and Demorieux (1972) discovered that the principal compressive stress is reduced, or "softened", by the principle tensile stress in the perpendicular direction. But without the proper equipment to

[1] Also refer to [28]

perform biaxial testing of 2-D elements, they could not formulate the softened stress-strain relationship of concrete in compression.

1.9.1. Stress –strain relationship of concrete in compression

Later, Vecchio and Collins (1981) proved that the softening coefficient of the compressive stress-strain curve of concrete was a function of the principal tensile strain ε_1, rather than the principal tensile stress.

So, incorporating the equilibrium equations, the compatibility equations and using the "softened stress – strain curve" of concrete, Collins and Mitchell (1980) developed the "*compression field theory*" (CFT), able to reproduce the non linear behavior of an element in the post-cracking region up to the peak point.

Afterward, Vecchio and Collins (1986) proposed the "*modified compression field theory*" (MCFT) which included a constitutive relationship for concrete in tension able to better model the post-cracking shear stiffness [30, 31, 52].

In 1988 Hsu, Belarbi and Pang (1995) performed biaxial tests on large 2-D elements. They confirmed that the softening coefficient is a function of principal tensile strain ε_1 and developed the "*rotating – angle softened truss model*" (RA-STM). This model introduced two mains improvements to the previous ones: (1) the tensile stress of concrete was taken into account so that the deformations could be correctly predicted and (2) average stress–strain curve of steel bars embedded in concrete was derived on the "smeared crack level" so that it could be correctly used in the equilibrium and compatibility equations which are based on continuous materials. [36]

Pang and Hsu (1996) and Hsu and Zhang (1997) introduced the *fixed - angle softened truss model* (FA-STM) able to predict the "concrete

contribution" V_c under the hypothesis that the cracks are oriented at the fixed angle, rather than the rotating one.

Zhu, Hsu and Lee (2001) derived a rational shear modulus as s function of the compressive and the tensile stress-strain curves of concrete.

Zhang and Hsu (1998) found that the softening coefficient was not only a function of the perpendicular tensile strain ε_1, but also a function of the compressive strength of concrete $f_c^{'}$.

Wang (2006) and Chintrakarn (2001), by experimental tests, proved that the softening coefficient was a function of deviation angle β.

So the overall coefficients which affect the softening coefficient are: ε_1, $f_c^{'}$ and β.

All these theories are able to predict only the pre-peak branch of the shear stress vs shear strain curve, but not the post-peak branch of the curves, since the Poisson effect of cracked reinforced concrete was neglected. Zhu and Hsu (2002) quantified the Poisson effect and quantified this property by two ratios. So they developed the *softened membrane model* (SMM), able to predict the monotonic response of the load-deformation curves, including the pre-cracking and the post-cracking responses, as well as the ascending and descending branches.

Mansour and Hsu (2005) extended the SMM to cycling loading, developing the *cyclic softened membrane model* (CSMM), which is able to evaluate the shear stiffness, the shear ductility and the shear energy dissipation of structures subjected to dominant shear (Hsu and Mansour, 2005).

1.10. ACI 318-08: shear design

As stated in the previous, in order to employ the *Equilibrium (Plasticity) Truss Model* for structural analysis the equilibrium condition must be met under the hypothesis of yield steel.
The equilibrium condition for beam shear can be derived referring to the isolated beam element of Figure 5b.

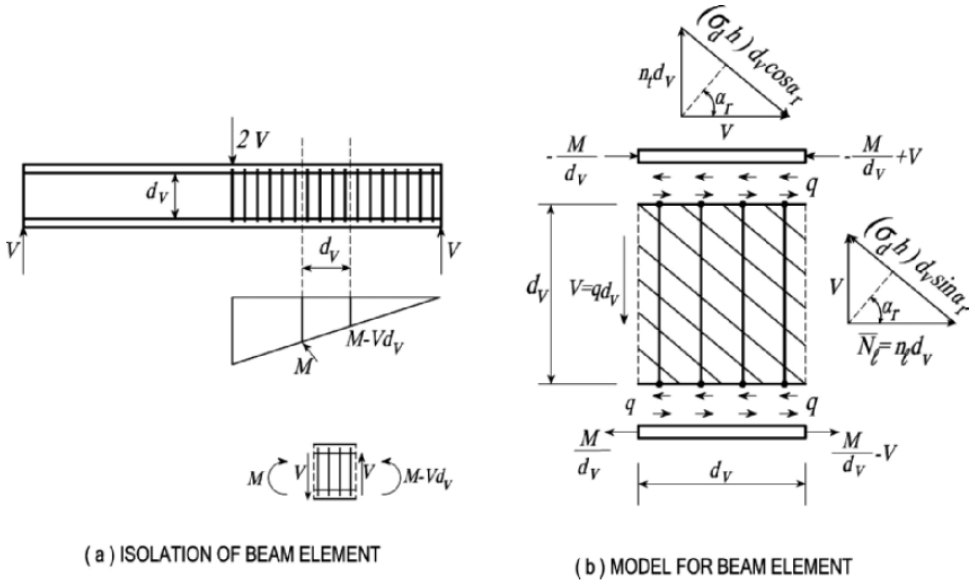

Figure 5. Equilibrium in beam shear, Hsu and Mo [36]

Referring to the setting up of Hsu and Mo [36], the following assumptions are made:

- **transverse direction:** the shear flow q is a constant over the depth of the beam, $V = \int q\mathrm{d}(d_v) = qd_v$;
- **longitudinal direction:** the shear flow q is distributed uniformly along the length of the beam and so the transverse steel stresses f_t and the stresses in the diagonal concrete struts σ_d vary uniformly along their lengths.

So, the equilibrium condition of the main body in the longitudinal, transverse and diagonal directions can be expressed as:

$$V = \overline{N}_l \cot \alpha_r \tag{1.1}$$

$$V = n_t d_v \tan \alpha_r \tag{1.2}$$

$$V = (\sigma_d h) d_v \sin \alpha_r \cos \alpha_r \tag{1.3}$$

where $\overline{N}_l$ and n_t are the values of longitudinal steel and transverse steel respectively, h is the thickness of the structural element.
The third equation,(1.3), allows checking the stress of concrete struts, in order to avoid the concrete crushing before the steel yielding.

[36] According to the ACI prescription, the shear strength V_n should be evaluated as:

$$V_n = V_c + V_s \tag{1.4}$$

where

- V_c is the contribution of concrete and can be evaluated by the following empirical expression (ACI318-08, ACI equation (11-3), [54]):

  $$V_c = 0{,}166\sqrt{f_c^{'}(MPa)}\, b_w d \tag{1.5}$$

  where $0{,}166\sqrt{f_c^{'}(MPa)}\, b_w d \le V_c \le 0{,}42\sqrt{f_c^{'}(MPa)}\, b_w d$ and $\frac{V_u d}{M_u} \le 1$

- V_s is the contribution of steel, which is the only one able to satisfy the equilibrium equation (1.3).
  According to the ACI Code, the following equations hold:

$$V_s = \frac{V_u}{\phi} - V_c \tag{1.6}$$

Taking $A_t = A_v$, $d_v = d$ and assuming the yielding of steel $f_t = f_{yt}$ and $\theta = 45°$ the (1.6) becomes:

$$\frac{A_v}{s} = \frac{V_s}{d \cdot f_{yt}} = \frac{V_u - \phi V_c}{\phi \cdot d \cdot f_{yt}} \tag{1.7}$$

The equation above refers to the transverse shear steel required in vertical legs of the cross section. The angle θ is taken as $45°$ and for the spacing s the following limits values are set:

$$\begin{aligned} s \le \frac{d}{2} &\rightarrow V_s \le 0,33\sqrt{f_c^{'}(MPa)}\, b_w d \\ s \le \frac{d}{4} &\rightarrow V_s > 0,33\sqrt{f_c^{'}(MPa)}\, b_w d \end{aligned} \tag{1.8}$$

1.11. Limitation of angle θ

Within the framework of the strain compatibility conditions, after the cracking of a RC 2-D element, the width of the cracks must be controlled, especially at the service load stage. This requirement affects the range of variation of angle θ, which represents the inclination of compressive strut on the longitudinal axis of the beam.
Each Code defines specific range of variation for θ:

- [36] ACI Code: $30° \le \theta \le 60°$
- [10] Eurocode2: $1 \le \cot\theta \le 2,5$, which corresponds to $21,8° \le \theta \le 45°$
- [5] NTC 2008: $1 \le \cot\theta \le 2,5$, which corresponds to $21,8° \le \theta \le 45°$

Usually both Codes and literature refer to experimental evidences and to qualitative evaluation of the crack width control to justify the limits of θ.
Recently Hsu and Mo (2010) [36] provided a rigorous demonstration based on the analysis of cracking condition at yielding of steel. In detail, they refer to two cases: (1) the yielding of the longitudinal steel and (2) the yielding of the transverse steel.
These analyses are briefly summarized in the following.
For the purpose of the analysis the normal strains have been defined:

- ε_l : the strain of the longitudinal steel
- ε_t : the strain of the transverse steel
- ε_r : the cracking strain
- ε_d : principal compressive strain, considered as a small given value
- $\alpha_r = 90° - \theta$

Referring to (1) the yielding of the longitudinal steel, the following condition is set:

$$\varepsilon_l = \varepsilon_y \tag{1.9}$$

The (1.9) guarantees the ductile behavior of the structural element, since the strain of longitudinal reinforcement corresponds to the yield stress of steel.

The transverse steel strain ε_t and the cracking strain ε_r can be expressed as a function of $\varepsilon_l, \varepsilon_d$ and α_r and the following nondimensional equations for ε_t and ε_r hold:

$$\frac{\varepsilon_t}{\varepsilon_y} = \frac{\varepsilon_d}{\varepsilon_y} + \left(1 - \frac{\varepsilon_d}{\varepsilon_y}\right) \tan^2 \alpha_r \tag{1.10}$$

$$\frac{\varepsilon_r}{\varepsilon_y} = 1 + \left(1 - \frac{\varepsilon_d}{\varepsilon_y}\right) \tan^2 \alpha_r \tag{1.11}$$

The graph of Figure 6 shows the variation of the transverse steel strain ratio, $\varepsilon_t / \varepsilon_y$, and the cracking strain ratio, $\varepsilon_r / \varepsilon_y$, as a function of α_r, according to (1.10) and(1.11).

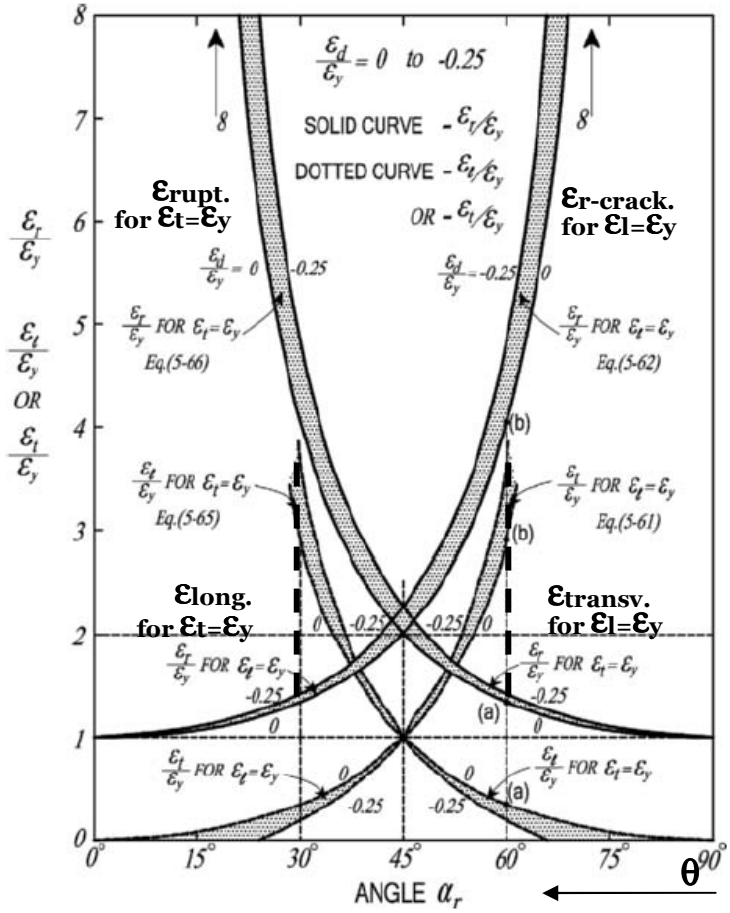

Figure 6. Cracking condition at yielding of steel, [36][2]

For each equation a range of $\varepsilon_d / \varepsilon_y$ ratios from 0 to –0,25 is given. The effect of $\varepsilon_d / \varepsilon_y$ ratio is small.

So, referring to some significant values of α_r the (1.10) and(1.11) give:

- $\alpha_r = 45° \Rightarrow \theta = 45°$, $\varepsilon_t = \varepsilon_y$ and $\varepsilon_r = 2\varepsilon_y - 2,25\varepsilon_y$;
- $\alpha_r = 60° \Rightarrow \theta = 30°$, $\varepsilon_t = 3\varepsilon_y - 3,5\varepsilon_y$ and $\varepsilon_r = 4\varepsilon_y - 4,75\varepsilon_y$

[2] Thurlimann (1979) provided for the first time the $\alpha_r - \varepsilon_r / \varepsilon_y$ graph, for the special case of $\varepsilon_d / \varepsilon_y = 0$ [29, 47].

If the value of α_r is furthered increased, the value of ε_r increases even faster.

Referring to (2) the yielding of the transverse steel, the following condition is set:

$$\varepsilon_t = \varepsilon_y \tag{1.12}$$

Following the same steps of the previous analysis, the longitudinal steel strain ε_l and the cracking strain ε_r can be expressed as a function of $\varepsilon_t, \varepsilon_d$ and α_r, giving the following nondimensional equations:

$$\frac{\varepsilon_l}{\varepsilon_y} = \frac{\varepsilon_d}{\varepsilon_y} + \left(1 - \frac{\varepsilon_d}{\varepsilon_y}\right)\cot^2 \alpha_r \tag{1.13}$$

$$\frac{\varepsilon_r}{\varepsilon_y} = 1 + \left(1 - \frac{\varepsilon_d}{\varepsilon_y}\right)\cot^2 \alpha_r \tag{1.14}$$

The functions above are plotted in the graph of Figure 6 and for some significant value of α_r they give:

- $\alpha_r = 45° \Rightarrow \theta = 45°$, $\varepsilon_l = \varepsilon_y$ and $\varepsilon_r = 2\varepsilon_y - 2{,}25\varepsilon_y$
- $\alpha_r = 30° \Rightarrow \theta = 60°$, $\varepsilon_l = 3\varepsilon_y - 3{,}5\varepsilon_y$ and $\varepsilon_r = 4\varepsilon_y - 4{,}75\varepsilon_y$

The trend of these two curves shows that the cracking strain ratio $\varepsilon_r / \varepsilon_y$ increases very rapidly after the first yield of steel when the angle α_r moves away from $45°$, which represents the inclination of isostatic tensile and compressive lines in the pre-cracking stage.

On the basis of this analysis the range of variation of $30° \leq \theta \leq 60°$ should fit the real behavior of the structural element and should allow controlling cracks' width.

1.11.1. Remarks

The graph of Figure 6 gives useful information to understand the structural behavior of a reinforced concrete beam starting from the pre-cracking state to the ultimate limit one.

According to the behavior of an idealized homogeneous body, the first cracks follow the inclination of the principal stress lines, which is about $45°$ on the longitudinal axis[3]. Under increasing loads, the tilt angle of the struts θ decreases and, referring to Figure 6, α_r increases.

1.12. Comments

As picked out by Hsu and Mo [36], the Equilibrium (Plasticity) Truss Model presents some weaknesses principally related to the strain compatibility condition for shear and torsion and the biaxial behavior of reinforced concrete 2-D elements.

In detail, among all the advantages of the method underlined by the authors, the following are especially significant for the purpose of this work: the equilibrium condition is completely satisfied and provides three equilibrium equations, useful for the design of the three components of the truss model: transverse steel, longitudinal steel and diagonal concrete struts. Moreover these equations satisfy the Mohr circle.

Referring to the shear behavior, the critical aspects deal mainly with the strain compatibility conditions that are not taken into account: so, shear and torsional deformations cannot be evaluated and the yielding of steel or

[3] For the analysis of the behavior of a beam during the prefailure stage, the development of the crack pattern and the evaluation of the structural resisting mechanisms see, Chapter 2.

the crushing of concrete cannot be rationally determined as well as the modes of failure.[36]

Chapter 2
Resistance to vertical shear in RC structures

2.1 Introduction

The majority of reinforced concrete flexural members have to resist to shearing forces in combination with flexure, axial loads and, in case, torsion. In order to indentify the effect of the only shear forces and the related mechanical models, it is useful to analyze all the possible interactions with the other structural actions [3].

If a flexural member, subjected to shear and flexure actions, fails before reaching the moment capacity, the structural collapse refers to “shear ultimate state” even if the structural behavior is ruled by shear and flexural

forces. Shear transfer relies more on compression and tension concrete elements than steel ones, which are usually subjected to low values of strain [13]. As a consequence, shear failures occur in concrete members and are usually non ductile.

The De Saint Venant theory, which is proper of homogeneous, isotropic and elastic bodies, is still expedient for the analysis of reinforced concrete structures at the prefailure stage and gives acceptable predictions about the localization and the shape of first cracks [3]. With the development of failure pattern, the distribution of stiffness and stresses within the member becomes very complex, as well as the related kinematic equations. This is the reason why the shear behavior of reinforced concrete beams can be reasonably described referring to two different stages: the first prefailure stage, and the second cracked stage, which correspond to two different structural models.

As stated previously, the uncracked stage can be reasonably analyzed referring to the classical concepts of shear stresses. As a confirmation, the crack patterns of a rectangular concrete beam, simply supported at the ends and subjected to uniform loads along the span, fit the isostatic lines of an ideal homogeneous, isotropic and elastic body, see Figure 1 and Figure 2, where flexure and shear combine to create a biaxial state of stress. So its behavior can be properly described by the classical formulation for the evaluation of strains and stresses [17].

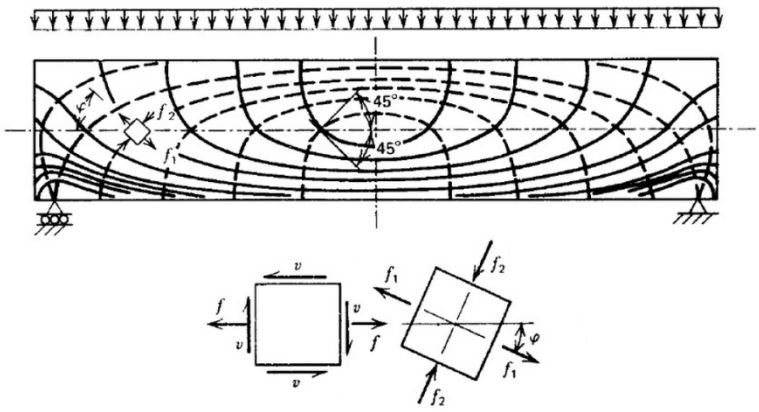

Figure 1. Trajectories of principal stresses
in a homogeneous isotropic beam [3]

When, under increasing magnitude of loads, the principal tensile stresses exceed the tensile strength of concrete, the second cracked stage occurs and the first failure is orthogonal to the principal tensile direction of the prefailure stage.

The analysis of crack patterns can be conducted in reference to the beam of Figure 2.

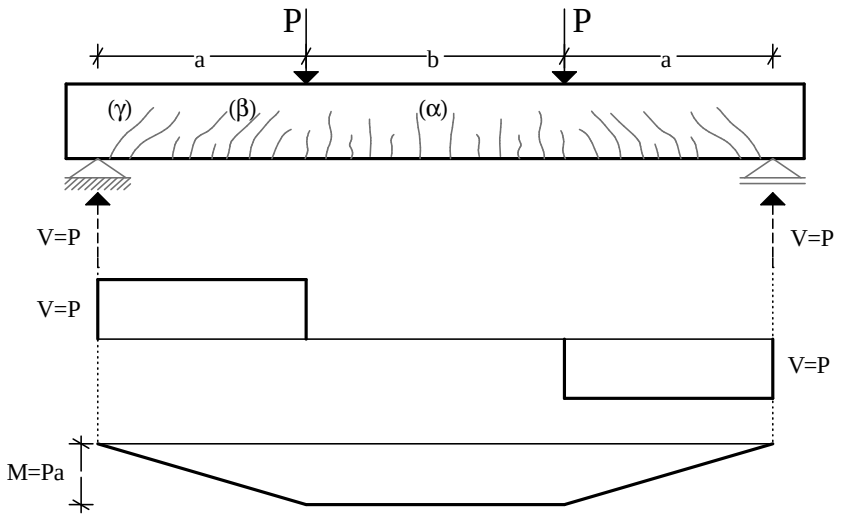

Figure 2. Reference beam model: possible cracking pattern

The well-known loading and constrain conditions of the beam allow dealing with shear and flexural effects *separately*: in detail, segment a is representative of the stresses and cracks of shear and segment b of the stresses-related cracks of flexure.

Briefly, the cracks within segment b are typical of flexural stresses and, starting from lower extreme tension fibers of the beam, where the tensile stress has the maximum value, they reach the neutral axis along vertical paths. Within segment a, instead, two kinds of failures can occur (γ) and (β), see Figure 2. The first type, (γ), is typical of portions of the beam where the shear stresses reach their maximum value and the flexural stresses the minimum value. They usually begin next to the neutral axis of

the beam and they propagate until the bottom chord along 45° inclined paths.

The second type, (β), is characteristic of portions of the beam where there are shear and flexural stresses in equal measure. They usually follow vertical paths next to the bottom chord and 45° inclined paths next to the neutral axis, in accordance with the distribution of stresses in each cross section [13].

Note that only the first cracks have the same characteristics of the ideal ones described above. In fact, they deal with the stresses of an ideal homogeneous body, before the first failure and before the related redistribution of stiffness and stresses.

The flexural member may collapse just after the formation of diagonal cracks or an entirely new shear carrying mechanism may develop, which is capable of sustaining further load in a cracked beam.

Usually, the second circumstance occurs thanks to some carrying mechanisms, proper to concrete beams without reinforcement, which will be described in detail in the following.

2.2 Resisting mechanisms in concrete beams

This section deals with all the resisting mechanisms occurring in reinforced concrete beams without web reinforcement.

Referring to the beam of Figure 2 and to (γ) type cracks described in the previous section, Figure 3 shows the equilibrium requirements for the shear span of the beam, subjected to constant shear force. The internal and external forces able to guarantee equilibrium can be easily identified.

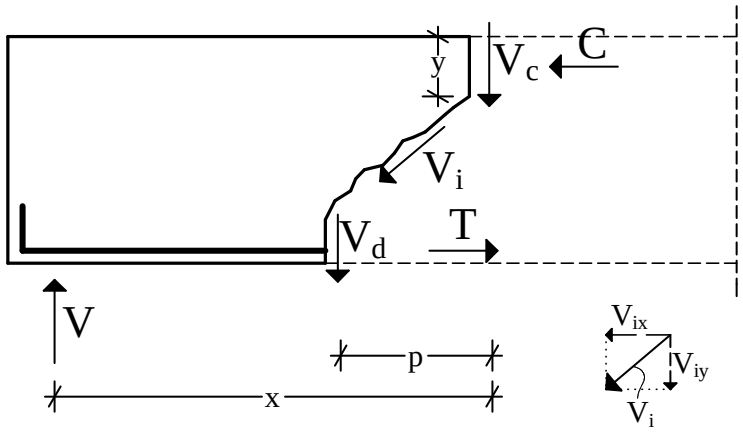

Figure 3. Equilibrium of the span *x* of the beam

The external transverse force V is resisted by the combination of:

- a shear force across the compression upper chord V_c;
- a dowel force transmitted across the crack by the flexural reinforcement V_d;
- the vertical components of inclined shearing stresses, V_i, transmitted across the inclined crack by means of interlocking of aggregate particles [3].

Note that the first term, V_c, is also present in uncracked members. The second and the third, instead, contribute to the resisting mechanism only in the presence of cracks, and the amount of their contribution depends on the relative displacements of the crack edges.

In addition to these three terms, the "arch action" can contribute to shear resistance by inclined compressive bars, see Figure 4. This resisting mechanism is activated near the constraints and especially with low slenderness values, l / z ratio (span of the beam to depth of the cross-section). In addition, in order for the arch action to work, it is necessary that the bottom longitudinal reinforcement runs through the span, with constant values of the cross-section, like the chains of arches.

The bearing capacity of the arch action depends on the geometrical and mechanical characteristics of the concrete struts (angle of the axis of gravity, concrete strength).

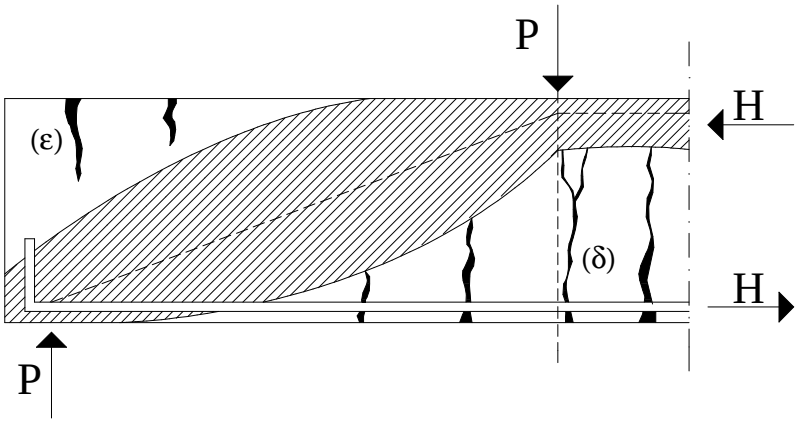

Figure 4. Arch action

The collapse of the arch within the beam may occur for the following reasons:

- the loss of bond of longitudinal reinforcement;
- the flexural failure of beams, (δ), starting from the bottom tension fibers, reaches the top compressive concrete chord and causes the reduction of the concrete struts cross-section, see Figure 4;
- the eccentricity between the compressive force of the strut and the top chord causes tensile stresses in the top fibers of the beam. When the tensile stress exceeds the tensile strength of concrete, (ε) failures come about and, depending on their length, they may reduce the area of the struts cross-section, see Figure 4;
- the diagonal compression stress of the struts reaches the compressive strength of concrete.

Extensive experimental works [18] show that the failures and the possible resisting mechanisms of the cracked beam develop in accordance with the a / d factor, which is the shear-span-to-depth ratio.

Concerning this, the results of experimental tests[1] conducted by Leonhardt and Walther [20] are meaningful, showing that the shear failure mechanisms fall in three approximate ranges of a / d ratio. In detail:

- Type I: the failures occur at or shortly after the application of the diagonal cracking load, with $3 < a / d < 7$. The arch mechanism is not able to resist to cracking load.
- Type II: shear compression or flexural tension failure of the compression zone above diagonal cracking load. This failure is typical of arch action, which occurs when $2 < a / d < 3$.
- Type III: failure by crushing or splitting of the concrete, when $a / d < 2{,}5$ [3].

The behavior of web reinforced concrete beams is not far from the one described above. The web reinforcement does not change the mechanisms of shear resistance, but improves them in different aspects[2].

In the following section the main resisting mechanisms of diagonally cracked beams are described in detail.

2.2.1 Concrete cantilevers, dowel action, aggregate interlock

Crack pattern, induced by load on a simply supported beam, see Figure 2, divides the tension zone into a number of blocks. Each of them may be considered to act as a cantilever with its end fixed at the upper compression zone and its free end just beyond the flexural tension reinforcement [3]. The shear load transfer from the tension reinforcement

[1] All the tests have been conducted on simply supported concrete beams, reinforced with lower longitudinal bars and subjected to point loads.

[2] For the detailed description of the shear resistance mechanisms for both reinforced and not reinforced concrete beams, see [3] and [13].

to the upper compressive chord depends on the bearing capacity of each cantilever.

In detail, referring to Figure 5, the actions on the concrete cantilever are the following:

- the bond force along the flexural reinforcement due to the increasing tensile force between two adjacent cracks
  $\Delta T = T_1 - T_2$;
- the forces induced by aggregate interlocking along the edges of the crack, v_{i1} and v_{i2}, see Figure 5 and Figure 6;
- the dowel forces V_{d1} and V_{d2} across the lower longitudinal reinforcement, see Figure 5 and Figure 7;
- the axial force P, the shear force V_h and the bending moment M_c that represent the reactions of the ideal cantilever fixed at the upper compressive chord and ensure the equilibrium of the "substructure" subjected to all the forces mentioned above [3];

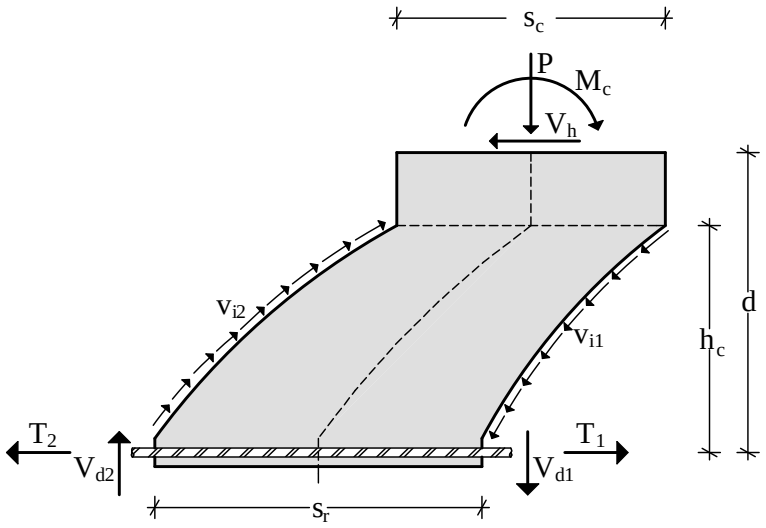

Figure 5. Concrete cantilever: equilibrium of the single element [3]

As regards the equilibrium condition of the cantilever, the moment induced by the bond forces, $\Delta T = T_1 - T_2$, is resisted by the aggregate

interlock forces, $\Delta v_i = v_{i2} - v_{i1}$, the dowel forces, $\Delta V_d = V_{d2} - V_{d1}$, and the bending moment M_c.

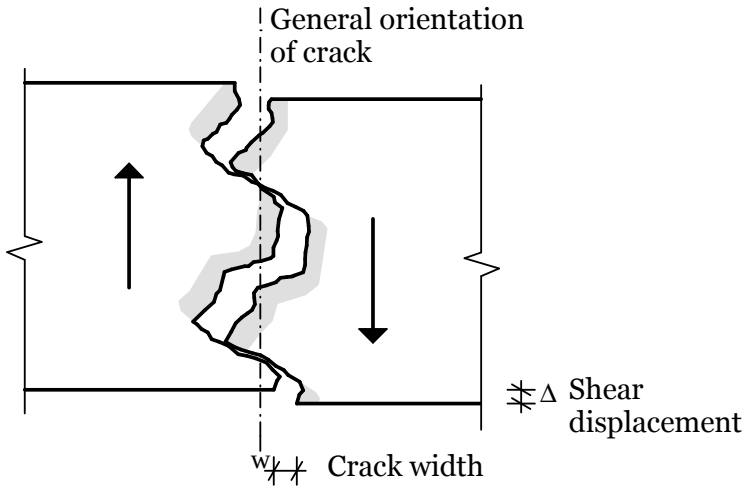

Figure 6. Displacement along a cracked shear plane:
aggregate interlock [3]

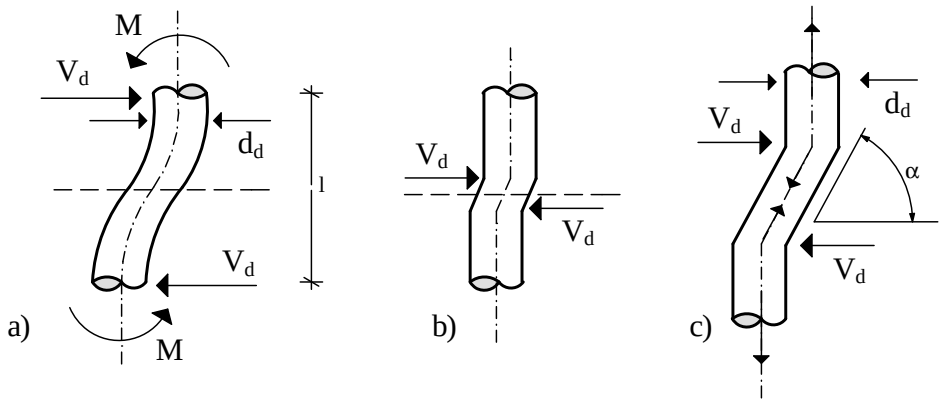

Figure 7. The mechanism of dowel action
across a shear interface [3]

So, the resistance of the concrete cantilever is ruled by the resistance of each mechanism whose weight in the overall structure bearing capacity depends mainly on geometrical factors.

Several experimental tests [1] showed that the flexural resistance of the cantilever depends on:

- the tensile strength of concrete;
- the distribution of stresses due to P, V_h and M_c;
- the depth s_c of the critical cantilever section.

As widely shown in a series of beams tested by Leonhardt and Walther [20], for common beams[3], at most 20% of the bond force can be resisted by the flexure of the "built – in end" of the concrete cantilever [3] and is determinate by the depth s_c of the critical cantilever section, which is usually small and especially at advanced stages of cracking. Moreover, the bearing capacity of the cantilever depends on the tensile and compressive strength of concrete, according to the stress of each fiber of the cantilever.

The bearing capacity of the dowel action of the flexural reinforcement, instead, can be activated by the shear displacement along the inclined cracks and depends on the tensile strength of cover concrete. In fact, splitting cracks reduce the stiffness and the effectiveness of the dowel action and, at the same time, reduce the bond performance of the bars[4]. The splitting strength of the concrete depends on the area around the bars and hence on the bar spacing.

Please note that the splitting and compressive strength of concrete is necessary to ensure the effectiveness of bond forces and, so, the overall effectiveness of the cantilever.

Several tests (see [20, 69]) showed that the dowel action does not exceed 25% of the total cantilever resistance. Moreover, it is more relevant in presence of stirrups, since they contribute to carry dowel forces right after the first cracks parallel to the flexural bar develop [3]. The stiffness of the dowel mechanism, in fact, depends on the position of a crack relative to the nearest stirrup which would be capable of sustaining the dowel force: dowel forces can be transferred by kinking of the bars, see Figure 7.

[3] Tested beams: $1 \leq \frac{a}{d} \leq 7$.

[4] Note that the bond performance of the bars is also related to the compressive strength of concrete. For more details, see [13].

When the width of the shear cracks is pretty narrow, small shear forces can be transmitted by means of the aggregate interlocking. The effectiveness of this mechanism, see Figure 6, depends mainly on the width and the coarseness of the crack, the shear displacement and the mechanical characteristics of concrete (concrete strength, size of aggregate compared to the width of the crack and the dimensions of the cross section). Among all the resisting shear mechanisms, the latter mentioned is the most efficient since it is able to bear 50% – 70% of the bond force[5].

The contribution of each mechanism (dowel action, aggregate interlock and flexural strength of the fixed end of the cantilever) to the shear capacity changes according to the evolution of the crack pattern and the three mechanisms are not necessary additive.

The carrying capacity of the fixed-end of the cantilever, in fact, decreases according to the developing of the inclined cracks. This phenomenon causes the rotation of the free-end cantilever, pushing to maximum the values of dowel action. Then, dowel cracks and secondary diagonal cracks near the reinforcement affect the aggregate interlock action, which represents the main shear carrying mechanism at this stage. The increase of cracks' width causes an instant reduction of the aggregate interlock forces on one side of the cantilever that causes imbalance. To restore the equilibrium condition a corresponding tension can be developed at the springing of the cantilever: the resulting tensile forces usually lead to further cracks that occur suddenly and, although they are about horizontal, these are referred to as diagonal tension failures. The shear carried by the compression zone above the diagonal cracks slowly increases according to the development of the cracks to a maximum of 25% to 40% of the total shear force across the section. Therefore the reminder shear must be carried by the tension zone of the beam by means of the aggregate interlock and the dowel mechanisms. But when they fail, the compression

[5] For more detail about the aggregate interlocking resisting mechanism see [1, 70, 71].

zone is usually unable to carry the increased shear in addition to the compression force resulting from the flexure and the beam fails [3].

2.3 Truss model for shear

Many kinds of truss models are able to reproduce the mechanical behavior of reinforced concrete structures useful for structural design [19]. Among all of them, the Mörsch truss is one of the most well-known and used to evaluate the shear resistance of reinforced concrete beams. It can be described as a system of prismatic members, usually called bars, connected each other by frictionless hinges and subjected only to forces applied to the joints. Since the bars are weightless and the hinges are ideal ones, each bar can be subjected also to normal tensile and compressive stress [17]. The analogy between the truss model and the web of the equivalent truss consists of stirrups acting as tension members and concrete struts as compressive ones. The struts run parallel to diagonal cracks and their grade depends on the spacing of the stirrups and the depth of the beam. The upper and the lower parallel chords represent the flexural concrete compression and reinforced tension zone, respectively [3,17].

The stress and the strain of bars can be determined only referring to equilibrium conditions.

The deformations that derive from beam and arch actions during the prefailure stage are not compatible with the ones coming from truss mechanisms: this strain incompatibility becomes less significant as the ultimate conditions are approached. [3]

In the most general case, tensile and compressive web elements are respectively inclined at α and θ to the horizontal. These information

suffice describing the topology of the truss and determining the value of the internal forces, since the structural system is internally determinate[6].
Referring to Figure 8, graphic remarks allow evaluating the value of stress and strain in each element of the truss, by assuming a graphic scale where the depth of the beam represents the magnitude of the shear **V**.

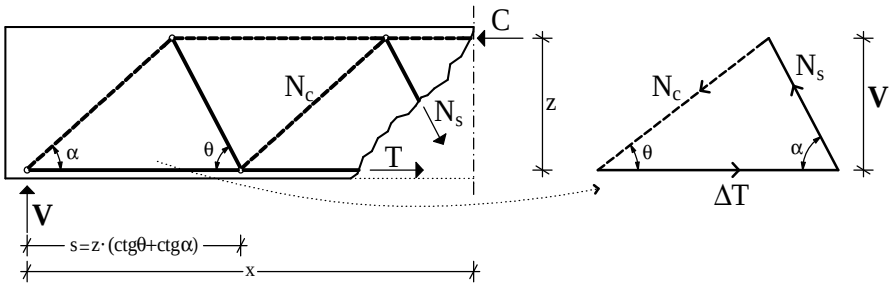

Figure 8. Internal forces in a generic truss

Therefore the following relation holds:

$$\mathbf{V} = N_c \cdot \sin\theta = N_s \cdot \sin\alpha \qquad (2.1)$$

where:

- N_c is the value of axial compressive stress in the compressive element;
- N_s is the value of axial tensile stress in the stirrup.

The overall shear resistance of the beam can be evaluated taking into account all the resisting mechanisms explained above – carrying mechanisms of beams without reinforcement and truss resisting mechanism - or just some of them, depending on the provisions of design codes.
Referring to the topology of the truss, the slope of the compression elements - struts - has been usually assumed to be $45°$ to the longitudinal axis of the beam and variable at the "discontinuity regions", as the boundaries of the beam [3]. Several studies based on strain energy

[6] Note that these remarks hold also for upper and lower chord only if the structure is externally statically determinate.

considerations, see [39], show that the optimum angle of compressive element along "beam regions" is about $38°$.

For the assessment of the compression strength of the struts, it is necessary considering some additional factors explained down below:

- in real reinforced concrete beams, concrete struts are subjected to bending moments, according to what has been explained above on the resisting mechanisms of beams without web reinforcement, see Figure 5. Moreover the assumption of "pin-jointed nodes" is a theoretical one;
- stirrups passing through transmit tension to these struts by means of bond [3], thus the compression strength of concrete is severely reduced by the biaxial state of stress and strain;
- the real load condition, far from being a uniform load applied to each node of the ideal truss, brings about eccentricities and transverse tensile stresses, which affect the real state of stress of each element.

The truss resisting mechanism in a reinforced concrete beam can be active only after the formation of the first diagonal cracks: in fact, in these conditions, the stirrups transfer the vertical shear across a diagonal crack. Moreover, the contribution of stirrups to the shear capacity of the beam can be evaluated also referring to the confinement action on concrete struts, which enhances the compressive strength of both concrete struts of the truss and the concrete elements of the arch on case of deep beams.

The use of horizontal web reinforcement, if considered, contributes to the shear resistance of beam by aiding crack control and increasing dowel action, but it does not affect the capacity of truss mechanism. In deep beams, as well, the arch mechanism can be greatly boosted by the addition of horizontal bars, if they are well anchored.

2.4 Resistance to vertical shear

According to the Italian National Code (Normativa Tecnica per le Costruzioni 2008), the design shear resistance of reinforced concrete structures should be determined by *suitable* truss models [5].
The structural members of the ideal truss are: the web reinforcement acting as tension member, the bottom longitudinal reinforcement, the flexural concrete compression zone and the concrete compressive struts.
For the Ultimate Limit State verification of shear, the following condition is set:

$$V_{Rd} \geq V_{Ed} \tag{2.2}$$

where:
V_{Ed} is the design value of shear demand and the shear capacity of the beam is defined as

$$V_{Rd} = \min\left(V_{Rsd}, V_{Rcd}\right) \tag{2.3}$$

The design capacity of tension web reinforcement should be evaluated as follows:

$$V_{Rsd} = 0,9 \cdot d \cdot \frac{A_{sw}}{s} \cdot f_{yd} \cdot \left(ctg\alpha + ctg\theta\right) \cdot \sin\alpha \tag{2.4}$$

The design strength of compressive web concrete members should be calculated as follows:

$$V_{Rcd} = 0,9 \cdot d \cdot b_w \cdot \alpha_c \cdot f'_{cd} \cdot \frac{\left(ctg\alpha + ctg\theta\right)}{\left(1 + ctg^2\theta\right)} \tag{2.5}$$

where:

f_{yd} is the design value of the yield strength of structural steel

d is the depth of the cross section

b_w is the width of the cross section

A_{sw} is the area of the web reinforcement's cross section

s is the spacing of steel bars

α is the tilt angle of tension bars to the longitudinal axis of the beam

θ is the tilt angle of compressive struts to the longitudinal axis of the beam

$f_{cd}^{'}$ is the reduced compressive strength of web concrete $f_{cd}^{'} = 0,5 \cdot f_{cd}$

α_c is an amplification factor that, in case of non-compressive members, as beams usually are, can be taken equal to 1.

Referring to the formula (2.4) and to Figure 9 and Figure 10, the meaning of each term is explained in the following:

- $0,9 \cdot d = z$ is the internal lever arm;
    - $z \cdot (ctg\alpha + ctg\theta)$, see Figure 9b, is the length of the representative span of the truss model, L_{rs}. This quantity, together with angles α and θ, gives all the useful information about the geometrical characteristics of the truss model adopted for the design. So, the ratio L_{rs} / s, gives the number, n, of trusses that contribute to the overall tensile shear strength of the beam;
- $A_{sw} \cdot f_{yd}$ is the tensile strength of the web reinforcement within L_{rs}, evaluated for the yield stress of the steel;
    - $A_{sw} \cdot f_{yd} \cdot \sin\alpha$ is the projection of the normal force of the tension bar on the vertical axis, $V_{R1t} = N_{R1t} \cdot \sin\alpha$.

So, the formulation (2.4) can be written as:

$$V_{Rsd} = A_{sw} \cdot f_{yd} \cdot \sin\alpha \cdot \frac{z \cdot (ctg\alpha + ctg\theta)}{s} = n \cdot N_{R1t} \cdot \sin\alpha \qquad (2.6)$$

So, the design shear strength of tensile members of the truss is evaluated referring to the single representative truss span, L_{rs}, since it is the product of the shear resistance of the single tension bar, multiplied by the number n of the bars, see (2.6).

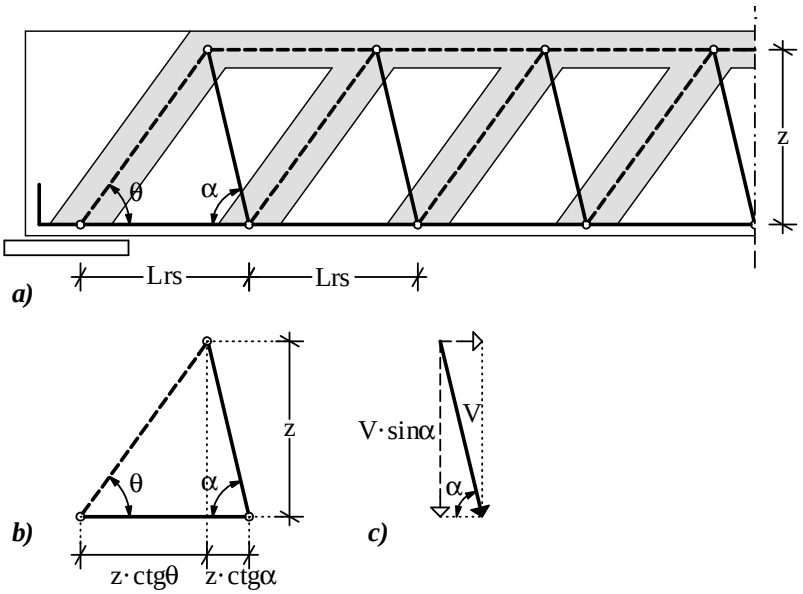

Figure 9. Single truss

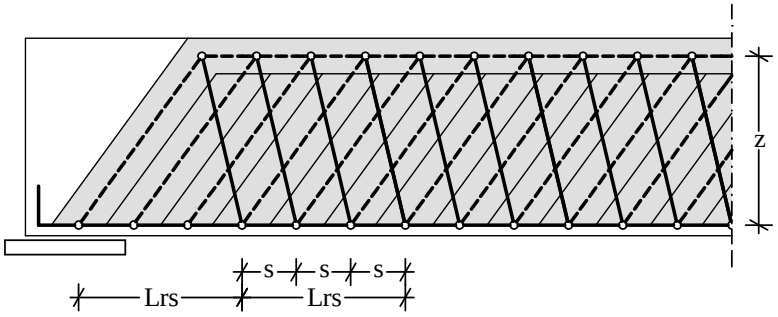

Figure 10. Multiple trusses

With reference to (2.5) and to Figure 9 and Figure 10, the meaning of each term can be explained as follows:

- $0,9 \cdot d = z$
  - $z \cdot (ctg\alpha + ctg\theta)$ has the same meaning explained above;
    - $b_w \cdot z \cdot (ctg\alpha + ctg\theta) \cdot \sin\theta = b_w \cdot L_{rs} \cdot \sin\theta = A_{st} \cdot \sin\theta$[7] gives the projection of the strut cross-section area on the plane orthogonal to the strut axis, see Figure 11;
    - $A_{st} \cdot f'_{cd} \cdot \sin\theta = N_{Rc} \cdot \sin\theta = V_{Rc}$ is the projection of the normal force of the compressive strut on the vertical axis, evaluated for the compressive strength of concrete.

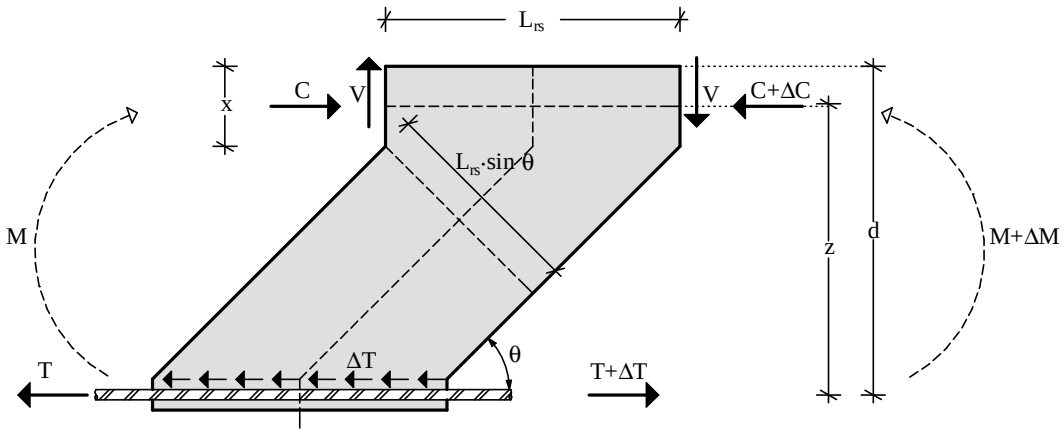

Figure 11. Compressive web member

So, the design strength of compressive web member is defined as the compressive strength of the cross-section of the strut of the single truss, whose depth is L_{rs}:

$$V_{Rc} = N_{Rc} \cdot \sin\theta \tag{2.7}$$

[7] Note that simple trigonometric transformations gives $\frac{1}{1+\cot^2\theta} = \sin^2\theta$

Note that by multiplying the numerator and the denominator by s, it is possible to express the overall strength of the strut as the sum of the contribution of n struts, each of which is ideally related to one tension bar.

$$V_{Rcd} = 0,9 \cdot d \cdot b_w \cdot \alpha_c \cdot f'_{cd} \cdot \frac{s}{s} \frac{\left(ctg\alpha + ctg\theta\right)}{\left(1 + ctg^2\theta\right)} = n \cdot b_w \cdot f'_{cd} \cdot s \cdot \sin^2\theta =$$

$$= n \cdot A_{s1\perp} \cdot f'_{cd} \cdot \sin\theta \Rightarrow \tag{2.8}$$

$$V_{Rcd} = n \cdot N_{R1c} \cdot \sin\theta$$

It makes clear that the Superposition Principle[8] underpins the method for the evaluation of tensile and compressive shear strength.

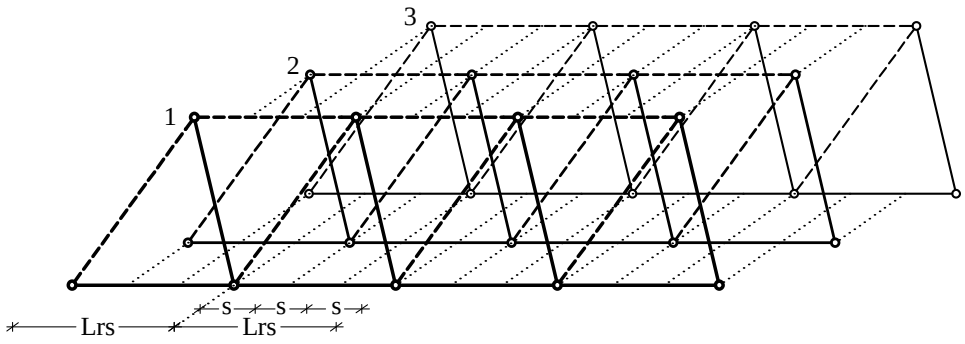

Figure 12. Superposition principle

So, the collapse load is defined as the minimum between the load (V_{Rsd}) that brings n tension bars to the yield stress and the one (V_{Rcd}) that brings the struts to the limit stress. Note that the number of tensile bars within L_{Rs}, as well as the depth of the struts, changes depending on the angle θ.

For design purposes, all terms in (2.4) and (2.5) can be chosen according to the design requirements. As far as the angle θ is concerned, note that it

[8] See next section

cannot be imposed, since it represents the *natural* inclination of the struts under the real load condition.

In fact, along the line of the commonly accepted theory of shear in reinforced concrete based on the variable angle strut, see Figure 13, the maximum shear capacity is attained when tension and compression elements fail simultaneously. Given this, the maximum shear capacity is attained when the two contributions (2.4) and (2.5) are made equal, by varying the value of θ according to the following limits set by the Italian National Code [5]:

$$1 \leq \cot\theta \leq 2{,}5 \tag{2.9}$$

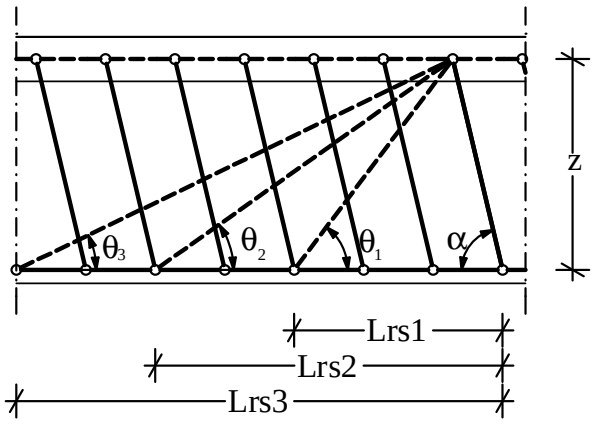

Figure 13. Variation of θ

Moreover, referring to (2.4), the value of V_{Rsd} depends on the number of tension bars, n, in the representative span length L_{rs}, the mechanical and geometrical characteristics of the single bar (area of the cross-section and yield stress of the steel) and the tilt angle, α. So, the value of V_{Rsd} increases as n, N_{R1t} and $\sin\alpha$ increase.

Referring to (2.5), instead, the value of the shear compressive strength depends only on the geometrical and mechanical properties of the strut cross-section. It should be noted that, assuming α and b_w as constant

values, since they are usually assigned data of the design, the area of the cross-section varies according to the angle θ[9].

By varying the value of θ , see Figure 13, both V_{Rsd} and V_{Rcd} change.

In detail, when the value of θ increases:

- the value of V_{Rsd} decreases, according to the number, n, of the tension bars within the shear representative span;
- the value of V_{Rcd} increases, according to the area of the cross-section, see Figure 14, where:

$$v_{Rcd} = \frac{(ctg\alpha + ctg\theta)}{(1 + ctg^2\theta)} \tag{2.10}$$

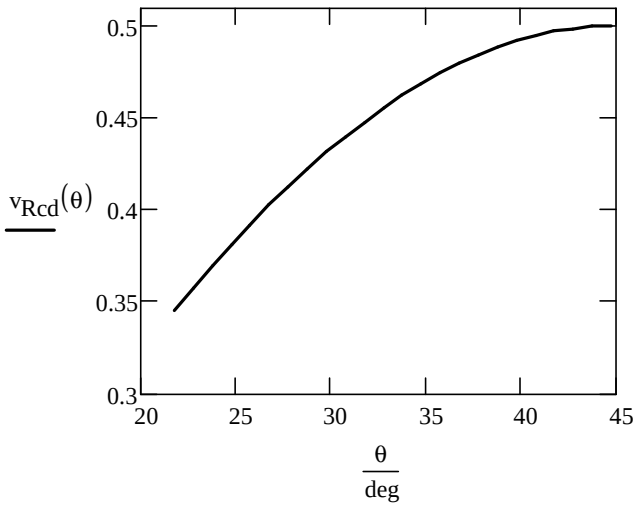

Figure 14. Variation of v_{Rcd} as function of θ

[9] Even if the number of struts related to each tensile bar changes, the overall area of the cross-section is constant, see Figure 10.

2.5 Analysis and critical aspects

The shear design criterion explained above shows some critical aspects, mainly related to the theory that underpins the design formulation.
In fact, the shear design method of the Italian National Code stems from the Lower Bound Theorem of Plasticity, also called Static Theorem, which states that:
"*If the load has such a magnitude that it is possible to find a stress distribution corresponding to stresses within the yield surface and satisfying the equilibrium conditions and the static boundary conditions for the actual load, then this load will not be able to cause collapse of the body.*" [22]
As long as the structure, subjected to any external loading condition, is able to guarantee the equilibrium by an internal stress resultant system, the external forces are less than the ones able to cause collapse of the structure. Referring to the structural safety, considering this external loading condition as the collapse one is a conservative choice, since the real collapse load will be either greater than the one considered or will refer to a different load condition. So, the equilibrium condition of the structural system is a necessary condition for the validity of the theorem.
This approach is widely used to establish the collapse criterion and to define possible collapse loading conditions for statically indeterminate structures.

Therefore, starting from (2.4) and (2.5), and referring to the collapse criterion explained above, the Italian National Code sets the following assumptions:

- the "equilibrium condition" is always met;
- the stress of all structural members (transverse reinforcement and struts) is taken equal to the limit value. So, the forces applied to the

overall structural system are able to cause the simultaneous failure of both the compressive struts and the steel ties.

- the design value of the shear capacity is the minimum value between the compressive resistance of the struts and the tensile resistance of the steel bars, referring to an arbitrary value of θ, within the range (2.9).

In the following sections, the analyses carried out to verify that the first two conditions can be contemporarily satisfied will be presented, with the additional objective of understanding the physical meaning of the bounds on θ and how they affect the validity of the theory behind the design method.

2.5.1 Equilibrium condition and ductile collapse

Referring to the structural model in Figure 13, the equilibrium condition can be expressed as follows:

$$V_{Rsd} = V_{Rcd} \tag{2.11}$$

According to the Lower Bound Theorem, Eq. (2.11) should be always met, since it represents the only equilibrated solution valid to evaluate the collapse load.

The Italian National Code, instead, does not impose the condition (2.11), but refers to it as the solution able to maximize the shear strength, see also [4], since it brings to collapse both concrete and steel members. Eq. (2.3), in fact, shows that, for the design purpose, it is possible to take into account as shear capacity the minimum between V_{Rsd} and V_{Rcd}, which means that the condition of equilibrium is not satisfied.

Moreover, the condition of minimum is not able to guarantee the pseudo-ductile shear collapse of the beam: in fact, if $V_{Rcd} < V_{Rsd}$, V_{Rcd} has to be considered as the design shear capacity and the concrete members will crush before the steel bars yield.

Furthermore, the approach of the variable angle truss model allows considering the value of θ able to guarantee the condition (2.2), by respecting the limits (2.9), without imposing any verification about the type of collapse – ductile or brittle – and about the real behavior of the structure, starting from the first prefailure stage (see previous section).
The selected value of θ, able to guarantee the equilibrium condition and to satisfy the design requirements, can be imposed in the *design model*, but it is not the real angle of the struts. Therefore, the real behavior of the structure could be different from the expected one. Concerning this, several experimental tests have been conducted, see [20, 23, 24], showing that, at collapse of flexural members, the value of θ depends on the amount and on the arrangement of shear and longitudinal reinforcement, and that, at the prefailure stage, the struts angle depends also on the axial stresses magnitude.

The critical aspects picked out above have been verified by means of analytical analyses on standard reinforced concrete beams.
For the purpose of studying the trend of V_{Rsd} and V_{Rcd} curves by varying the angle θ, (2.4) has been expressed as a function of the mechanical reinforcement ratio μ_{sw}. In detail:

$$\mu_{sw}(\phi, s) = \frac{f_y \cdot A_{sw}(\phi)}{f_{cd}^{'} \cdot b_w \cdot s \cdot \sin\alpha} \tag{2.12}$$

By substituting (2.12) in (2.6), the following relation holds:

$$V_{Rsd} = \mu_{sw} \cdot f'_{cd} \cdot b_w \cdot \sin^2 \alpha \cdot z \cdot (ctg\alpha + ctg\theta) \tag{2.13}$$

Then, referring to (2.13) and (2.5), the normalized tensile and compressive shear capacity can be expressed as follows:

$$v_{Rsd}(\theta, \mu_{sw}) = \frac{V_{Rsd}(\theta, \mu_{sw})}{f'_{cd} \cdot b_w \cdot z} = \mu_{sw} \cdot \sin^2 \alpha \cdot (ctg\alpha + ctg\theta) \tag{2.14}$$

$$v_{Rsc}(\theta) = \frac{V_{Rcd}(\theta)}{f'_{cd} \cdot b_w \cdot z} = \alpha_c \cdot \frac{(ctg\alpha + ctg\theta)}{(1 + ctg^2\theta)} \tag{2.15}$$

Since the value of V_{Rsd} is a function of θ and $\mu_{sw}(\phi, s)$ and V_{Rcd} is a function of θ, the trend of the functions $v_{Rsd}(\theta, \mu_{sw})$ and $v_{Rsd}(\theta)$ can be analyzed referring to: θ, μ_{sw}, s.

Note that the angle of the tensile shear reinforcement, α, has been considered equal to $90°$, since in most civil constructions the tension web bars are made from vertical stirrups. Moreover, the values of $\mu_{sw}(\phi)$ have been calculated referring to the following set of diameters: $\phi = [8,10,12]$ mm .

The results of the analyses are summarized in the graphs below.

Before starting to comment each case study, it is useful to underline that all the graphs, which show how the value of $v_{Rsd}(\theta, \mu_{sw})$ and $v_{Rsc}(\theta)$ changes depending on θ for three different values of μ_{sw}, have to be read referring to the real behavior of structures, from the prefailure state to the ultimate limit state (see previous section).

Therefore, starting from $\theta \approx 45°$, the first value of v_{Rd} is the one corresponding to the intersection point between the vertical line drawn

starting from $\theta = 45°$ and the curve, $v_{Rsd}(\theta, \mu_{swi})$ or $v_{Rcd}(\theta)$. Then, moving along the curve under consideration[10], the value of v_{Rd} changes as the angle θ decreases.

The first graph, see Figure 15, refers to s=100 mm and shows that the equilibrium condition ($v_{Rsd} = v_{Rcd}$) is met for each value of μ_{sw}.

Under the hypothesis of shear demand v_D=0.3 - horizontal gray line – there are three different design solutions able to meet the resistance requirement:

- $\mu_{sw} = \mu_{sw0}$; $\theta \approx 23°$;
- $\mu_{sw} = \mu_{sw1}$; $\theta \approx 36°$;
- $\mu_{sw} = \mu_{sw2}$; $\theta \approx 45°$.

With reference to the second design solution and starting from the prefailure state, for $\theta = 45°$ the beam shear capacity will equal the strength of n[11] yielded steel bars. As the shear force increases, until the shear demand v_D, the value of θ decreases and the number of yielded steel bars increases up to the value of v_D. Then, under the design shear load v_D all the steel bars within L_{rs} will be yielded and the stress of concrete will be less than the ultimate one.

This solution, as well as the third one, ensures a pseudo-ductile shear behavior, but does not meet the equilibrium condition that can be satisfied for different values of θ, naturally reached under larger values of shear demand.

The third design solution, as well, is the only one that, for the specific shear demand under analysis, is able to meet both equilibrium and resistance requirements.

[10] Referring to (2.3), the reference curve is the first one intersected by the vertical line.

[11] Number of bars in L_{rs}, whose length depends on θ .

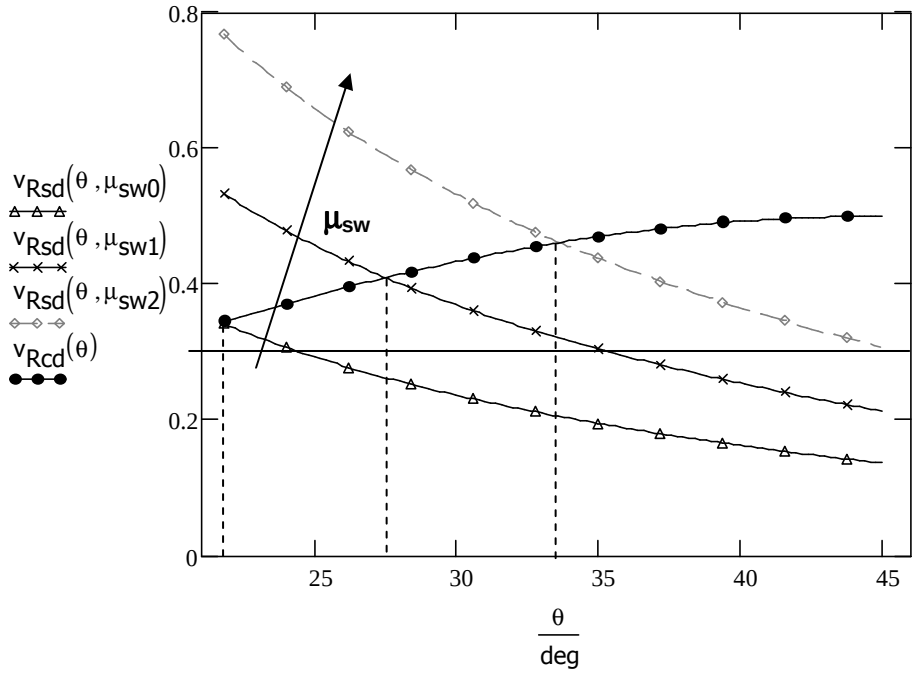

Figure 15. s=100 mm, C25/30, S355, $\alpha_c = 1$

Figure 16 refers to $s = 200\text{mm}$. Unlike the previous case, the equilibrium condition can be met only for $\mu_{sw} = \mu_{sw2}$.

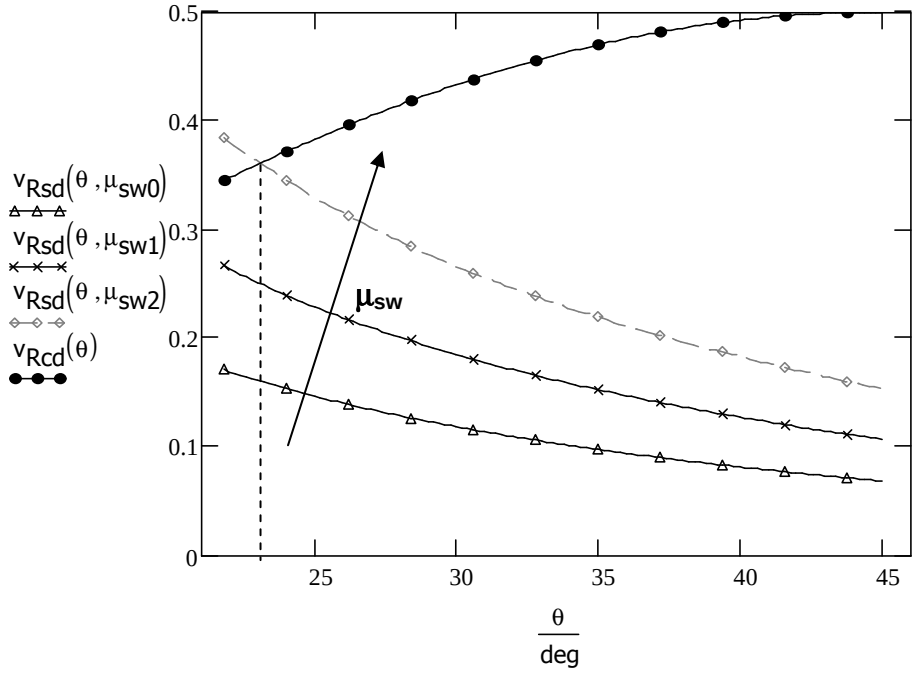

Figure 16. s=200 mm, C25/30, S355, $\alpha_c = 1$

Figure 17, as well, refers to $s = 300\ \text{mm}$ and shows that the equilibrium solution cannot be satisfied for any value of μ_{sw}.

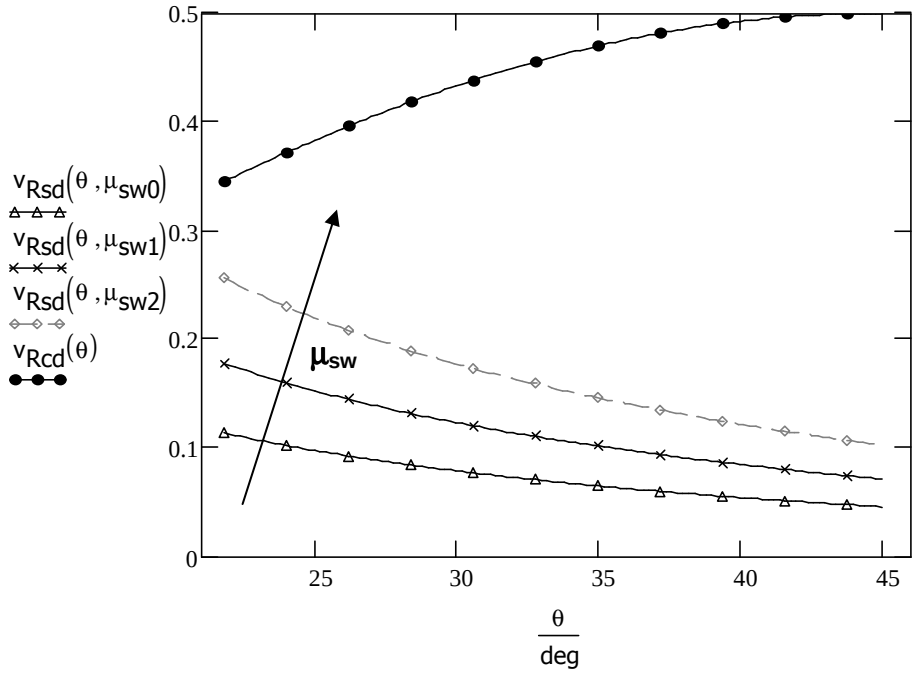

Figure 17. s=300 mm, C25/30, S355, $\alpha_c = 1$

The three cases above show that the equilibrium condition, which is a necessary requirement for the validity of the Lower Bound Theorem, cannot always be met, also for all those design solution quite common in civil constructions.

The graph below, see Figure 18, refers to an uncommon constructive solution, but is able to represent another limit of the theoretical approach of the Italian National Code.

In fact, the graph shows that the equilibrium solution cannot be met for any value of μ_{sw} and θ and, most of all, it proves that all solutions refer to brittle shear behavior.

Starting from $\theta = 45°$, the vertical line intersects the curve v_{Rcd}, which represents the limit strength of concrete. Note that the value of the shear

resistance cannot increase, not only because it represents the maximum value along the curve v_{Rcd}, but also because the brittle collapse does not allow the development of additional resisting mechanisms.

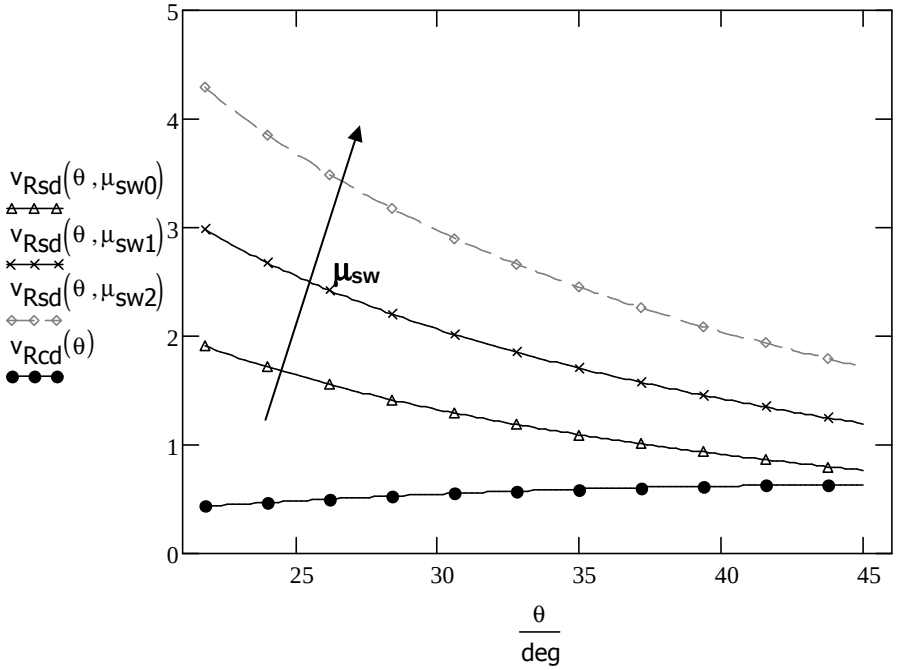

Figure 18. s=50 mm, b_w=200, C16/20, S450, $\alpha_c = 1$

Moreover, note that the variation of θ cannot be continuous, since it depends on the spacing of transverse reinforcement, s. Therefore the equilibrium condition, that in some cases represents the only possible solution of the problem, see Figure 15, cannot be met because of the arrangement of the reinforcement and the limits of the range of variation of θ, see (2.9).

2.5.2 Constitutive law and superposition principle

According to the theory behind the formulations of the Italian National Code, tensile and compressive forces are taken into account with their respective maximum values: the yield stress for steel, f_{yd}, and the compressive strength for concrete, $f_{cd}^{'}$.

This condition has two critical aspects: the first one refers to the constitutive laws, which cannot be satisfied for both the compressive and the tensile member; the second one concerns the superposition principle, which is only valid for linear analysis.

In fact, as explained above, at shear demand v_D, the variable angle truss is characterized by:

- θ, the angle of compression struts;
- n, the number of tension bars, which is a function of θ, see (2.8).

The overall resisting substructure, characterized by L_{rs}, can be considered as the sum of n trusses, see (2.6) (2.8). But within the framework of plasticity theory, the assumption of applicability of the superposition principle does not seem appropriate.

Chapter 3
Simplified model

3.1 Introduction

This section deals with the development of a new simplified mechanical model of CSCB capable of predicting the yield of shear steel bars and the corresponding stress in concrete elements. The proposed model stems from a variational approach, able to meet both the compatibility and the equilibrium conditions.

The problem has been set by means of the displacement method of analysis, under the hypotheses of infinite stiffness of the beam upper chord. Then the equilibrium condition has been found using the Principle of Minimum Potential Energy.

The first section of the chapter briefly outlines the theoretical background of variational methods for finding the solution of boundary mixed linear elastic problems[1].
The second section deals with the description of the proposed model and the theoretical assumptions behind it, the definition of all the adopted symbols, and the solution of the structural system, obtained by minimizing the potential energy functional.
In the next part the concept is deepened of "shear demand" for the proposed model, by making use of the capacity design concept.
In the last section, as well, some geometrical remarks are presented in order to explain the physical meaning of each term of the proposed formulation and the lower and upper limits set for the value of each of them.

3.2 Variational approach

The solution of mixed boundary linear elastic problems can be found by means of three different general methods: direct, inverse and semi-inverse. The direct method allows determining the exact solution by direct integration of field equations (15 differential equations), which express compatibility conditions, equilibrium conditions and constitutive laws. Boundary conditions have to be satisfied exactly.
According to the inverse method, particular displacements or stresses have to be selected and then it is necessary to identify the specific problem that can be solved by the solution field.
By the semi-inverse method, part of the displacement and/or stress field is specified "a priori" and the remaining part is determined by means of the field equations (usually using direct integration) and boundary conditions.

[1] This definition of the problem refers, respectively, to the mixed boundary conditions, since they deal with both displacements and forces, and to the linear equations, able to describe the problem.

As an example, De Saint Venant's problem is set according to this method [25].

All the methods defined above require finding the solution of the field equations that can be found by means of several mathematical techniques: analytical solutions procedures, approximate solution procedures and numerical solution procedures. [25]

Within the framework of approximate solution procedures, *variational methods,* which are related to energy theorems, allow obtaining values of unknown displacements or forces at specific points of the structure by finding an extreme of a particular integral functional. In structural mechanics, the reference functional is usually the total energy of the system and includes all the features of the problem – governing equations, boundary and/or initial conditions and constraint condition. [64].

In the following, some basic concepts related to variational methods for finding the solution of boundary mixed linear elastic problems are briefly presented.

3.2.1 Strain Energy and Work

The strain energy can be defined as the amount of energy stored in a structural element during its deformation, due to applied external loads.

Consider the simplest case of a spring with non-linear constitutive law, gradually loaded with a force F along its longitudinal axis. The load-displacement graph is shown in Figure 1: by increasing the applied force by a small amount, δF , the displacement increases of an amount δy .

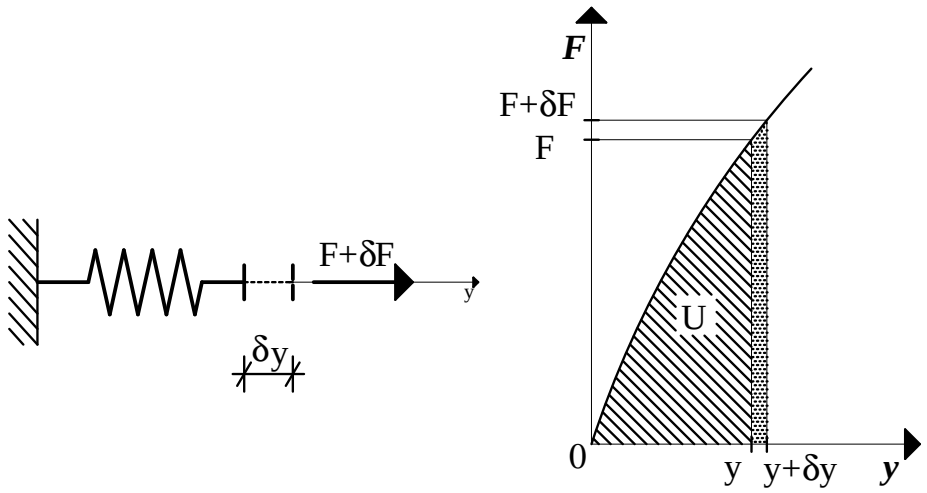

Figure 1. Strain energy: linear constitutive law

The dotted area of the graph underneath the curve $F = f(y)$ represents the strain energy stored in the spring during the last increase of the load, see (3.1), which, neglecting the second order infinitesimal, is given by:

$$\delta U = F \cdot dy \tag{3.1}$$

Therefore, the overall strain energy stored in the spring when the load increases gradually from 0 to F, see the striped area in Figure 1, can be expressed as the sum of the strain energy related to each small increase of displacement. So the following relation holds:

$$U = \int_0^y F dy \tag{3.2}$$

The strain energy stored in the spring can be also seen as a measure of the *internal work,* W_i.

Referring to the case of linear constitutive law of the spring, the curve in Figure 1 becomes a line, whose function is $F = ky$, where k represents the stiffness of the spring.

So, referring to (3.2), the strain energy – which is equal to the internal work – can be expressed as:

$$U = W_i = \int_0^y F dy = \int_0^y k \cdot y dy = k \cdot \frac{y^2}{2} = \frac{1}{2} \cdot F \cdot y \tag{3.3}$$

For conservative systems, the internal work is equal to the external one, done by the force F. So, the following relation holds:

$$W_e = W_i \tag{3.4}$$

The work of external forces, W_e, on an elastic solid is completely stored as strain energy, U, within the solid.
Moreover, as F is a conservative force, it is also possible to define the *potential energy*, which is a function of the external forces. The variation of the potential energy can be expressed as:

$$W_e = -\Delta V \tag{3.5}$$

As shown in (3.5), ΔV has a negative sign since the positive work causes a reduction in the potential.

3.2.2 Total potential energy

The total potential energy is defined as the algebraic sum of the internal strain energy and the potential energy function of the external load, V.

$$\Pi = U + \Delta V \tag{3.6}$$

By substituting (3.3) and (3.5) into (3.6), the following formulation holds:

$$\Pi = \frac{1}{2} k y^2 - F y \tag{3.7}$$

Before expounding the Principle of Virtual Work, in the following all the terms used in the next section are briefly introduced.
In the framework of the theory of deformable bodies, consider a mixed boundary value problem, where all the equations are linear and the boundary conditions deal with both forces and displacement. The generalized Hooke's law for anisotropic bodies can be written as follows:

$$[T] = [C][E] \tag{3.8}$$

Where $[C]$ is the fourth order elastic modulus tensor (stiffness tensor), whose components represent the bounded functions of the variable $x \in V$: for the general case of anisotropic materials, it has 3^4 elements. $[T]$ and $[E]$ are the second order stress and the Cauchy strain tensors, respectively. Referring to the $ij-th$ element of the tensor $[T]$, (3.8) gives:

$$\sigma_{ij} = C_{ijkl}\varepsilon_{kl} \tag{3.9}$$

Because of the rotational equilibrium of the body, $[T]$ is symmetric and the following equation holds:

$$\sigma_{ij} = \sigma_{ji} \Rightarrow \sigma_{ij} = C_{ijkl}\varepsilon_{kl} = \sigma_{ji} = C_{jikl}\varepsilon_{kl} \Rightarrow C_{ijkl} = C_{jikl} \tag{3.10}$$

The symmetry of the tensor $[E]$, as well, gives:

$$\varepsilon_{kl} = \varepsilon_{lk} \Rightarrow \sigma_{ij} = C_{ijkl}\varepsilon_{kl} = C_{ijlk}\varepsilon_{lk} \tag{3.11}$$

Then, the following equation can be written:

$$C_{ijkl} = C_{jikl} = C_{ijlk} \tag{3.12}$$

This property of the tensor $[C]$ is called "minor symmetry" and reduces the number of matrix elements from 81 to 36.

Moreover, for hyperelastic materials, since the stress-strain relation can be derived from a strain energy[2] density functional, see(3.13), the "major symmetry" holds, see (3.14), which reduces the number of matrix elements to 21 independent terms.

$$\sigma_{ij} = \frac{\partial \varphi}{\partial \varepsilon_{ij}} \Rightarrow C_{ijkl} = \frac{\partial^2 \varphi}{\partial \varepsilon_{ij} \partial \varepsilon_{kl}} \tag{3.13}$$

$$C_{ijkl} = C_{klij} \tag{3.14}$$

Moreover, in the case of an isotropic body, the independent elements of $[C]$ become 2 : the in-plane shear modulus, G , and the Lame's coefficient, λ , defined as follows:

$$\lambda = \frac{E \cdot \nu}{\left[(1+\nu)+(1-2\nu)\right]} \tag{3.15}$$

where E is the Young modulus and ν is the Poisson's ratio.

[2] The work done by surface and body forces on an elastic body is stored inside it in the form of strain energy. For an idealized elastic body, this stored energy turns on zero when the body returns to the unstrained configuration.

3.2.3 The Principle of Virtual Work

The principle of virtual work provides the basis for all the approximate solution procedures. The Virtual Work is the work done on a deformable body by actual forces in moving through a hypothetical or virtual displacement that is consistent with the geometric constrains [64].
It states that if $\sigma(u)$ is a statically admissible stress field (equilibrium conditions are met) and $u(x)$ is a geometrically admissible displacement field (compatibility conditions are met), the following formulation holds

$$\int_V \sigma_{ij}\varepsilon_{ij}(u)\mathrm{d}V = \int_V f_i u_i \mathrm{d}V + \int_S p_i u_i \mathrm{d}S + \int_S r_i \delta_i \mathrm{d}S \tag{3.16}$$

where:

- f_i represents the $i-th$ body force
- p_i is the $i-th$ surface force
- r_i is the constraint reaction force
- δ_i is the displacement at the support, along the same direction of r_i

Therefore, the virtual work of internal forces, represented by the left-hand side of the equation, is equal to the virtual work of external forces, made up of the virtual work of body forces, surface forces and the work of support reactions due to the displacements of constrains.

Eq. (3.16) can be written as:

$$\int_V \sigma_{ij}\varepsilon_{ij}(u)\mathrm{d}V - \int_V f_i u_i \mathrm{d}V - \int_S p_i u_i \mathrm{d}S - \int_S r_i \delta_i \mathrm{d}S = 0 \tag{3.17}$$

Thus, the total virtual work for a body in equilibrium is zero.
Under the assumptions $\delta_i = 0$ and $f_i = 0$, which represent the most common case in real structures, (3.17) becomes:

$$\int_V \sigma_{ij}\varepsilon_{ij}(u)\mathrm{d}V - \int_S p_i u_i \mathrm{d}S = 0 \tag{3.18}$$

The strain energy, see (3.3), stored by the solid can be expressed as:

$$\Theta = \int_V \sigma_{ij}\varepsilon_{ij} dV \tag{3.19}$$

The density of local strain energy, as well, can be written as:

$$\Theta_0 = \int_0^{\varepsilon} \sigma_{ij} d\varepsilon \tag{3.20}$$

Moreover, the complementary strain energy density can be written as:

$$\Theta_0 = \int_0^{\sigma} \varepsilon_{ij} d\sigma \tag{3.21}$$

The strain energy is the area underneath the stress-strain curve up to the point of deformation, see Figure 2.

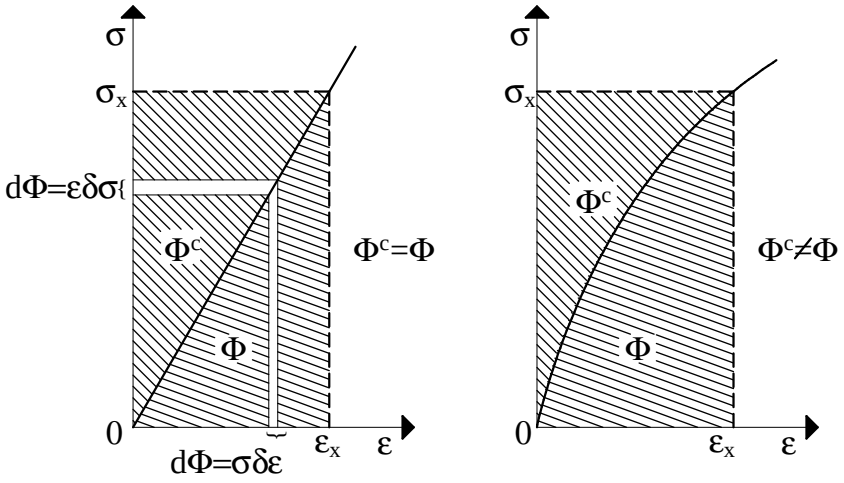

Figure 2. Strain and complementary energy for linear and non-linear elastic materials

Note that just for linear elastic materials the value of the strain energy equals that of the complementary one.
In case of uniaxial tension, when all the stress components of the tensor $[T]$ are zero, except σ_{ii}, the linear strain energy density can be written as:

$$\Theta_0 = \int_0^{\varepsilon} \sigma_{ii} d\varepsilon = \frac{1}{2}\int_0^{\varepsilon} (E\varepsilon_{ii}) d\varepsilon = \frac{E\varepsilon_{ii}^2}{2} = \frac{1}{2}\sigma_{ii}\varepsilon_{ii} \tag{3.22}$$

Referring to the axial strain energy, the following formulations hold:

$$\sigma_{ii} = E\varepsilon_{ii} \qquad \varepsilon_{ii} = \frac{du}{dx}(x) \tag{3.23}$$

$$\Theta = \int_V \frac{1}{2} E\varepsilon_{ii}^2 dV = \int_L \left[\int_A \frac{1}{2} E \left(\frac{du}{dx} \right)^2 dA \right] dx = \int_L \left[\frac{1}{2} \left(\frac{du}{dx} \right)^2 \int_A E dA \right] dx \tag{3.24}$$

The following condition can be set:

$$\Theta_{0,l} = \frac{1}{2} EA \left(\frac{du}{dx} \right)^2 \tag{3.25}$$

It represents the strain energy per unit length. Then, the strain energy is:

$$\Theta = \int_L \Theta_{0,l} dx \tag{3.26}$$

The complementary strain energy density and the complementary strain energy can be written, respectively, as follows:

$$\Theta_0^c = \frac{1}{2} \frac{N^2}{EA} \tag{3.27}$$

$$\Theta^c = \int_L \Theta^c dx \tag{3.28}$$

3.2.4 Principle of Minimum Potential Energy

As stated in the previous section, the potential energy can be denoted as $\Pi = U + \Delta V$. According to the Virtual Work Principle, the variation of potential energy for an equilibrium configuration is zero. It means that the potential energy is *stationary* for equilibrium configurations. The potential energy, under this condition, will reach its *local extremum*, either minimim or maximum value. As demonstrated by Sokolnikoff (1956) or Reismann and Pawlik (1980), the potential energy function has a *local minimum* in the equilibrium configuration. This leads to the Principle of Minimum Potential Energy: *of all displacements satisfying the given boundary conditions of an elastic solid, those that satisfy the equilibrium equations make the potential energy a local minimum* [25].
So, under the hypotheses that the body is subjected to conservative forces, that it is made up of elastic materials regardless of whether the stress-strain law is linear or nonlinear and starting from known displacements, the following formulation holds:

$$\Pi(u) = \frac{1}{2}\int_V \varepsilon^T(u) \cdot C_{ijkh} \cdot \varepsilon(u) dV - \int_V \varepsilon^T(u) \cdot C_{ijkh} \cdot \varepsilon(u) dV \tag{3.29}$$

3.3 Proposed model

This section deals with the research and the solution of a new mechanical model able to describe the structural behavior of CSCB and to define a reliable design and verification method consistent with the requirements of the National Code.

Starting from the model in Figure 3, which represents the main resistant elements of composite steel and concrete beams, the simplified model in Figure 4 has been defined, in order to fulfill the following requirements:

- reproducing the real mechanical behavior of the structure, with reference to all the (compressive and tensile[3]) resisting elements and to their stiffness and resistance, for any possible arrangement of the steel elements of the beam;
- providing a model which can be the basis for a reliable procedure of design and verification of structural elements, especially referring to the pseudo- ductile behavior of a beam failing in shear;
- putting forward a solution methodology able to guarantee the attainment of both equilibrium and compatibility conditions.

Referring to the first requirement, by means of a preliminary strut-and-tie modeling, the internal truss system has been organized in two groups of elements: those belonging to the flanges and those belonging to the web. The flanges are the upper compressed chord made of concrete and the bottom tension chord made generally by a steel plate.

The web is made of the following elements:

T - Steel bars, either vertical or inclined, generally in tension

R - Rods made of concrete and steel, generally in compression

S - Diagonal struts made of concrete

The flanges are devoted to the flexural capacity, while the web to the shear capacity. Moreover, all geometrical and mechanical characteristics of the

[3] Please note that compressive and tensile elements have been defined referring to the most common load condition for beams in static conditions: uniform load.

model are parametric quantities, which allow describing any beam configuration.

Referring to the shear capacity, the overall resisting system can be described referring separately to the steel tensile bars (T) and the compressive steel and concrete elements ($R+S$), where the former fix the tensile shear resistance of the beam and the latter the compressive shear resistance. It should be noted that, unlike the variable angle model for reinforced concrete structures, see Chapter 2, the mechanical model of a CSCB is fixed, since both θ_R and θ_S angles are defined by the steel truss geometry. So, the tensile and compressive shear resistance depends on the mechanical characteristics of the beam and the geometrical arrangement of the steel truss.

This remark allows considering the set of T, S and R, which converge onto a common node, as a "representative substructure" of the shear resistance of the overall CSCB, see Figure 4 and Figure 9.

Therefore, starting from this substructure, a design procedure, based on the capacity design criterion, has been defined, which seeks the equality between shear demand and tensile shear capacity, while verifying crushing of concrete compressive elements and lateral buckling of compressive steel bars.

In the application of the capacity design criterion, this setting of the model allows considering the capacity of the tensile elements as the externally acting force that must be equilibrated by the compressive elements.

Note that, as explained in detail in the "Shear Demand" section of this Chapter, the shear demand V_D used in the proposed model is defined by referring to the bending moment capacity of the cross section, since the shear design procedure refers to the 2nd stage, see Chapter 1.

This setting of the design procedure is able to ensure both global and local ductile behavior of the beam.

The structural model, which is a statically indeterminate one, has been solved by referring to a variational method, as described in a previous

section: in detail, starting from a compatibility solution under the hypothesis of infinite stiffness of the upper chord, see Figure 4, the equilibrium condition has been found by minimizing the total potential energy. As a result, the vertical displacement of the node of the structure has been expressed as a function of the shear demand and the stiffness of the compressive elements. Moreover, since the stiffness values of each compressive element are known after the solution of the system, it is possible to evaluate the stress of both concrete and steel compressive elements in order to check, respectively, the crack width and the buckling of bars.

3.3.1 Symbols

In the following Figure 3 and Table 1 all the symbols used to describe and analyze the proposed simplified model are summarized. Note that in the model the slight angle of the bars in the cross-section is neglected.

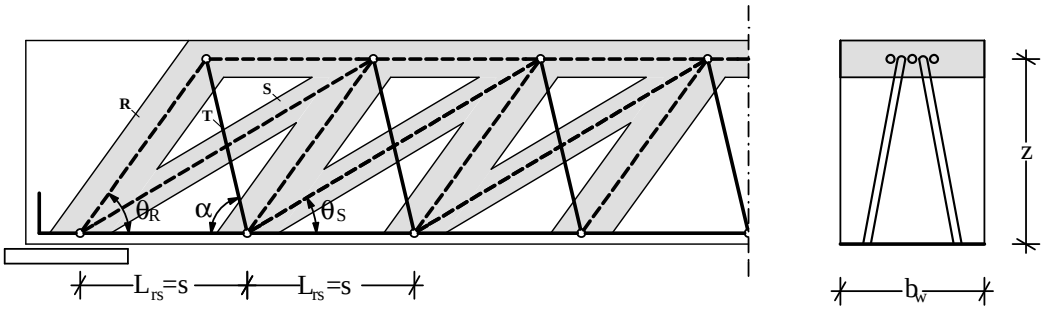

Figure 3. Composite Steel-Concrete Beams: model

Table 1. Symbols

	Tension bar	**Rod**[4]	**Strut**
symbol	T	R	S
area	$A_T = A_{sw}$	$A_R = n_E \cdot A_{sw} + b_w \cdot \nu_R \cdot s$	$A_S = b_w \cdot \nu_S \cdot s$

[4] The "Rod element" is made up of steel and concrete , with the following cross section area: $A_R = n_E \cdot A_{sw} + b_w \cdot \nu_R \cdot s$, where $n_E = \frac{E_S}{E_c}$

angle	α	$\theta_R = \operatorname{acot}\left(\frac{1}{\zeta} - \cot\alpha\right)$	$\theta_S = \operatorname{acot}\left(\frac{2}{\zeta} - \cot\alpha\right)$
Young modulus	E_s	E_c, E_s	E_c
length	$l_T = \frac{z}{\sin\alpha}$	$l_R = \frac{z}{\sin\theta_R(\alpha)}$	$l_S = \frac{z}{\sin\theta_S(\alpha)}$
glob. displ.	v	v	v
loc. displ.	$v \cdot \sin\alpha$	$v \cdot \sin\theta_R$	$v \cdot \sin\theta_S$
strain	$\varepsilon_T = \frac{v}{z}\sin\alpha$	$\varepsilon_R = \frac{v}{z} \cdot \sin\theta_R$	$\varepsilon_S = \frac{v}{z} \cdot \sin\theta_S$
stress	$E_s \cdot \varepsilon_T$	$E_c \cdot \varepsilon_R$	$E_c \cdot \varepsilon_S$
aixal forces	N_T	N_R	N_S

3.3.2 Solution of the simplified model

Figure 4 shows the simplified model of the structure and Table 2 the meaning of the symbols used to describe and solve the system.

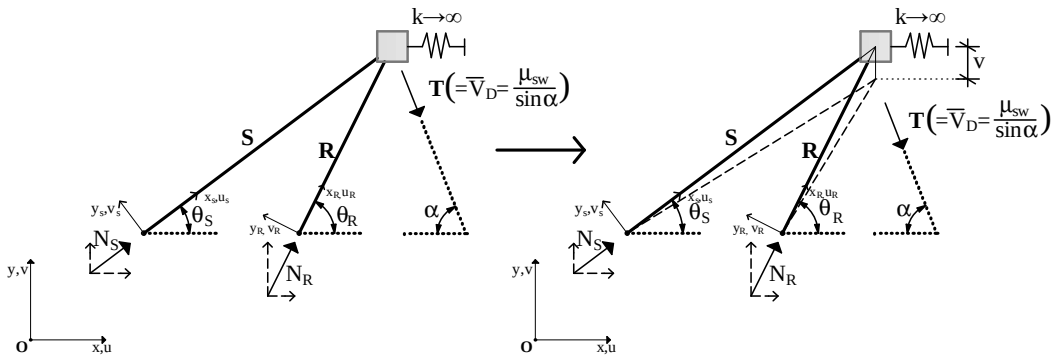

Figure 4. Simplified model

Table 2. Symbols for potential energy formulation

	Global reference system (GRS)	**Local reference system (LRS)**	**Dimensionless quantity (GRS)**	**Dimensionless quantity (LRS)**
Stiffness	K	k	$\overline{K}$	$\overline{k}$
Shear demand	V_D	v_D	$\overline{V}_D$	$\overline{v}_D$
Axial force	N_R, N_S	n_R, n_S	$\overline{N}_R, \overline{N}_S$	$\overline{n}_R, \overline{n}_S$
Displacement	V	v_R, v_S	$\overline{V}$	$\overline{v}$

The geometrical characteristics of the truss along the longitudinal axis are expressed through the *aspect ratio*, defined as:

$$\zeta = \frac{z}{s} \tag{3.30}$$

Referring to the simplified model, see Figure 4, the potential energy function can be written as follows:

$$\Pi(V, \nu) = \frac{1}{2} \cdot K_R \cdot V^2 + \frac{1}{2} \cdot K_S \cdot V^2 - V_D \cdot V \tag{3.31}$$

The term V, see Figure 4, is the vertical displacement of the node. K_R and K_S are the axial stiffness of, respectively, the rod and the strut, in the global reference system. They can be expressed as functions of the relative local stiffness:

$$\begin{aligned} K_R &= k_R \sin^2 \theta_R \\ K_S &= k_S \sin^2 \theta_S \end{aligned} \tag{3.32}$$

Moreover, the local stiffnesses are:

$$\begin{aligned} \mathrm{k_R} &= \frac{E_c A_R}{l_R} \\ \mathrm{k_S} &= \frac{E_c A_S}{l_S} \end{aligned} \tag{3.33}$$

For the meaning of the symbols E_c, A_R, l_R, A_s, l_S, refer to Table 1.
So (3.33) can be expressed as:

$$\begin{aligned} \mathrm{k_R} &= \frac{E_c A_R}{z}\sin^3\theta_R \\ \mathrm{k_S} &= \frac{E_c A_S}{z}\sin^3\theta_S \end{aligned} \tag{3.34}$$

By substituting (3.34) in (3.31), the following formulation holds:

$$\begin{aligned} \Pi(\mathrm{V},\nu) &= \frac{1}{2}\left(\frac{E_c A_R}{z}\sin^3\theta_R + \frac{E_c A_S}{z}\sin^3\theta_S\right)\mathrm{V}^2 - \mathrm{V_D}\cdot u \\ &= \frac{1}{2}\frac{E_c}{z}\left(A_R\sin^3\theta_R + A_S\sin^3\theta_S\right)\mathrm{V}^2 - \mathrm{V_D}\cdot u \\ &= \frac{1}{2}\frac{E_c}{z}\left[\left(n_E A_{sw} + b_w \nu_R s\right)\sin^3\theta_R + \nu_S s b_w \sin^3\theta_S\right]\mathrm{V}^2 - \mathrm{V_D}\cdot u \\ &= \frac{1}{2}\frac{E_c}{z}\left[\left(\frac{n_E A_{sw}}{s} + b_w\nu_R\right)\sin^3\theta_R + \nu_S b_w \sin^3\theta_S\right] s\cdot\mathrm{V}^2 - \mathrm{V_D}\cdot u \end{aligned}$$

Recalling that the aspect ratio is defined as $\zeta = \frac{z}{s}$, then

$$\begin{aligned} &= \frac{1}{2}E_c\left[\left(\frac{n_E}{\zeta}\frac{A_{sw}}{s} + \frac{b_w\nu_R}{\zeta}\right)\sin^3\theta_R + \frac{\nu_S b_w}{\zeta}\sin^3\theta_S\right]\cdot\mathrm{V}^2 - \mathrm{V_D}\cdot u \\ &= \frac{1}{2}E_c b_w\left[\left(\frac{n_E}{\zeta}\frac{A_{sw}}{s\cdot b_w} + \frac{\nu_R}{\zeta}\right)\sin^3\theta_R + \frac{\nu_S}{\zeta}\sin^3\theta_S\right]\cdot\mathrm{V}^2 - \mathrm{V_D}\cdot u \end{aligned} \tag{3.35}$$

By introducing the mechanical reinforcement ratio $\mu_{sw} = \frac{f_y A_{sw}}{f_c b_w s}$

and the ratio $n_f = \frac{f_y}{f_c}$, the formulation becomes:

$$= \frac{1}{2} E_c b_w \left[\frac{1}{\zeta} \left(\frac{n_E}{n_f} \mu_{sw} + \nu_R \right) \sin^3 \theta_R + \frac{\nu_S}{\zeta} \sin^3 \theta_S \right] \cdot \mathrm{V}^2 - \mathrm{V_D} \cdot u$$

By introducing the dimensionless displacement, defined as $\overline{\mathrm{V}} = \frac{\mathrm{V}}{\mathrm{s}}$ and

the dimensionless value of shear demand, $\overline{\mathrm{V}}_{\mathrm{D}} = \frac{\mathrm{V_D}}{f_c b_w s}$

$$\Pi\left(\overline{\mathrm{V}}, \nu\right) = \frac{1}{2} E_c b_w \left[\frac{1}{\zeta} \left(\frac{n_E}{n_f} \mu_{sw} + \nu_R \right) \sin^3 \theta_R + \frac{\nu_S}{\zeta} \sin^3 \theta_S \right] \cdot \overline{\mathrm{V}}^2 \cdot s^2 - \overline{\mathrm{V}}_{\mathrm{D}} \cdot f_c b_w s^2 \overline{\mathrm{V}}$$

$$= b_w s^2 \left\{ \frac{1}{2} E_c \left[\frac{1}{\zeta} \left(\frac{n_E}{n_f} \mu_{sw} + \nu_R \right) \sin^3 \theta_R + \frac{\nu_S}{\zeta} \sin^3 \theta_S \right] \cdot \overline{\mathrm{V}}^2 - \overline{\mathrm{v}}_{\mathrm{D}} \cdot f_c \overline{\mathrm{V}} \right\}$$

$$= b_w s^2 f_c \left\{ \frac{1}{2} \frac{E_c}{f_c} \left[\frac{1}{\zeta} \left(\frac{n_E}{n_f} \mu_{sw} + \nu_R \right) \sin^3 \theta_R + \frac{\nu_S}{\zeta} \sin^3 \theta_S \right] \cdot \overline{\mathrm{V}}^2 - \overline{\mathrm{V}}_{\mathrm{D}} \overline{\mathrm{V}} \right\}$$

The potential energy can be expressed as a dimensionless quantity, defined as:

$$\overline{\Pi}\left(\overline{\mathrm{V}}, \nu\right) = \frac{\Pi\left(\overline{\mathrm{v}}, \nu\right)}{b_w s^2 f_c} \tag{3.36}$$

then:

$$\overline{\Pi}\left(\overline{\mathrm{V}}, \nu\right) = \frac{\Pi\left(\overline{\mathrm{v}}, \nu\right)}{b_w s^2 f_c} = \left\{ \frac{1}{2} \frac{E_c}{f_c} \left[\frac{1}{\zeta} \left(\frac{n_E}{n_f} \mu_{sw} + \nu_R \right) \sin^3 \theta_R + \frac{\nu_S \sin^3 \theta_S}{\zeta} \right] \cdot \overline{\mathrm{v}}^2 - \overline{\mathrm{v}}_{\mathrm{D}} \overline{\mathrm{v}} \right\} \tag{3.37}$$

So, the values of the dimensionless rod and strut stiffness in the global reference system can be expressed as:

$$\overline{\mathrm{K}}_{\mathrm{R}} = \frac{E_c}{f_c} \frac{\frac{n_E}{n_f}\mu_{sw} + \nu_R}{\zeta} \sin^3 \theta_R \tag{3.38}$$

$$\overline{\mathrm{K}}_{\mathrm{S}} = \frac{E_c}{f_c} \frac{\nu_S}{\zeta} \sin^3 \theta_S \tag{3.39}$$

Then the (3.31) can be expressed as:

$$\overline{\Pi}\left(\overline{\mathrm{V}}, \nu\right) = \frac{1}{2}\left[\overline{\mathrm{K}}_{\mathrm{R}} + \overline{\mathrm{K}}_{\mathrm{S}}\right] \cdot \overline{\mathrm{V}}^2 - \overline{\mathrm{V}}_{\mathrm{D}} \cdot \overline{\mathrm{V}} \tag{3.40}$$

According to the Principle of Minimum Potential Energy, the equilibrium solution can be found as the minimum of the function $\overline{\Pi}\left(\overline{\mathrm{v}}, \nu\right)$.

$$\frac{\partial}{\partial \overline{\mathrm{V}}} \overline{\Pi}\left(\overline{\mathrm{V}}, \nu\right) = 0 \tag{3.41}$$

$$\begin{aligned} &\frac{\partial}{\partial \overline{\mathrm{V}}}\left(\frac{1}{2}\left[\overline{\mathrm{K}}_{\mathrm{R}} + \overline{\mathrm{K}}_{\mathrm{S}}\right]\overline{\mathrm{V}}^2 - \overline{\mathrm{V}}_{\mathrm{D}}\,\overline{\mathrm{V}}\right) = \left[\overline{\mathrm{K}}_{\mathrm{R}} + \overline{\mathrm{K}}_{\mathrm{S}}\right]\overline{\mathrm{V}} - \overline{\mathrm{V}}_{D} = 0 \Rightarrow \\ &\overline{\mathrm{V}}_E = \frac{\overline{\mathrm{V}}_{\mathrm{D}}}{\left[\overline{\mathrm{K}}_{\mathrm{R}} + \overline{\mathrm{K}}_{\mathrm{S}}\right]} \end{aligned} \tag{3.42}$$

All the formulas above refer to the global reference system. For the purpose of evaluating the magnitude of axial forces in each element for the equilibrium solution, in the following the values of displacements and stiffness are expressed referring to the local reference system.

$$\begin{aligned} \overline{\mathrm{k}}_{\mathrm{R}} &= \frac{\overline{\mathrm{K}}_{\mathrm{R}}}{\sin^2 \theta_R} \\ \overline{\mathrm{k}}_{\mathrm{S}} &= \frac{\overline{\mathrm{K}}_{\mathrm{S}}}{\sin^2 \theta_S} \end{aligned} \tag{3.43}$$

$$\begin{aligned}\bar{v}_R &= \bar{v}_E \sin\theta_R \\ \bar{v}_S &= \bar{v}_E \sin\theta_S\end{aligned} \tag{3.44}$$

Then, the dimensionless axial force in each element can be expressed as:

$$\begin{aligned}\bar{n}_R &= \bar{k}_R \cdot \bar{v}_R = \frac{\bar{\bar{K}}_R}{\sin^2\theta_R}\bar{v}_E \cdot \sin\theta_R = \frac{\bar{\bar{K}}_R}{\sin\theta_R}\bar{v}_E \\ \bar{n}_S &= \bar{k}_S \cdot \bar{v}_S = \frac{\bar{\bar{K}}_S}{\sin^2\theta_S}\bar{v}_E \cdot \sin\theta_S = \frac{\bar{\bar{K}}_S}{\sin\theta_S}\bar{v}_E\end{aligned} \tag{3.45}$$

Referring to(3.42) the formula above becomes:

$$\begin{aligned}\bar{\bar{n}}_R &= \frac{\bar{\bar{K}}_R}{\sin\theta_R}\bar{\bar{v}}_E = \frac{\bar{\bar{K}}_R}{\sin\theta_R} \cdot \frac{\bar{v}_D}{\left[\bar{\bar{K}}_R + \bar{\bar{K}}_S\right]} \\ \bar{\bar{n}}_S &= \frac{\bar{\bar{K}}_S}{\sin\theta_S}\bar{\bar{v}}_E = \frac{\bar{\bar{K}}_S}{\sin\theta_S} \cdot \frac{\bar{v}_D}{\left[\bar{\bar{K}}_R + \bar{\bar{K}}_S\right]}\end{aligned} \tag{3.46}$$

3.4 Geometrical variables

In the following sections the analyses carried out to define the range of variation of all the dimensionless parameters chosen to describe the geometry and the mechanical characteristics of the model will be presented.
The results of this study are embedded in the simplified model, since they allow selecting automatically the admissible set of parameters that define the structure.

3.4.1 Range of variation of ζ

The range of variation of the aspect ratio, $\zeta = z/s$, has been defined referring to the most common shapes of trusses, along the longitudinal axis.

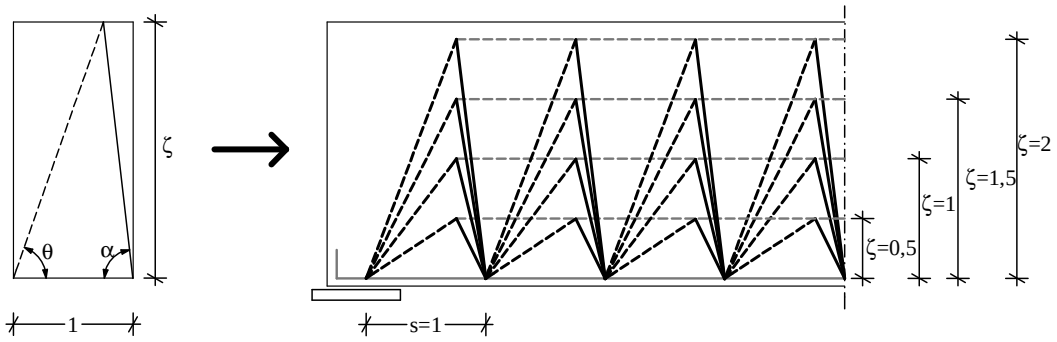

Figure 5. Range of variation of ζ

The following limits have been set:

$$0,5 \leq \zeta \leq 4 \tag{3.47}$$

where the range up to 2 represents common building typologies and that up to 4 refers to industrial buildings.

3.4.2 Range of variation of α as a function of ζ

The bar angle α is an independent variable of the model, such as ζ. The following geometrical considerations show that the two quantities can change independently, but, since they are related by a geometrical relationship, the range of variation of α changes according to the value of ζ, as shown in Figure 6.

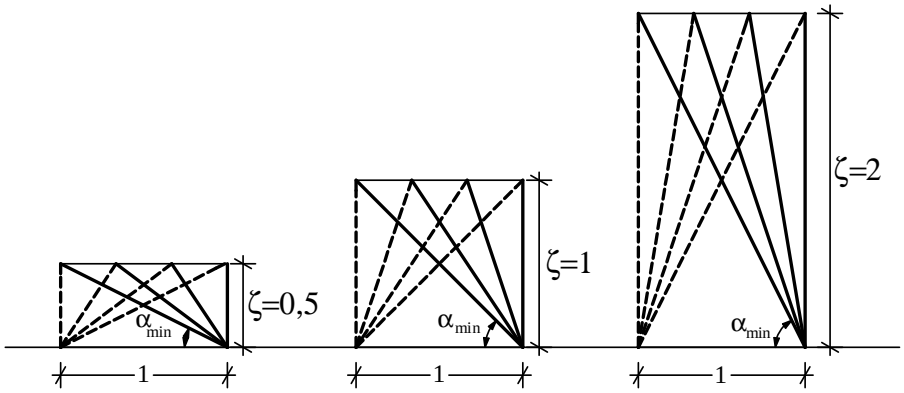

Figure 6. Variation of lower bound of α as a function of ζ

For the purpose of the analysis, the function $\alpha_H(\alpha,\zeta)$ has been defined:

$$\alpha_H(\alpha,\zeta) = \alpha \cdot H_\alpha(\alpha,\zeta) \tag{3.48}$$

where

$$H_\alpha(\alpha,\zeta) = \arctan(\zeta) \le \alpha \le 90° \tag{3.49}$$

Eq. (3.49) defines the range of variation of α, which is related to geometrical conditions: the lower bound depends on the aspect ratio of the truss, $\zeta = z/s$, while the upper one , is $90°$, which is the maximum angle of tensile bars in common beams.

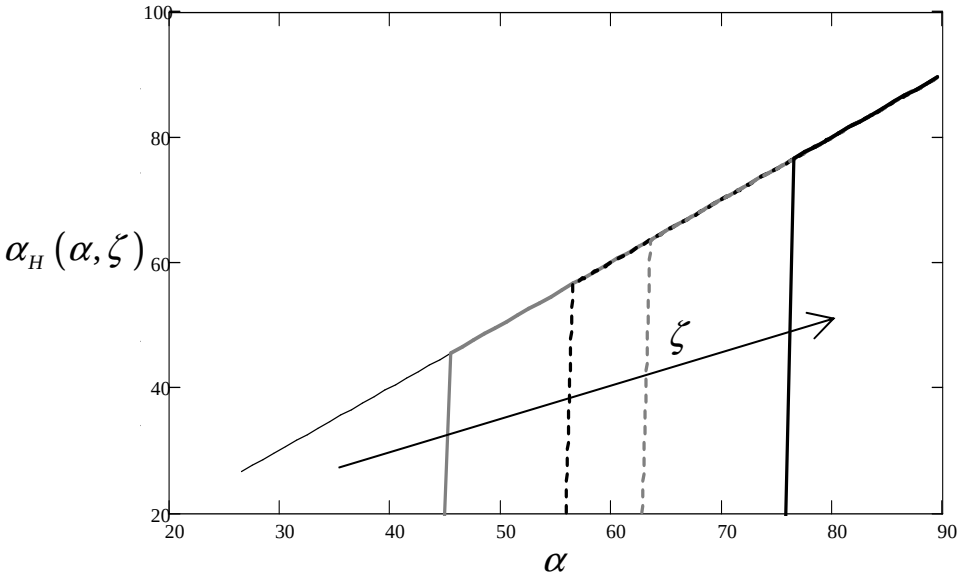

Figure 7. Range of variation of α

Figure 7 shows that, as the value of ζ increases, the range of variation of α becomes narrower.

Thus, in the optimization process, carried out in Chapter 5, when a given value of ζ_i is taken into account for the evaluation of the goal function, the values of α change within the related geometrical admissible range: α_{i_range}.

3.4.3 Range of variation of μ_{sw}

The transverse reinforcement mechanical ratio, μ_{sw}, can be defined as:

$$\mu_{sw} = n_f \rho_{sw} \tag{3.50}$$

where:

- $\rho_{sw} = \frac{A_{sw}}{s \cdot b_w}$ is the geometrical ratio of transversal tensile reinforcement with respect to concrete volume
- $n_f = \frac{f_y}{f_c}$ is the ratio between the yield strength of steel and the compressive strength of concrete, as previously defined, see (3.35).

Then, (3.50) can be written as

$$\mu_{sw} = n_f \frac{A_{sw}}{s \cdot b_w} \tag{3.51}$$

which shows that the reinforcement mechanical ratio gives information about the capacity of each structural element within the representative distance[5].

In the optimization function later defined, μ_{sw} is an independent variable, such as ζ, but the limits of the mechanical transverse reinforcement ratio depend on the aspect ratio, as shown in the following.

Eq. (3.51) can be expressed as a function of ζ

$$\mu_{sw} = n_f \frac{A_{sw}}{z \cdot b_w} \cdot \zeta \tag{3.52}$$

If the quantities n_f, A_{sw}, z, b_w in (3.52) are constant, the value of μ_{sw} changes according to ζ. Particularly, if the value of s increases, the value of μ_{sw} decreases, since the same amount of transversal reinforcement refers to a longer representative length. Also note that the value of μ_{sw} does not depend on z, see(3.52), since the reinforcement ratio is constant along the depth of the cross section.

[5] Note that the length of the representative distance, L_{rs}, is equal to s.

Starting from these remarks, the range of variation of μ_{sw} has to be defined according to the values of ζ: in fact, the same amounts of reinforcement, expressed as functions of maximum and minimum diameters of steel bars, give different reinforcement ratios as the value of ζ changes.

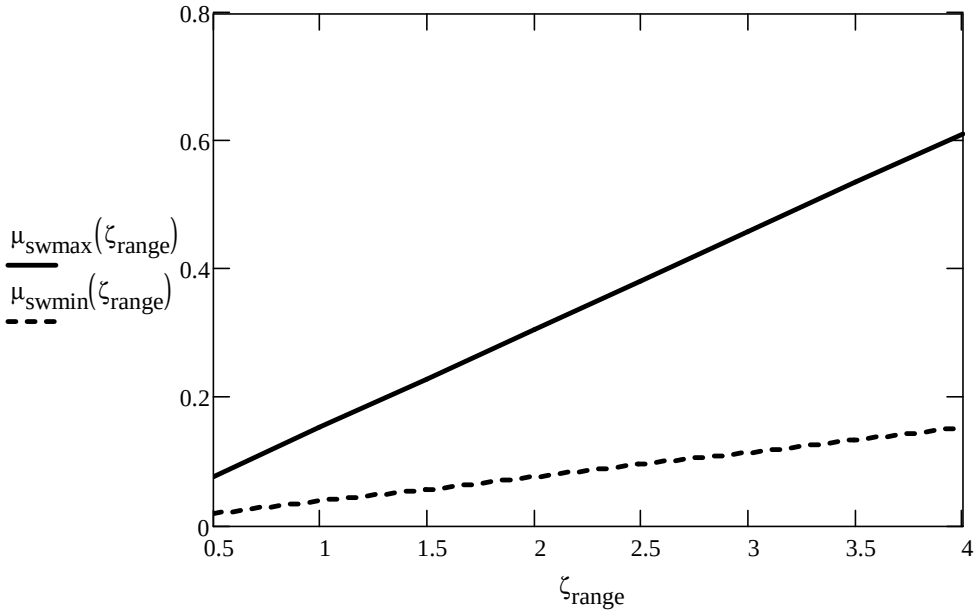

Figure 8. Range of variation of μ_{sw}. The dashed line represents the lower bound, while the solid line represents the upper bound, both expressed as a function of ζ.

Referring to Figure 8, the values $\mu_{sw\_\min}$ and $\mu_{sw\_\max}$ have been defined as follows:

$$\mu_{sw\_\min}(\zeta) = n_f \frac{\pi}{2} \frac{\phi_{\min}^2}{z \cdot b_w} \zeta \tag{3.53}$$

$$\mu_{sw\_\max}(\zeta) = n_f \frac{\pi}{2} \frac{\phi_{\max}^2}{z \cdot b_w} \zeta \tag{3.54}$$

where, according to the most common geometrical and mechanical characteristics of these beam, the values of $\phi_{\min}$ and $\phi_{\max}$ have been taken equal to $12mm$ and $24mm$, respectively.

The graph in Figure 8 shows that the range of variation of μ_{sw} becomes wider as the value of ζ increases. A useful key to understanding the graph is by considering that along the x axis the value of s decreases. It allows relating the area of steel to the area of concrete in the representative distance $b_w \cdot s$.

Given the relationship between the value of ζ and the range of variation of μ_{sw}, it is also possible to establish the inverse relationship, by expressing the bounds of ζ as functions of the value of μ_{sw}:

$$\zeta_{\min}(\mu_{sw}) = \frac{2}{\pi} \cdot \frac{\mu_{sw}}{\phi_{\max}^2} \cdot \frac{b_w \cdot z}{n_f} \tag{3.55}$$

$$\zeta_{\max}(\mu_{sw}) = \frac{2}{\pi} \cdot \frac{\mu_{sw}}{\phi_{\min}^2} \cdot \frac{b_w \cdot z}{n_f} \tag{3.56}$$

So the following condition can be set:

$$\zeta_{\min}(\mu_{sw}) \le \zeta \le \zeta_{\max}(\mu_{sw}) \tag{3.57}$$

This condition will be used in the optimization function, to be defined at a subsequent stage.

3.4.4 Limits for considering compressed concrete elements

The angles θ_R and θ_S are dependent variables, since their values depend on both α and ζ.

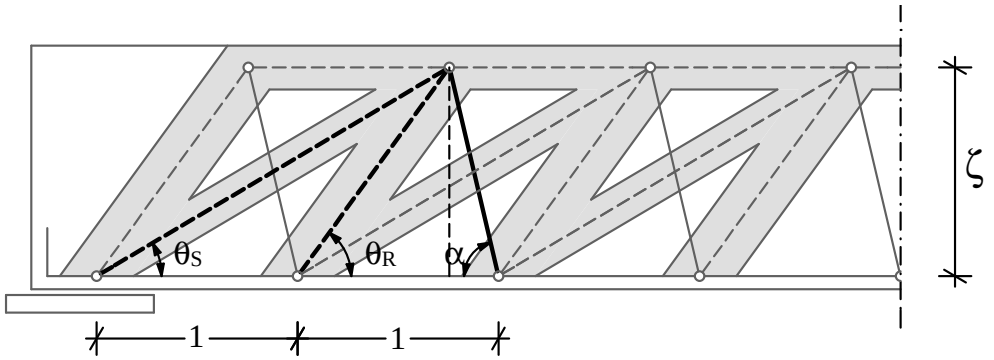

Figure 9. Angles θ_R and θ_S

Referring to Figure 9, the following relations hold:

$$\zeta\left(\cot\theta_R+\cot\alpha\right)=1\Rightarrow\cot\theta_R=\frac{1}{\zeta}\left(1-\zeta\cot\alpha\right)\Rightarrow$$
$$\theta_R\left(\alpha,\zeta\right)=\operatorname{acot}\left(\frac{1}{\zeta}-\cot\alpha\right) \tag{3.58}$$

$$2\zeta\cot\theta_R+\zeta\cot\alpha=\zeta\cot\theta_S\Rightarrow$$

referring to the previous expression:

$$\zeta\cot\theta_S=2\left(1-\zeta\cot\alpha\right)+\zeta\cot\alpha\Rightarrow\zeta\cot\theta_S=2-\zeta\cot\alpha\Rightarrow \tag{3.59}$$
$$\cot\theta_S=\left(\frac{2}{\zeta}-\cot\alpha\right)\Rightarrow$$
$$\theta_S\left(\alpha,\zeta\right)=\operatorname{acot}\left(\frac{2}{\zeta}-\cot\alpha\right)$$

Since θ_R and θ_S are dependent variables, also their range of variation has to depend on both α and ζ.

The bounds of the angles of the compressive elements have been evaluated taking into account the limitation imposed on θ [6] by the National Code (NTC2008) [5], while adding the further consideration that , due to the observed geometrical dependence, the maximum and minimum values of θ_R and θ_S have been defined in terms of α, as follows:

$$1-\cot\alpha \le \cot\theta \le 3{,}5-\cot\alpha \tag{3.60}$$

For the purpose of the analysis, the following functions have been introduced:

$$\theta_{\sup}(\alpha,\zeta) = \operatorname{acot}(1-\cot\alpha) \tag{3.61}$$

$$\theta_{\inf}(\alpha,\zeta) = \operatorname{acot}(3{,}5-\cot\alpha) \tag{3.62}$$

$$H_{\theta R}(\alpha,\zeta) = \theta_{R\_\inf}(\alpha,\zeta) \le \theta_R(\alpha,\zeta) \le \theta_{R\_\sup}(\alpha,\zeta) \tag{3.63}$$

$$H_{\theta S}(\alpha,\zeta) = \theta_{S\_\inf}(\alpha,\zeta) \le \theta_S(\alpha,\zeta) \le \theta_{S\_\sup}(\alpha,\zeta) \tag{3.64}$$

So the geometry equations, which include the bounds, become:

$$\theta_{RH}(\alpha,\zeta) = \theta_R(\alpha,\zeta)\cdot H_{\theta R}(\alpha,\zeta) \tag{3.65}$$

$$\theta_{SH}(\alpha,\zeta) = \theta_S(\alpha,\zeta)\cdot H_{\theta S}(\alpha,\zeta) \tag{3.66}$$

The following graphs, see Figure 10, Figure 11, Figure 12, show the results of the parametric analysis carried out to evaluate the geometrical conditions that allow considering the compressive elements as part of the

[6] θ refers to the angle of the strut, within the framework of the variable angle strut. Note in NTC2008 that the lower bound of 1 has to do with the representative de Saint Venant length (which has to equal at least the depth), while the upper bound of 2.5 has to do with the lowest angle by which the compressed element is deemed to be contributing to the shear capacity.

structural model. Each graph refers to a specific value of the aspect ratio, ζ, and shows:

- the limits set by the National Code (NTC2008), represented with grey horizontal straight lines;
- the new limits introduced by this study: the lower and upper bounds are represented by the dashed black curves;
- the values of $\cot\theta_S$, along the black line;
- the values of $\cot\theta_R$, along the black dashed line.

The first graph in Figure 10 refers to $\zeta = 0{,}5$ and shows that the contribution of the concrete strut cannot be taken into account. The contribution of the rod, instead, can be considered for $\alpha \geq 45°$.
It means that also the rod cannot be considered in the structural model.

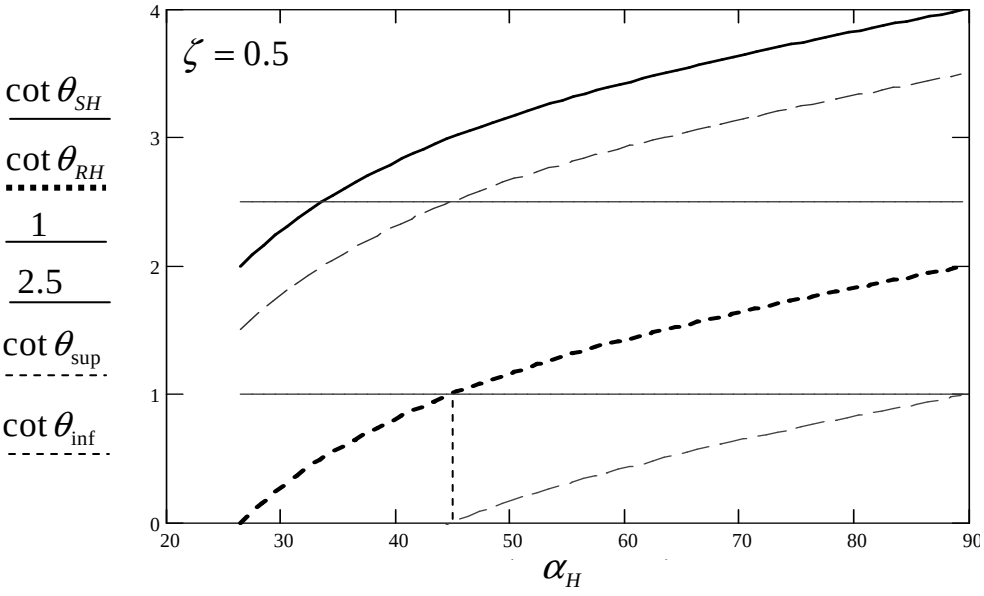

Figure 10. Limits for considering compressed struts, $\zeta = 0{,}5$

The second graph in Figure 11, instead, concerns the case of $\zeta = 1$. It shows that both the strut and the rod are part of the mechanical model for all the admissible values of α, see Figure 7.

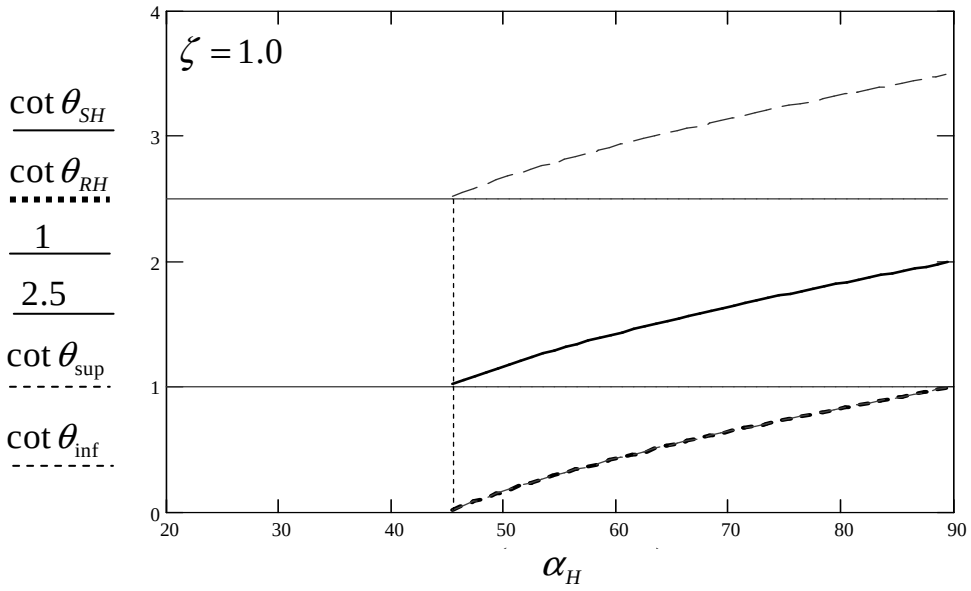

Figure 11. Limits for considering compressed struts, $\zeta = 1$

The third graph in Figure 12 deals with $\zeta = 1{,}5$ and displays that just the strut can be considered in the mechanical model if $\alpha \geq 73°$approx. for all the admissible values of α. Note that, by considering the bounds of the National Code, the contribution of the rod should have been ignored.

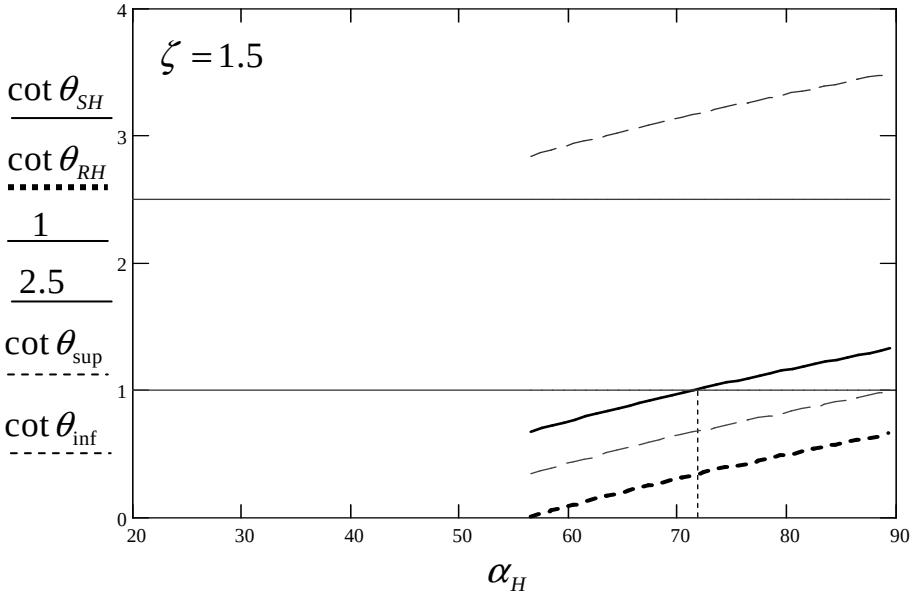

Figure 12. Limits for considering compressed struts, $\zeta = 1{,}5$

On the basis of the results of the parametric analysis above, some considerations about the mechanical model have been carried out.

Starting from $\zeta = 1{,}5$, the contribution of the concrete part of the rod should not be considered in the mechanical model, since the cotangent of its angle is smaller than 1.

Referring to Figure 13, note that the rod is made up of two steel bars and of the concrete included between them.

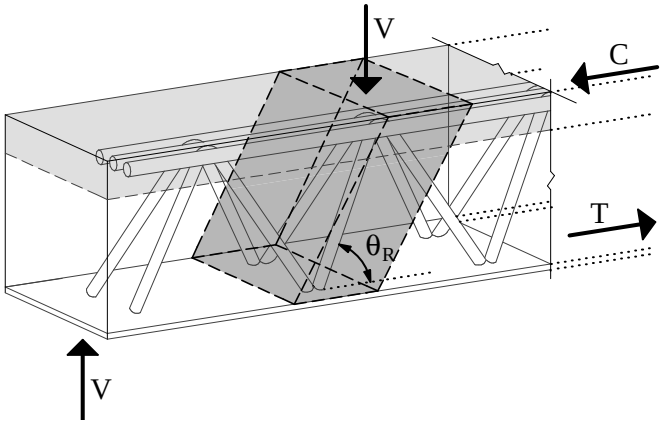

Figure 13. Geometry of the concrete rod.

The strain of the steel rods, which are always part of the mechanical model apart from the value of the angle θ_R, involves the concrete component as a resistance element of the model. So it seems appropriate to consider just the upper bound of the condition (3.63).

3.4.5 Mechanical transverse reinforcement ratio

The mechanical transverse reinforcement ratio has been evaluated by referring separately to the tension and compression web steel bars.

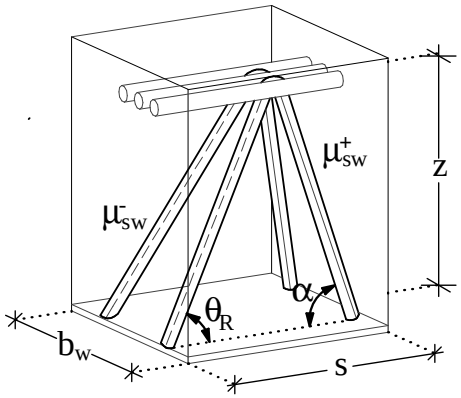

Figure 14. Tension and compression web reinforcement

The reinforcement mechanical ratio is evaluated referring to the volumes of concrete and steel and to their respective strength. So, referring to the tension steel bars, it can be expressed as follows:

$$\mu_{sw}^{+} = \frac{f_y \cdot A_{sw}}{f_c \cdot z \cdot b_w \cdot s} \cdot \frac{z}{\sin\alpha} = \frac{f_y \cdot A_{sw}}{f_c \cdot b_w \cdot s} \cdot \frac{1}{\sin\alpha} \tag{3.67}$$

where α is the angle of the tension bars.

The reinforcement mechanical ratio of compression bars, as well, can be expressed as:

$$\mu_{sw}^{-} = \frac{f_y \cdot A_{sw}}{f_c \cdot b_w \cdot s \cdot z} \cdot \frac{z}{\sin\theta} = \frac{f_y \cdot A_{sw}}{f_c \cdot b_w \cdot s} \cdot \frac{1}{\sin\theta} \tag{3.68}$$

where θ is the angle of compression steel bars.

Thus, the overall transverse reinforcement mechanical ratio, including both tension and compression bars, can be expressed as:

$$\mu_{sw}^{TOT} = \mu_{sw}^{+} + \mu_{sw}^{-} = \frac{f_y A_{sw}}{f_c b_w s} \cdot \left(\frac{1}{\sin\alpha} + \frac{1}{\sin\theta} \right) \tag{3.69}$$

Referring to (3.67) and (3.68), the following relation holds:

$$\mu_{sw}^{-} = \mu_{sw}^{+} \frac{\sin\alpha}{\sin\theta_R} \tag{3.70}$$

Thus, the overall mechanical transverse reinforcement ratio, μ_{sw}^{TOT} can be expressed as a function of μ_{sw}^{+}:

$$\mu_{sw}^{TOT} = \mu_{sw}^{+} \cdot \left(1 + \frac{\sin\alpha}{\sin\theta_R} \right) \tag{3.71}$$

Note that the equation for evaluating the mechanical transverse reinforcement ratio is usually given as:

$$\mu_{sw} = \frac{f_y A_{sw}}{f_c b_w s} \tag{3.72}$$

It still represents the ratio between the volumes of steel and concrete, weighted by their respective strength, but for the specific and most common case of just tensile reinforcement and $\alpha = 90°$.
Given the above, (3.69) can be expressed as:

$$\mu_{sw}^{TOT} = \mu_{sw}^{+} + \mu_{sw}^{-} = \mu_{sw} \cdot \left(\frac{1}{\sin\alpha} + \frac{1}{\sin\theta} \right) \tag{3.73}$$

The graph in Figure 15 shows the variation of the ratio $\mu_{sw}^{TOT} / \mu_{sw}$ by changing the value of α within the admissible range for each ζ. The

curves prove that the reinforcement mechanical ratio evaluated referring to the angles changes its value according to the different length of the steel bars. This consideration confirms that the mechanical reinforcement ratio must be evaluated referring to the volumes of structural materials.

Moreover, the graph in Figure 16 shows the variation of the ratio $\mu_{sw}^{TOT} / \mu_{sw}^{+}$ according to the value of α. By increasing the value of the angle of tensile bars, which means by decreasing θ_R for each ζ, the amount of reinforcement devoted to resist tensile stresses decreases and the compressive one increases. So the function $\mu_{sw}^{TOT} / \mu_{sw}^{+}$ always has an increasing trend.

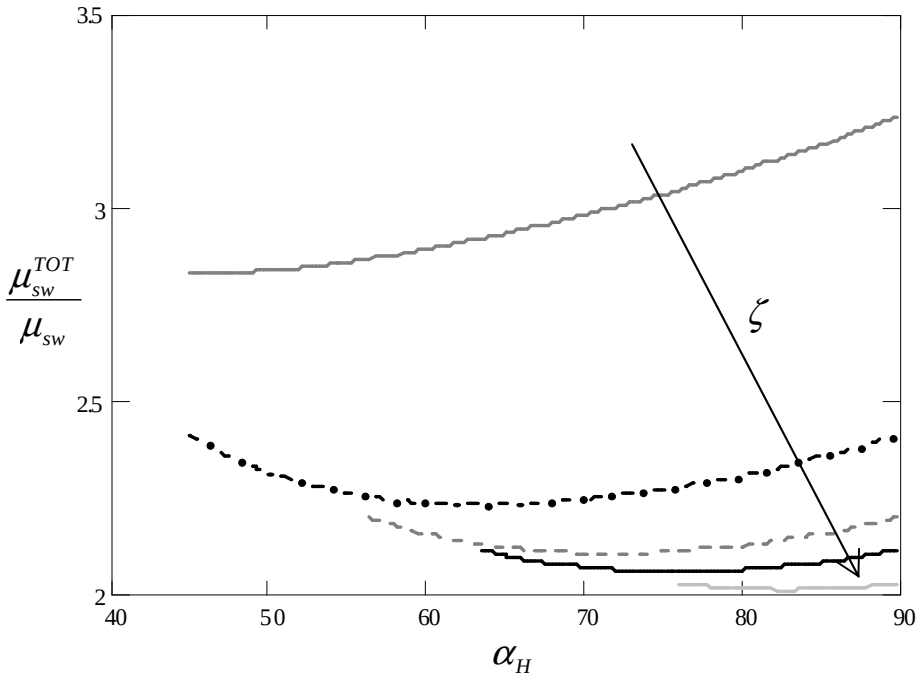

Figure 15. Ratio $\mu_{sw}^{TOT} / \mu_{sw}$

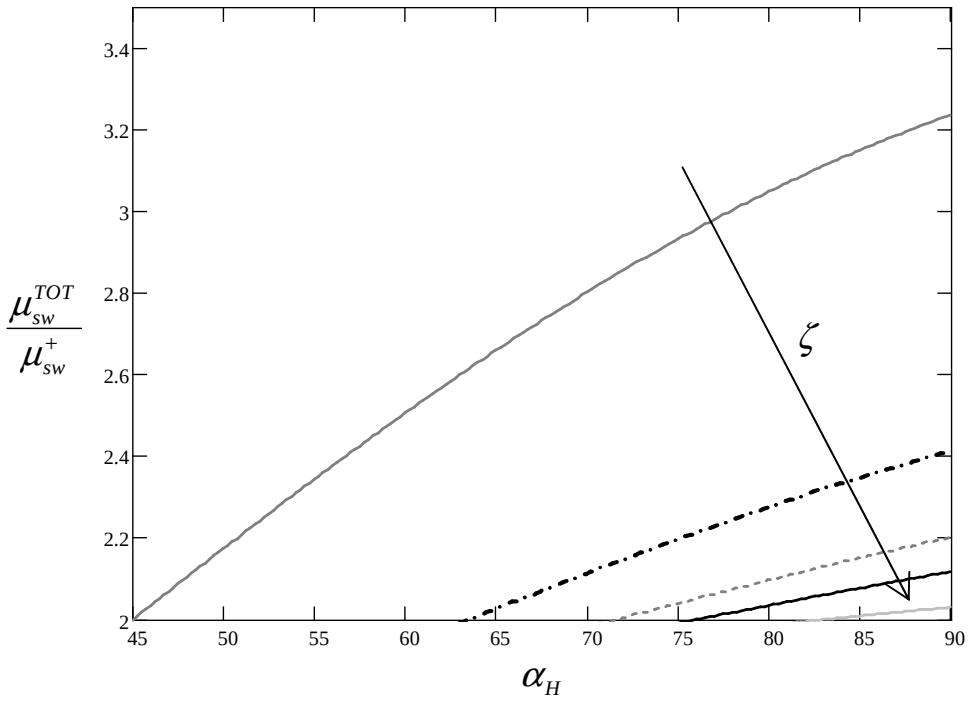

Figure 16. Ratio $\mu_{sw}^{TOT} / \mu_{sw}^{+}$

3.5 Lateral buckling

For the evaluation of the optimal shape of the truss, the resistance of the rod has been evaluated referring to the compressive strength of the composite cross section and to the lateral buckling resistance.

According to the formulation of the National Code [5] the following condition has to be met:

$$\chi = \frac{1}{\phi + \sqrt{\phi^2 - \overline{\lambda}^2}} \leq 1 \tag{3.74}$$

where ϕ is defined as:

$$\phi = 0,5\left[1+\alpha\left(\overline{\lambda}-0,2\right)\right)+\overline{\lambda}^2\Big] \tag{3.75}$$

where α is a factor related to the imperfections of the structural elements, and according to the Table 4.2.VI [5] has been considered equal to $0,49$ and $\overline{\lambda}^2$ can be evaluated as follows:

$$\overline{\lambda}^2 = \frac{N_{pl,RK}}{N_{cr}} \tag{3.76}$$

where $N_{pl,RK}$ and N_{cr} are, respectively, the compressive force related to the strength of the composite cross-section and the Euler's critical load:

$$N_{pl,RK} = A_{sw}\cdot f_y + 0,85\cdot f_c \cdot b_w \cdot s \tag{3.77}$$

$$N_{cr} = \frac{\pi^2 \left(EJ\right)_{eff}}{l_0^2} \tag{3.78}$$

The quantities A_{sw}, f_y, f_c, b_w, s have been defined previously, see Table 1. $\left(EJ\right)_{eff}$ is the bending stiffness of the cross section, accounting for second order effects. According to [5], it has been evaluated as follows:

$$\left(EJ\right)_{eff,II} = k_0\left(E_s J_B + k_{e,II} E_{cm} J_R\right) \tag{3.79}$$

where $k_0 = 0,9$, $k_{e,II} = 0,57$, J_B and J_R are the inertia moments of steel and concrete components of the rod, respectively. In detail:

[7] Note that $k_{e,II}E_{cm} = \frac{f_c}{\varepsilon_c}$, where $\varepsilon_c = 0,2\%$

$$J_B = A_{sw} \cdot \frac{\phi_B^2}{32} \tag{3.80}$$

$$J_R = \frac{1}{8} \cdot \frac{b_w^3 \cdot s}{12} \tag{3.81}$$

Note that J_R has been evaluated referring to the rod cross-section area of each web bar and the width of the cross section, $b_w / 2$, has been considered as the minor axis of inertia.
By substituting (3.79), (3.80) and (3.81) in (3.78), N_{cr} can be expressed as:

$$N_{cr} = \left(\frac{\pi}{\beta_0 l}\right)^2 k_0 \left[E_s A_{sw} \frac{\phi_B^2}{32} + \frac{f_c}{E_c} \cdot \frac{1}{8} \cdot \frac{b_w^3 s}{12} \right] = \left(\frac{\pi \sin\theta_R}{\beta_0 z}\right)^2 k_0 \left[\frac{f_y}{E_y} A_{sw} \frac{\phi_B^2}{32} + \frac{f_c}{E_c} \cdot \frac{1}{8} \cdot \frac{b_w^3 s}{12} \right] \tag{3.82}$$

By normalizing for $f_c b_w s$, both $N_{pl,RK}$ and N_{cr}, $\overline{\lambda}^2$ can be expressed as:

$$\overline{\lambda}^2 = \frac{\mu_{sw} + 0{,}85}{\left(\frac{\pi \sin\theta_R}{\beta_0 z}\right)^2 k_0 \left[\frac{1}{\varepsilon_y} \mu_{sw} \frac{\phi_B^2}{32} + \frac{1}{\varepsilon_c} \cdot \frac{1}{8} \cdot \frac{b_w^2}{12} \right]} \tag{3.83}$$

where

$$\mu_{sw} = \frac{f_y A_{sw}}{f_c b_w s} \tag{3.84}$$

Moreover, by introducing the following relations

$$\varepsilon_y = \varepsilon_c = \varepsilon_{\lim} \text{ and } \phi_B = \varphi_B \cdot s \tag{3.85}$$

the Eq. (3.84) can be written as:

$$\overline{\lambda}^2 = \frac{\mu_{sw} + 0{,}85}{\left(\frac{\pi \sin\theta_R}{\beta_0 \zeta s}\right)^2 \frac{k_0}{\varepsilon_{\lim}}\left[\mu_{sw}\frac{\varphi_B^2 s^2}{32} + \frac{1}{8}\cdot\frac{b_w^2}{12}\right]} = \frac{\mu_{sw} + 0{,}85}{\left(\frac{\pi \sin\theta_R}{\beta_0 \zeta}\right)^2 \frac{k_0}{\varepsilon_{\lim}}\left[\mu_{sw}\frac{\varphi_B^2}{32} + \frac{1}{8}\cdot\frac{b_w^2}{12s^2}\right]} = \frac{\mu_{sw} + 0{,}85}{\left(\frac{\pi}{\beta_0}\right)^2 \frac{k_0}{32\cdot\varepsilon_{\lim}}\left[\mu_{sw}\varphi_B^2 + \frac{1}{3}\cdot\frac{b_w^2}{s^2}\right]} \cdot \frac{\zeta^2}{\sin^2\theta_R} = \tag{3.86}$$

The following condition is laid down:

$$\beta_w = \frac{b_w}{s} = \frac{\zeta \cdot b_w}{z} \tag{3.87}$$

Then, the Eq. (3.86) becomes

$$\overline{\lambda}^2 = \frac{\mu_{sw} + 0{,}85}{\left(\frac{\pi}{4\beta_0}\right)^2 \frac{k_0}{2\cdot\varepsilon_{\lim}}\left[\mu_{sw}\varphi_B^2 + \frac{1}{3}\cdot\beta_w^2\right]} \cdot \frac{\zeta^2}{\sin^2\theta_R} \Rightarrow$$
$$\overline{\lambda} = \frac{4\beta_0}{\pi}\sqrt{\frac{2\cdot\varepsilon_{\lim}}{k_0}}\sqrt{\frac{\mu_{sw} + 0{,}85}{\left[\mu_{sw}\varphi_B^2 + \frac{1}{3}\cdot\beta_w^2\right]}} \cdot \frac{\zeta}{\sin\theta_R} \tag{3.88}$$

The lateral buckling phenomenon depends on the real dimensions of the structural element, and this issue must be taken into account for parametrical analyses. For this purpose, the dimensionless parameter φ_B, see (3.89) has been defined:

$$\varphi_B = \frac{\phi_B}{s} = \frac{\phi_B \cdot \zeta}{z} \Rightarrow \frac{1}{\varphi_B} = \frac{z}{\phi_B \cdot \zeta} \tag{3.89}$$

It represents the inverse of the steel bar's slenderness, expressed as the ratio between the diameter ϕ_B and the bar spacing s. A useful key to the reading is by expressing $s = z/\zeta$: since the value of z is constant, the slenderness of the bar increases when ϕ_B or the aspect ratio ζ decreases, that means by increasing the value of s.

In order to analyze the phenomenon of lateral buckling, a preliminary analysis about the range of variation of φ_B has been carried out, see Figure 17 and Figure 18. For assigning the values of s the following vector has been defined:

$$s_{pl} = [0,2 \quad 0,3 \quad 0,4 \quad 0,5 \quad 0,6]\,m \tag{3.90}$$

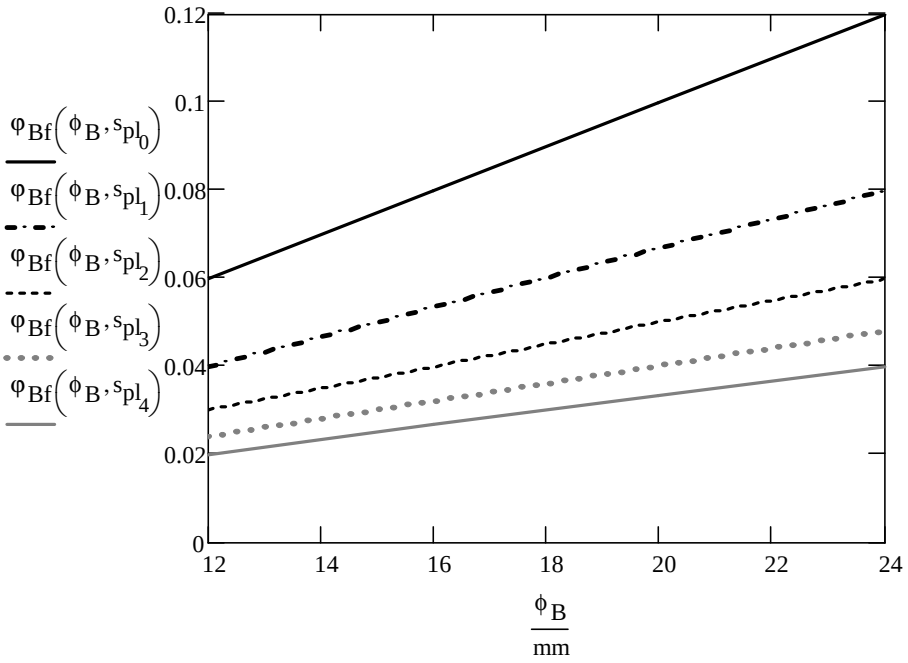

Figure 17. Range of variation of φ_B (1)

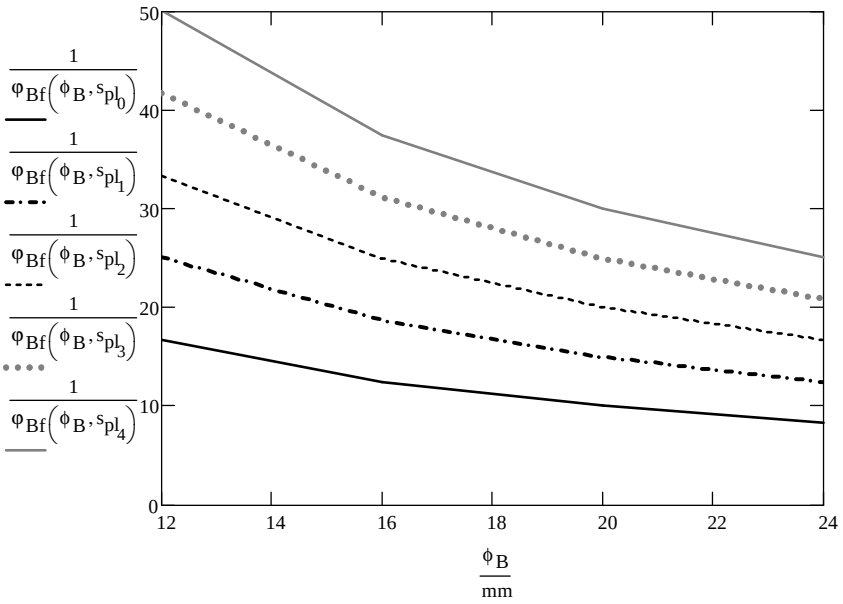

Figure 18. Range of variation of φ_B (2)

The graph in Figure 17 shows that the value of φ_B varies within the range $0,02-0,12$. Note that the bounded cases refer to unlikely pairs of $\phi_B - s$ values in real structures: the lower bound value deals with $\phi_B = 12mm$, $s = 600mm$ and the upper one with $\phi_B = 24mm$, $s = 200mm$.

The physical meaning of the function φ_B is shown in Figure 18, which shows that the value of the slenderness of the bar decreases as the value of the diameter increases, for each value of s.

On the basis of these results, the following analysis has been conducted referring to a mean value of $\varphi_B = 0,05$.

As stated in the previous, the condition (3.74) must be met to satisfy the verification of compressive bars for lateral buckling. Referring to (3.74) and(3.75), χ depends only on $\overline{\lambda}$.

The formula (3.88) shows that, by assigning the values of $\beta_0 = 0,8$ [8], $k_0 = 0,9$ (see above) and $\varepsilon_{\lim} = 0,2\%$ the value of $\bar{\lambda}$ changes according to ζ φ_B and α, since $\theta_R(\alpha, \zeta)$.

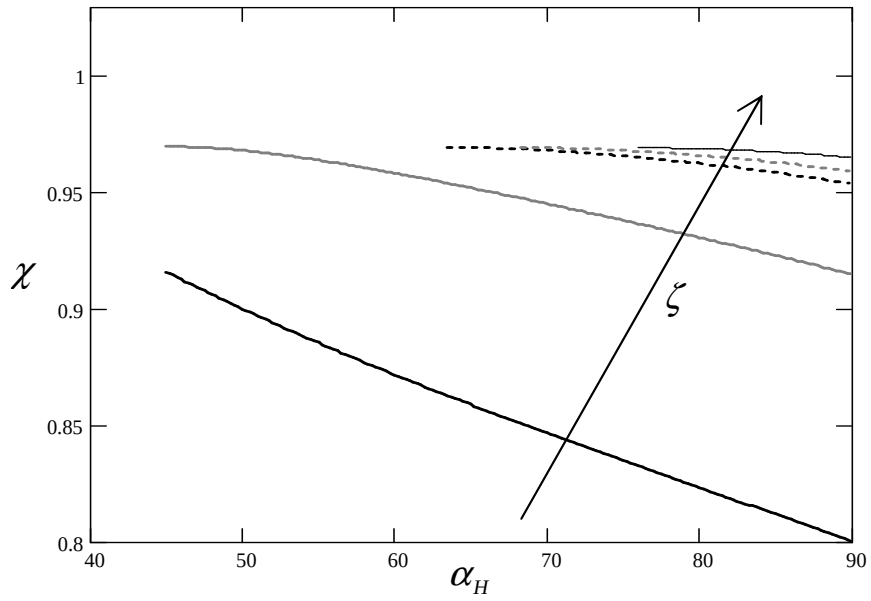

Figure 19. Limits of variation of χ

The graph above shows that the condition (3.74) is always met for all the admissible geometrical conditions. Note that the range of variation of α depends on ζ, see (3.48) and (3.49), whose range of values is (3.47).

Note that the mechanical transverse reinforcement ratio μ_{swTOT} in Figure 19 refers to the overall mechanical reinforcement ratio, see (3.69).

[8] From the analysis of experimental results [26]

3.6 Shear demand

In agreement with Eurocode 8 and NTC2008, the design shear demand, V_D, shall be determined according to capacity design rules, referring to the beam equilibrium under the following loads: the transverse (vertical) load coming from the seismic loading combination and the end bending moments $M_{i,d}$ (the subscript $i=1,2$ refers to the end sections of the beam), corresponding to plastic hinges formation for positive and negative directions of seismic loading.

In detail, see Figure 20, at the end section i, two values of the acting shear force should be evaluated, i.e. the maximum $V_{Ed,\max,i}$ and the minimum $V_{Ed,\min,i}$ corresponding to the maximum positive and the maximum negative end moments $M_{i,d}$, that can develop at ends 1 e 2 of the beam. End moments, $M_{i,d}$, may be evaluated as follows:

$$M_{i,d} = \gamma_{rd} M_{Rb,i} \tag{3.91}$$

where

- γ_{Rd} is the factor accounting for possible overstrength due to steel strain hardening, which in the case of DCM (medium ductility level) beams may be taken equal to 1;
- $M_{Rb,i}$ is the design value of the beam moment of resistance at the end i in the sense of the seismic bending moment under the considered sense of the seismic action; [65]

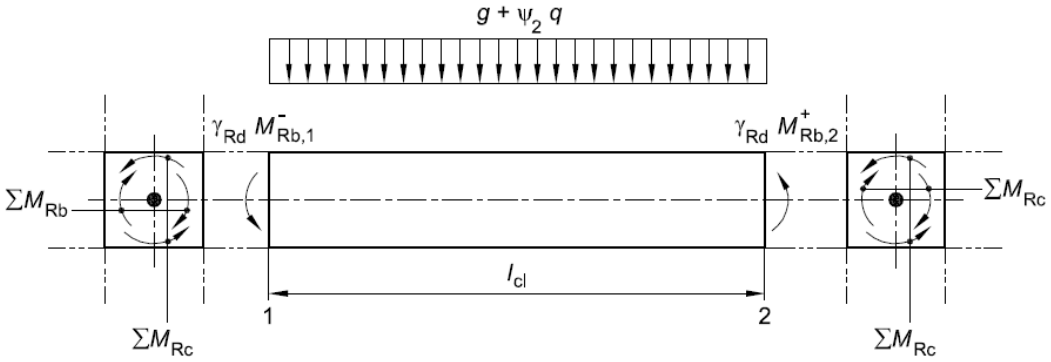

Figure 20. Capacity design values of shear forces on beams [65]

So, the shear demand shall be calculated as follows:

$$V_D = g + \psi_2 q + \frac{\gamma_{Rd}}{l_{cl}}\left(M^{-}_{Rb,1} + M^{+}_{Rb,2}\right) \tag{3.92}$$

For the purpose of evaluating the value of dynamic loads affecting the shear demand, bending moments coming from the dynamic combination of actions have been expressed as function of the bending moments coming from static loads. The static and dynamic combinations of actions are respectively:

$$\gamma_G G_k + \gamma_Q Q_k = w \tag{3.93}$$

$$G_k + \psi_2 Q_k + E = w_E \tag{3.94}$$

where:

- G_k is the characteristic permanent action;
- Q_k is the characteristic variable action;
- E is the effect of seismic actions;
- $\gamma_G = 1{,}3$ is the partial factor for permanent actions;
- $\gamma_Q = 1{,}5$ is the partial factor for variable actions;

- $\psi_2 = 0,3$ is the factor defining the representative values of variable actions for quasi-permanent loads.

Referring to (3.93) and (3.94), the overall factors for static and dynamic load combinations can be considered equal to $1,5$ and 1, respectively, so the following equality holds:

$$w = 1,5 w_E \tag{3.95}$$

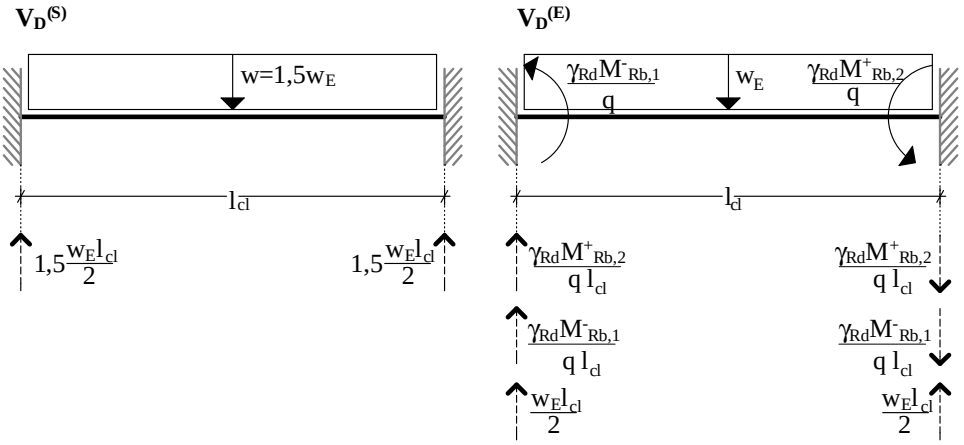

Figure 21 Shear demand

The design values of the bending resistance moment are:

$$M_{Rd}^{(S)} = \gamma_{Rd} \cdot 1,5 \cdot \frac{w_E l_{cl}^{\ 2}}{12} \tag{3.96}$$

$$M_{Rd}^{(E)} = \frac{w_E l_{cl}^{\ 2}}{12} + \frac{\gamma_{Rd}}{q} \max\left(M_{Rb,1}^{-}, M_{Rb,2}^{+}\right) \tag{3.97}$$

where $\gamma_{Rd} = 1,35$ and q is the structure factor, which may fall in the range $1,5$ to $4,5$.

The design values of the resistance of the composite section to vertical shear are:

$$V_{Rd}^{(S)} = V_D^{(S)} = \gamma_{Rd} \cdot 1,5 \cdot \frac{w_E l_{cl}}{2} \tag{3.98}$$

$$V_{Rd}^{(E)} = V_D^{(E)} = \frac{w_E l_{cl}}{2} + \frac{\gamma_{Rd}}{q \cdot l_{cl}} \left(M_{Rb,1}^{-} + M_{Rb,2}^{+} \right) \tag{3.99}$$

By setting the following relation:

$$M_{Rb,1}^{-} + M_{Rb,2}^{+} = \alpha \frac{w_E l_{cl}^{\ 2}}{12} \tag{3.100}$$

it is possible to express the condition by which the value of shear demand due to dynamic loads is larger than the static one.

$$\begin{gathered} V_D^{(E)} > V_D^{(S)} \Leftrightarrow \frac{w_E l_{cl}}{2} + \frac{\gamma_{Rd}}{q \cdot l} \alpha \frac{w_E l_{cl}^{\ 2}}{12} > \gamma_{Rd} \cdot 1,5 \cdot \frac{w_E l_{cl}}{2} \Rightarrow \\ \gamma_{Rd} \frac{\alpha}{6 \cdot q} + 1 > \gamma_{Rd} 1,5 \Rightarrow \alpha > 4,5 \cdot q \end{gathered} \tag{3.101}$$

Under the hypothesis

$$M_{Rb,1}^{-} = M_{Rb,2}^{+} = M_e \Rightarrow M_e = \frac{\alpha}{2} \cdot \frac{w_E l^2}{12} \tag{3.102}$$

$$M_{Rd}^{(E)} = \frac{w_E l_{cl}^2}{12} + \frac{\gamma_{Rd}}{q} \cdot \frac{\alpha}{2} \cdot \frac{w_E l_{cl}^2}{12} \tag{3.103}$$

$$\begin{gathered} M_{Rd}^{(E)} > M_{Rd}^{(S)} \Leftrightarrow \frac{w_E l_{cl}^2}{12} + \frac{\gamma_{Rd}}{q} \cdot \frac{\alpha}{2} \cdot \frac{w_E l_{cl}^2}{12} > \gamma_{Rd} \cdot 1,5 \cdot \frac{w_E l_{cl}^{\ 2}}{12} \Rightarrow \\ 1 + \frac{\gamma_{Rd}}{2q} \cdot \alpha > \gamma_{Rd} \cdot 1,5 \Rightarrow \alpha > 1,52 \end{gathered} \tag{3.104}$$

The dimensionless shear demand for the parametrical analyses has been defined as follows:

$$\bar{v}_D = \frac{\mu_{sw}}{\sin\alpha} = \frac{f_y A_{sw}}{f_c b_w s} \cdot \frac{1}{\sin\alpha} = \mu_{sw}^{+} \tag{3.105}$$

The expression of μ_{sw} is defined in (3.72), which refers to the tensile bars whose angle is $\alpha = 90°$.

Chapter 4
Complete model

4.1 Introduction

This section deals with the construction of a parametric complete structural model of the CSCB, carried out by means the classical displacement method, able to describe the structural behavior of several types of beams, subjected to any kind of vertical load condition.

The developed model has been embedded in a worksheet capable to evaluate stresses and strains of the whole beam, the collapse load and the ductile or brittle behavior of the structure.
The aim is to verify the validity of the results of the simplified mechanical model shown in the previous Chapter.

4.2 Stiffness matrix

4.2.1 Displacement method of analysis

All structures must satisfy equilibrium of forces, compatibility of displacements and constitutive laws in order to ensure their safety. In case of statically indeterminate structures, there are two different methods to satisfy these requirements: the *force method* and the *displacement method*. The fist one is based on identifying the unknown redundant forces and then satisfying the structure's compatibility equations. To do that, all the displacements are expressed as functions of loads by using the load-displacement relations. The solution of these equations gives the redundant reactions and then the equilibrium equations allow determining the remaining reactions on the structure.
The *displacement method*, instead, requires satisfying equilibrium equations for the structure. So, the unknown displacements are written as functions of loads by using the constitutive laws. The solution of these equations gives the displacements. Then, the unknown loads are determined from the compatibility conditions, using the load-displacement equations. [2]

The equation which establish the relation between forces and displacement can be written, in its general form, as:

$$\sum_{j=1}^{\nu} k_{ij} u_j = F_i^{(n)} \qquad (i = 1....\nu) \tag{4.1}$$

$$[K] \cdot \{u\} = \{F^{(n)}\} \tag{4.2}$$

Referring to(4.1):

- k_{ij} are the stiffness coefficients: the subscripts refer, respectively, to the direction of the force i and the direction of the displacement j with respect to which the stiffness coefficient is evaluated;
- u_j is the displacement of the node, along the direction j;
- $F_i^{(n)}$ is the force applied to the node along the direction i. The superscript (n) refers to the n nodes of the structure.

The formula (4.2) has the same meaning of (4.1) but it is expresses by matrices.

So, the (4.1) imposes the equilibrium condition between external forces, which are known, and internal forces, which depend on stiffness and the displacement, for each node n.

The external forces set up the vector of the constant terms and the internal ones are expressed as functions of nodes' displacements and the stiffness matrix, K. Note that all the admissible displacements of the nodes represent the degrees of freedom (d.o.f.) of the structure.

Given the assumption of linear-elastic behavior of structure, each bar of the truss beam can be modeled like a spring, whose stiffness is k, subjected to forces at the ends that cause displacements.

4.2.2 Truss analysis using stiffness method

A standard procedure for determining the stiffness matrix of trusses is developed in the following.
Since the truss is composed of many members, the matrix of the overall structure can be considered as the result of the assembling of n the *member stiffness matrix*, see K_m in(4.3).
So, the first step is defining the stiffness matrix of the generic $m$bar in the local reference system (L.R.S.). This matrix defines the relationship between the displacement of the joints and the external forces.

$$f_M = K_l^m u_M \tag{4.3}$$

Note that, by imposing that the $i-th$ component of the vector u_M is equal to 1 and all the others are equal to 0, the vector of internal forces, f_M, is the $i-th$ column of the stiffness matrix K_l^m.

So, a useful method to evaluate the terms of the member matrix is assigning to one node from time to time a unit displacement, along one of the two directions in the L.R.S., and by imposing that all the other displacements are 0. It means that for each member, one node is held fixed and the other one is constrained with sliding support properly placed.
Such a system can be solved referring also to equilibrium conditions.
Moreover, the physical meaning of each term of the member stiffness matrix k_{ij} can be explained as follows: it represent the force at joint i when a unit displacement is imposed at joint j. So, if $i = j = 1$, then k_{11} is the force at the near joint when the far joint is held fixed and the near joint undergoes a displacement of $u = 1$.

For the generic element m, the procedure of construction of the member stiffness matrix is presented in the following. Note that the global reference system (G.R.S.) is (O, x, y) and the local one (L.R.S.) is (O, ξ, η), see Figure 1. For the sake of convention, the global coordinates will be considered positive x to the right and positive y upward. For the local ones, the same convention will be adopted.

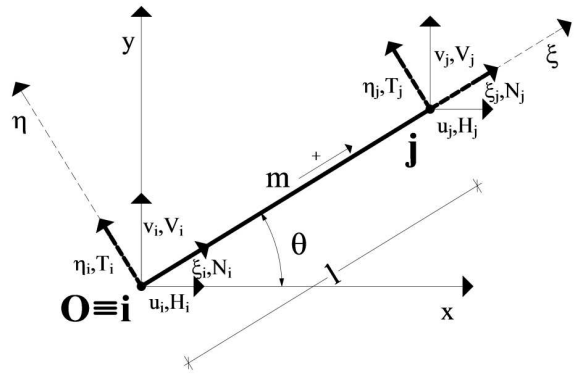

Figure 1. Element m: local and global reference system

First column

In order to obtain the fist column of the member stiffness matrix, the unit displacement has been assigned to the node i, along the direction ξ.
Then the following relations hold:

$$\xi_i = 1, \quad \eta_i = \xi_j = \eta_j = 0 \tag{4.4}$$

The bar m is compressive, and the magnitude of the axial force is:

$$N_i = \frac{EA}{l}\Delta l = \frac{EA}{l}\xi_i = \frac{EA}{l} \tag{4.5}$$

By imposing the equilibrium condition, it is possible to evaluate the value of all the forces in m caused by the displacement $\xi_i = 1$. The relationship between forces and displacement represents just the constitutive law.

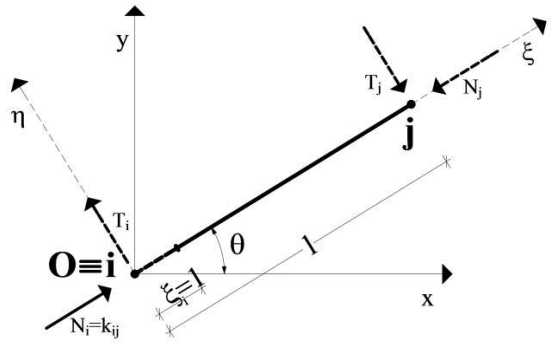

Figure 2. First column

$$N_i = K_{ij} \cdot \xi_A = \frac{EA}{l} \cdot 1 = -N_j$$
$$T_i = T_j = 0 \tag{4.6}$$

The results of the expression (4.6) represent the terms of the first columns of the matrix K_m in the L.R.S., see (4.7).

$$\begin{matrix} \xi_i \\ \eta_i \\ \xi_j \\ \eta_j \end{matrix} \begin{bmatrix} \frac{EA}{l} \\ 0 \\ -\frac{EA}{l} \\ 0 \end{bmatrix} \tag{4.7}$$

Second column

In order to evaluate the terms of the second column, the displacement $\eta_i = 1$ has been imposed to the node i.

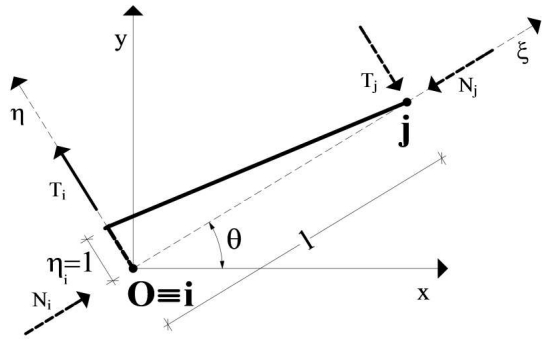

Figure 3. Second column

$$N_i = K_{ij} \cdot \xi_i = \frac{EA}{l} \cdot 1 = -N_j = 0$$
$$T_i = T_j = 0 \tag{4.8}$$

Under the hypothesis of small displacement, all the forces are equal to 0.

$$N_i = N_j = T_i = T_j = 0 \tag{4.9}$$

Then:

$$\begin{matrix} \xi_i \\ \eta_i \\ \xi_j \\ \eta_j \end{matrix} \begin{bmatrix} 0 \\ 0 \\ 0 \\ 0 \end{bmatrix} \tag{4.10}$$

Third column

For the third column, the displacement $\zeta_j = 1$ has been imposed to the node j.

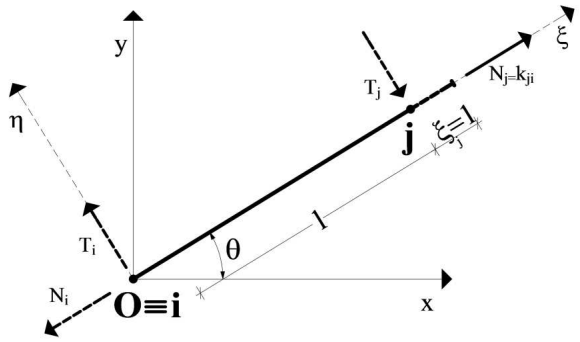

Figure 4. Third column

$$N_j = K_{ji} \cdot \xi_j = \frac{EA}{l} \cdot 1 = -N_i$$
$$T_i = T_j = 0 \tag{4.11}$$

Then:

$$\begin{matrix} \xi_i \\ \eta_i \\ \xi_j \\ \eta_j \end{matrix} \begin{bmatrix} -\frac{EA}{l} \\ 0 \\ \frac{EA}{l} \\ 0 \end{bmatrix} \tag{4.12}$$

Fourth column

The values of the fourth column have been evaluated by imposing the displacement $\eta_j = 1$

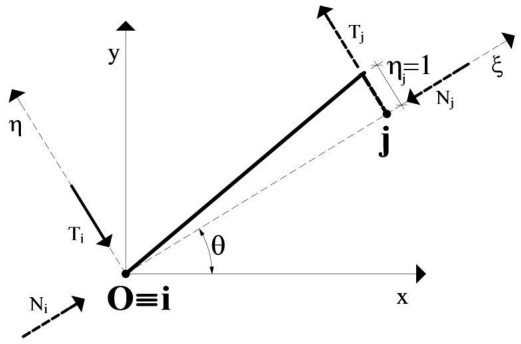

Figure 5. Fourth column

$$N_i = N_j = T_i = T_j = 0 \tag{4.13}$$

Then:

$$\begin{matrix} \xi_i \\ \eta_i \\ \xi_j \\ \eta_j \end{matrix} \begin{bmatrix} 0 \\ 0 \\ 0 \\ 0 \end{bmatrix} \tag{4.14}$$

Assembling the vectors above, allows obtaining the stiffness matrix of the single member not constrained, in the local reference system (O,ξ,η)

$$\left[K_l^M\right] = \frac{EA}{l}\begin{bmatrix} 1 & 0 & -1 & 0 \\ 0 & 0 & 0 & 0 \\ -1 & 0 & 1 & 0 \\ 0 & 0 & 0 & 0 \end{bmatrix} \tag{4.15}$$

Since the truss is composed of many members, in the following is developed a method for transforming the member forces and displacements defined in local coordinates to global coordinates. For this purpose, the coordinate system rotation matrix $[R]$ has been introduced.

Generally speaking, the rotation is a linear transformation which depends on the angle θ, see Figure 1, able to transform the vector (ξ,η) in the vector (x,y).

The rotation θ matrices for respectively counterclockwise and anti-counterclockwise rotation around the origin of axis, can be expressed the follows:

$$\begin{bmatrix} x \\ y \end{bmatrix} = \begin{bmatrix} \cos\theta & \sin\theta \\ -\sin\theta & \cos\theta \end{bmatrix} \begin{bmatrix} \xi \\ \eta \end{bmatrix}, \quad [R] = \begin{bmatrix} \cos\theta & \sin\theta \\ -\sin\theta & \cos\theta \end{bmatrix} \tag{4.16}$$

$$\begin{bmatrix} x \\ y \end{bmatrix} = \begin{bmatrix} \cos\theta & -\sin\theta \\ \sin\theta & \cos\theta \end{bmatrix} \begin{bmatrix} \xi \\ \eta \end{bmatrix}, \quad [R'] = \begin{bmatrix} \cos\theta & -\sin\theta \\ \sin\theta & \cos\theta \end{bmatrix} \tag{4.17}$$

Referring to the generic element m, the rotation from the local reference system to the global one can be expressed as follows:

$$\begin{bmatrix} \xi_i \\ \eta_i \\ \xi_j \\ \eta_j \end{bmatrix} = \begin{bmatrix} \cos\theta & \sin\theta & 0 & 0 \\ -\sin\theta & \cos\theta & 0 & 0 \\ 0 & 0 & \cos\theta & \sin\theta \\ 0 & 0 & -\sin\theta & \cos\theta \end{bmatrix} \begin{bmatrix} u_j \\ v_j \\ u_j \\ v_j \end{bmatrix} = \begin{bmatrix} R & 0 \\ 0 & R \end{bmatrix} \begin{bmatrix} u_i \\ v_i \\ u_j \\ v_j \end{bmatrix} \tag{4.18}$$

The formulation above can be concisely expressed as:

$$\begin{aligned} s_L &= Tu \\ f_L &= Tf \end{aligned} \qquad [T] = \begin{bmatrix} R & 0 \\ 0 & R \end{bmatrix} \tag{4.19}$$

$[T]$ is an orthogonal matrix, so $[T]^{-1} = [T]^T$. The stiffness matrix of the generic $i-th$ member in the global reference system can be expressed as:

$$f_l = K_l u_l \Rightarrow T^i f = K_l T^i u \Rightarrow f = T^{iT} K_l T^i u \Rightarrow K^i = T^{iT} K_l T^i \tag{4.20}$$

where:

$$u = \begin{bmatrix} 1 \\ 0 \\ 0 \\ 0 \end{bmatrix}$$

in order to taking into account only axial strains.
After a few counts, the stiffness matrix of member m in the global reference system (O, x, y), in case of anti-counterclockwise θ and counterclockwise rotation α respectively, becomes:

$$K_g^m = \frac{EA}{l} \begin{bmatrix} \cos^2\theta & \cos\theta\sin\theta & -\cos^2\theta & -\cos\theta\sin\theta \\ \cos\theta\sin\theta & \sin^2\theta & -\cos\theta\sin\theta & -\sin^2\theta \\ -\cos^2\theta & -\cos\theta\sin\theta & \cos^2\theta & \cos\theta\sin\theta \\ -\cos\theta\sin\theta & -\sin^2\theta & \cos\theta\sin\theta & \sin^2\theta \end{bmatrix} \tag{4.21}$$

$$K_g^m = \frac{EA}{l} \begin{bmatrix} \cos^2\alpha & \cos\alpha\sin\alpha & -\cos^2\alpha & -\cos\alpha\sin\alpha \\ \cos\alpha\sin\alpha & \sin^2\alpha & -\cos\alpha\sin\alpha & -\sin^2\alpha \\ -\cos^2\alpha & -\cos\alpha\sin\alpha & \cos^2\alpha & \cos\alpha\sin\alpha \\ -\cos\alpha\sin\alpha & -\sin^2\theta & \cos\alpha\sin\alpha & \sin^2\alpha \end{bmatrix} \tag{4.22}$$

The matrices above are singular[1] since, as stated in the previous, they refer to an unconstrained member, whose degree of freedom refers to the length variation. So, just one of the four components of displacement deals with the strain and the remaining three define displacements of rigid body.

[1] $\det K_l^m = 0$

Generally speaking, *member stiffness matrices* can be divided into four sub-matrices, whose order is equal to the degrees of freedom of each joint. For the subject matter case, the sub-matrix is a 2nd order one.
The mechanical meaning of each sub-matrix can be explained as follows: the matrices on the main diagonal, K_{uu}^{m} and K_{vv}^{m}, refer to the effects of the displacement of i or j node on the forces on the same node. Instead, the matrices out of the main diagonal, $K_{uv}^{m} = K_{vu}^{m} = \left[K_{vu}^{m} \right]^{T}$ consider the effects of the displacement of i or j node on F_j and Fi respectively.
Then, the (4.21) (or (4.22)) can be written as:

$$K^{m} = \begin{bmatrix} K_{uu}^{m} & \left(K_{uv}^{m}\right)^{T} \\ K_{vu}^{m} & K_{vv}^{m} \end{bmatrix} \tag{4.23}$$

The stiffness matrix of the overall structure, K_{TOT} ,is a square matrix $2n$-th order, where n represents the number of all the nodes of the structure, an2 2 is the number of degrees of freedom for each of them.
So the order of the matrix represents the number of the equilibrium equation and the number of the displacements (unknowns) of the unconstrained structure.

The matrix K_{TOT} can be divided in $2\text{x}2$ sub-matrices as well, each of which has the same meaning explained above speaking of the member stiffness matrix.

$$K_{TOT} = \begin{bmatrix} k_{11} & k_{12} & k_{13} & k_{14} \\ & k_{22} & k_{23} & k_{24} \\ & sym & k_{33} & k_{34} \\ & & & k_{44} \end{bmatrix} \tag{4.24}$$

The assembly process of matrix should be done element by element. The method is briefly developed in the following.
By naming each node of the structure with a capital letter, the stiffness coefficient k_{uu}^{A-m} represents the stiffness of the node A given by the bar m and the coefficient k_{uu}^{A-p} represents the stiffness of the node A given by the bar p and so on. Then, the overall coefficient k_{uu}^{A} is equal to the sum of the coefficients, with the same subscripts, of all the elements which converge in the same node A: if n members converge in the node A, k_{uu}^{A} will be made up of the sum of n terms. So, the k_{vv}^{A} can be found the same procedure. Ea
Referring to the coefficients out of the main diagonal, the same procedure allows obtaining the values of $k_{uv}^{A-m} = k_{vu}^{A-m}$ and $k_{uv}^{A-p} = k_{vu}^{A-p}$.

K_{TOT} is a singular matrix, since it refers to the unconstrained structure. By deleting the arrows and columns of the constrained degrees of freedom, it is possible to obtain the stiffness matrix of the constrained structure, which is not singular. This is a necessary condition to solve the equilibrium equation by finding the displacements of the nodes, see (4.25):

$$\{U_i\} = [K_{TOT}]^{-1} \cdot \{F_i\} \tag{4.25}$$

where:

- $\{U_i\}$ is the vector of the displacements of nodes;
- $\{F_i\}$ is the vector of the external forces.

In order to obtain the value of stresses in each member, it is necessary referring to the vector of displacements and to the stiffness matrix of each element, see Figure 1:

$$\left\{K^m\right\}\begin{bmatrix} u_i \\ v_i \\ u_j \\ v_j \end{bmatrix}^m = \begin{bmatrix} H_i \\ V_i \\ H_j \\ V_j \end{bmatrix}^m \tag{4.26}$$

The axial forces and the values of stress can be found referring to the following well known formulas:

$$\begin{aligned} \left|N^m\right| &= \sqrt{\left(H_i^m\right)^2 + \left(V_i^m\right)^2} \\ \left|\sigma_m\right| &= \frac{\left|N^m\right|}{A_m} \end{aligned} \tag{4.27}$$

As an alternative, it is possible to evaluate the stress in each bar by calculating at first the strain ε^m and then by using the constitutive laws:

$$\sigma_i = \varepsilon_i E \tag{4.28}$$

4.3 Case of study

The case of study deals with the construction of the parametric stiffness matrix of a composite steel and concrete truss beam, whose shape is shown in Figure 6: the continuous lines represent the steel elements of the beam and the dotted ones the possible additional concrete elements. Please note that, depending on the loading and geometry conditions, concrete elements can be part or not of the resisting system and the steel ones, as well, can be made up of steel and concrete.

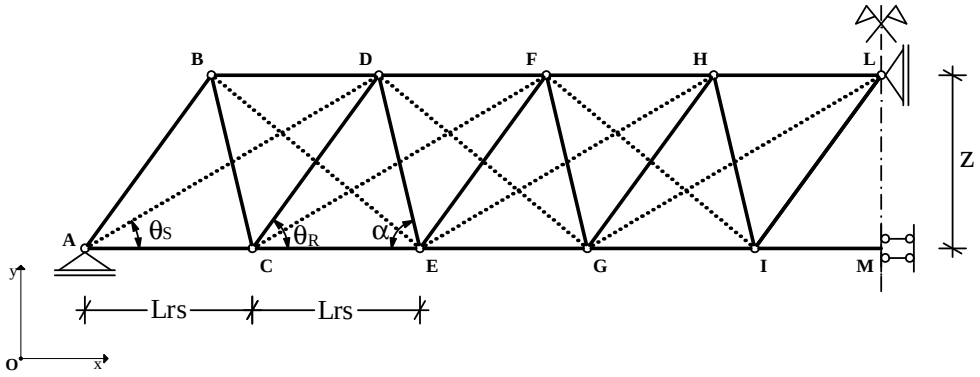

Figure 6. Shape of truss

The stiffness of each element in the local reference system can be expressed as follows:

	Angle	Steel	Concrete
web bars	α	$\kappa_{s,\alpha} = \frac{E_s A_{wb}}{z} \sin\alpha$	$\kappa_{c,\alpha} = \frac{E_c A_{c,R}}{z} \sin\alpha$
	θ_R	$\kappa_{s,\theta_R} = \frac{E_s A_{wb}}{z} \sin\theta_R$	$\kappa_{c,\theta_R} = \frac{E_c A_{c,R}}{z} \sin\theta_R$
	θ_S	–	$\kappa_{c,\theta_S} = \frac{E_c A_{c,S}}{z} \sin\theta_S$
lower chord	–	$\kappa_{s,lc} = \frac{E_s A_{s,lc}}{z(\cot\alpha + \cot\theta)}$	–

upper chord	–	$\kappa_{s,uc} = \dfrac{E_s A_{s,uc}}{z\left(\cot\alpha + \cot\theta\right)}$	$\kappa_{c,uc} = \dfrac{E_c A_{c,uc}}{z\left(\cot\alpha + \cot\theta\right)}$

Table 1. Stiffness of each element in the local reference system

For the meaning of each term in the table above, refer to Chapter 3.

As stated in the previous, for the purpose of assembling the overall stiffness matrix in the global reference system (G.R.S.) it is necessary to preliminary construct the stiffness matrix of each element in the G.R.S. by using the rotation matrices, (4.21) (4.22), and then filling out each term of the global matrix according to the topology of the beam.

For the subject matter case, to give an example of the possible terms of the stiffness matrix it is necessary to preliminary define a loading condition, see Figure 7, since the contribution of concrete affects only the compressive elements.

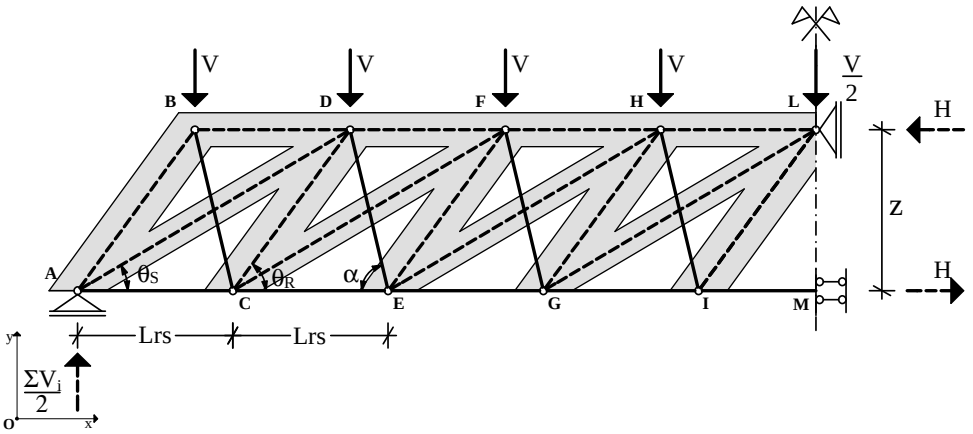

Figure 7. Possible loading condition

The structure shown above is externally statically determinate with respect to vertical loads and internally statically indeterminate $\left(2n < a + v \Rightarrow 2\times 11 < 22 + 4\right)$. The structure in the plane $\left(O, x, y\right)$ has 18 degrees of freedom, so the overall stiffness matrix is an 18 order one. The formula (4.29) shows the structure of the matrix, which mainly depends on the placing of the nodes and their respective d.o.f. in the matrix.

$$K = \begin{bmatrix} k_{uu}^{A} & k_{uA-vB} & k_{uA-vD} & k_{uA-uB} & k_{uA-uC} & 0 & \dots & 0 \\ & k_{vv}^{B} & k_{vB-vD} & k_{vB-uB} & k_{vB-uC} & k_{vB-vC} & \dots & 0 \\ & & k_{vv}^{D} & 0 & k_{vD-uC} & k_{vD-vC} & \dots & 0 \\ & & & k_{uu}^{B} & k_{uB-uC} & k_{uB-vC} & \dots & 0 \\ & & & & k_{uu}^{C} & k_{uC-vC} & \dots & 0 \\ & & sym & & & k_{vv}^{C} & \dots & 0 \\ & & & & & & \ddots & k_{vI-vL} \\ & & & & & & & k_{vv}^{L} \end{bmatrix} \tag{4.29}$$

So, referring to Figure 7 and formula (4.29), the expressions of the parametric stiffness of nodes A and B are:

$$k_{uu}^{A} = \left(\kappa_{s,\theta_R} + \kappa_{c,\theta_R}\right)\cos^2\theta_R + \kappa_{s,lc} = \\ = \frac{1}{z}\left[\left(E_s A_{wb} + E_c A_{c,R}\right)\sin\theta_R \cos^2\theta_R + \frac{E_s A_{s,lc}}{\left(\cot\alpha + \cot\theta\right)}\right] \tag{4.30}$$

$$k_{vv}^{B} = \left(\kappa_{s,\theta_R} + \kappa_{c,\theta_R}\right)\sin^2\theta_R + \kappa_{s,\alpha}\sin^2\alpha = \\ = \frac{1}{z}\left[\left(E_s A_{wb} + E_c A_{c,R}\right)\sin^3\theta_R + E_s A_{wb}\sin^3\alpha\right] \tag{4.31}$$

$$k_{uu}^{B} = \left(\kappa_{s,\theta_R} + \kappa_{c,\theta_R}\right)\cos^2\theta_R + \kappa_{s,\alpha}\cos^2\alpha + \kappa_{s,uc} + \kappa_{c,uc} = \\ = \frac{1}{z}\left[\left(E_s A_{wb} + E_c A_{c,R}\right)\sin\theta_R \cos^2\theta_R + E_s A_{wb}\sin\alpha\cos^2\alpha + \right. \\ \left. + \frac{E_s A_{s,uc} + E_c A_{c,uc}}{\left(\cot\alpha + \cot\theta\right)}\right] \tag{4.32}$$

$$k_{uv}^{B} = k_{vu}^{B} = \left(\kappa_{s,\theta_R} + \kappa_{c,\theta_R}\right)\sin\theta_R \cos\theta_R + \kappa_{s,\alpha}\sin\alpha\cos\alpha = \\ = \frac{1}{z}\left[\left(E_s A_{wb} + E_c A_{c,R}\right)\sin^2\theta_R \cos\theta_R + E_s A_{wb}\sin^2\alpha\cos\alpha\right] \tag{4.33}$$

Such a stiffness matrix, where each term is a parameter, is able to describe the structural behavior of several types of beams, subjected to any vertical load condition.

The matrix, moreover, has been embedded in a worksheet able to evaluate the values of stress and strain in each element, the collapse load and the ductile or brittle behavior of the structure.

The collapse load is calculated by means of the loads multiplier α_{cl}, whose expression is:

$$\alpha_{cl} = \frac{f_{y/c}}{\sigma_{y/c}} \tag{4.34}$$

where:

- $f_{y/c}$ is the value of the yield or compressive strength, depending on the element under analysis;
- $\sigma_{y/c}$ is the value of the stress, tension or compression, in each element.

So, given a beam and a loading condition, each steel or concrete element of the beam is characterized by a specific value of α_{cl}, which represents how much the value of stress is far from the limit one. Then, the minimum value among all α_{cl} coefficients corresponds to the multiplier of the loads able to bring on collapse the structure, which means the collapse of at least one of all the elements of the overall structure.

Moreover, each value of α_{cl} refers to a specific kind of collapse: yield of compressive or tensile steel bars, lateral buckling of composite elements or compressive strength of compressive concrete elements. So the minimum value of the multiplier of loads allows knowing if the collapse is a ductile or brittle one. The verification methods and the theoretical assumptions behind them are explained in the following section.

4.3.1 Verifications

As stated above, the collapse of the structure corresponds to the collapse of at least one of the structural elements of the beam. So, within the worksheet, the stress of each bar is compared with the corresponding limit one. In detail, in the structural model all the compressive elements are made up of steel and concrete, so they are subjected to three different verifications: the yield strength of steel bar, the compressive strength of concrete element and the verification to lateral buckling of composite cross section. Referring to tensile bars, instead, the reference value of stress for verifications is the yield strength of steel.

4.3.1.1 Compressive elements

Referring to the first two verifications of compressive elements, the limit values for the yield stress of steel and compressive strength of concrete refer to those provided by the National Code [5] and depend on the adopted materials, see section 4.3.2 Materials.
The area of the cross sections, as well, has been evaluated as follows:

- steel bars: $A_C = A_{sw} = \pi \frac{\phi^2}{2}$. Since it refers to the area of two steel bars, under the hypothesis of symmetrical behavior in the cross section[2];
- concrete elements: $A_R = b_w \cdot \nu_R \cdot s$, where $s = L_{rs}$ and b_w is the width of the cross section.

With reference to the verification to lateral buckling, all the details about the formulation and geometrical assumptions are explained in the following section.

[2] As confirmed by experimental tests, see Chapter 5.

4.3.1.1.1 Lateral buckling

The buckling resistance of all the compressive elements of the structural system, see Figure 7, has been verified in accordance with the formulation of NTC2008 [5], in detail:

$$\frac{N_E}{N_{b,R}} \leq 1 \tag{4.35}$$

where:

N_E is the compressive force in the local reference system

$N_{b,R}$ is the buckling resistance of the bars, calculated as follows:

$$N_{b,R} = \frac{\chi A f_{ym}}{\gamma_{M1}} \tag{4.36}$$

with:

$$\chi = \frac{1}{\phi + \sqrt{\phi^2 - \bar{\lambda}^2}} \leq 1 \tag{4.37}$$

$$\phi = 0,5\left[1 + \alpha\left(\bar{\lambda} - 0,2\right) + \bar{\lambda}^2\right] \tag{4.38}$$

Referring to the value of $\bar{\lambda}$, a distinction has been made for the bars of the upper chord, $\bar{\lambda}_{uc}$,and the bars of the web truss $\bar{\lambda}_{wt}$.

In fact the first ones have been verified referring to the formulation for steel structures, the second ones referring to the formulation of steel and concrete composite structures. So:

$$\overline{\lambda}_{uc} = \sqrt{\frac{A_{uc} \cdot f_{ym}}{N_{cr}}} \tag{4.39}$$

$$\overline{\lambda}_{wt} = \sqrt{\frac{N_{pl,R}}{N_{cr}}} \tag{4.40}$$

where

$$N_{pl,R} = 0,85 \cdot A_c \cdot f_{cm} + A_s \cdot f_{ym} \tag{4.41}$$

N_{cr} has been calculated referring to the Euler's critical load. In detail:

$$N_{cr} = \frac{\pi^2 EJ}{l_0^2} \tag{4.42}$$

For the evaluation of the bending stiffness of the composite cross section for limit state verifications, the second order effects have been taken into account. So, the following bending stiffness has been considered:

$$\left(EJ\right)_{eff,II} = k_0 \left(E_s J_s + k_{e,II} E_{cm} \cdot J_c\right) \tag{4.43}$$

where:

$$k_0 = 0,9 \tag{4.44}$$

$$k_{e,II} = 0,5 \tag{4.45}$$

J_s is the moment of inertia of the web truss' bars, J_c is the moment of inertia of the rods[3].

As stated in the previous, the numerical model refers to a standard model of beam, in which the upper chord is made up of 3 bars and the web truss is made up of 2 bars. Since the aim is the evaluation of the shear resistance, for all the steel elements the moment of inertia refers to the single bar and the area of the cross section to the sum of all of them.

Also notice that the use of $k_{e,II}$ reduces the value of the tangent modulus of elasticity of concrete, as that that the buckling is evaluated with cracked concrete section.

As for the evaluation of $l_0 = \beta l$, according to the behavior of steel beams during the experimental tests, β has been considered as follows:

element	β
web bars	0,8
upper/lower chord	0,5

Table 2. Values of β coefficient

A is the area of the steel cross section under consideration and f_{ym} the mean value of steel yield strength.

According to the Table 4.2.VI [5], the factor α, related to the imperfections of the structural elements, has been considered equal to $0,49$ for both the solid circular cross sections of the web and the upper flange.

Moreover, the partial factor γ_{M1} for structural steel applied to resistance of members to instability has been considered equal to $1,05$.

[3] Notice that J_c has been calculated referring to the rod cross section's area proper of each web bar. $b_w / 2$, has been considered as the minor axis of inertia, since along the longitudinal plane of the beam, it seems reasonable that the lateral buckling of the cross section has a very low likelihood of occurrence.

4.3.1.2 Tensile bars

The verification of tensile bars has been conducted by comparing the yield stress of steel provided by the National Code [5] with the stress of each tensile steel bar, under the hypothesis of no tensile concrete, see section 4.3.2 Materials.
As for the compressive steel bars, the area of the cross sections has been evaluated as follows:

- steel bars: $A_T = A_{sw} = \pi \frac{\phi^2}{2}$. Since it refers to the area of two steel bars, under the hypothesis of symmetrical behavior in the cross section[4];

[4] As confirmed by experimental tests, see Chapter 5.

4.3.2 Materials

The numerical analysis has been conducted referring to the mean values of concrete and steel strength, f_{cm} and f_{ym}.

All the mechanical characteristics of materials, in fact, are part of input data of the analysis and they have to be taken into account with mean values so that also the output result can be considered as "the mean value" of the function.

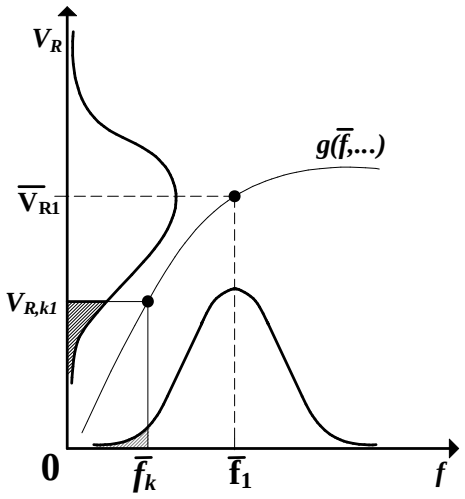

4.3.2.1 Steel

All the steel grades used for this kind of composite beams have been taken into account for the analysis, as shown in Table 3.

steel grade	f_{tk}	f_{yk}	f_{yd}	f_{ym}
*S*235	360	235	224	271
*S*275	430	275	262	317

$S355$	510	355	338	409
$S450$	550	440	419	488

Table 3. Mechanical characteristics for each steel grade [N/mm²]

The Young modulus for every steel grade has been considered equal to $210.000 N/mm^2$.

The mean value of yield stress, f_{ym}, has been evaluated taking into account the coefficient of variation (CV) [14] for each steel grade. CV is the normalized measure of dispersion of a probability distribution and shows the accuracy of the measures of the collected data, usually coming from experimental tests. Referring to a finite number of samples:

$$CV = \sqrt{\frac{1}{n}\sum_{i=1}^{n}\left(\frac{x_i}{|\mu|}-1\right)^2} = \frac{\sigma}{|\mu|} \tag{4.46}$$

In the subject matter case:

$$\sigma = \sqrt{\frac{\sum_{i=1}^{n}\left(f_{yi}-f_m\right)^2}{n-1}};\ f_{ym} = \frac{\sum_{i=1}^{n} f_{yi}}{n} \tag{4.47}$$

σ and f_{ym} allow to calculate the characteristic value of the yield strength of steel, f_{yk}, that Eurocode EN1990 [9] defines as the 5% fractile of its statistical distribution where a minimum value of the property is the nominal failure limit, and as the 95% fractile where a maximum value is the limiting value. Then:

$$f_{yk}^{+} = f_{ym} + K \cdot \sigma \tag{4.48}$$

$$K = 1{,}645 \tag{4.49}$$

With reference to NTC2008:

steel grade	***CV***
$S235 - S355$	8%
$> S355$	6%

Table 4. Coefficient of variation for each steel grade

So all the useful data are available to evaluate f_{ym}.

As stated in the previous, all the analyses have been conducted under the hypotheses of linear behavior of materials, until the collapse of one of them. Referring to the steel elements, it occurs when at least one bar reaches the yield compressive or tensile stress or reaches the buckling critical load.

The following bilinear constitutive law has been considered for the steel:

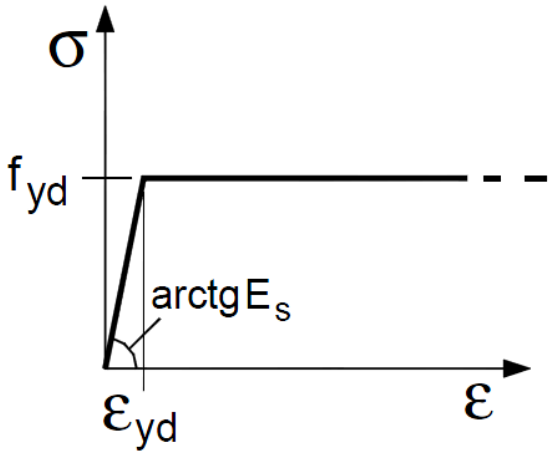

Figure 8. Constitutive law for steel: $\sigma - \varepsilon$ diagram [5]

4.3.2.2 Concrete

The mechanical characteristics of concrete have been calculated following the formulation of NTC2008 [5].
For the evaluation of f_{ck} and f_{cm}, respectively the characteristic and mean value of the cylinder compressive strength of concrete at 28 days can be calculated starting from the value of the compressive strength of cubes:

$$f_{ck} = 0,83 \cdot R_{ck} \tag{4.50}$$

$$f_{cm} = f_{ck} + 8 \tag{4.51}$$

The value of design strength of concrete, as well, has been evaluated taking into account the partial factor $\gamma_M = 1,5$ for concrete property, also accounting for model uncertainties and dimensional variations. And the value of Young modulus has been calculated as:

$$E_{cm} = 22.000\left[\frac{f_{cm}}{10}\right]^{0,3} \tag{4.52}$$

concrete strength classes	**f_{ck}**	**f_{cm}**	**f_{cd}**	**E_{cm}**
$C20/25$	20,75	28,75	13,83	30.200
$C25/30$	24,9	32,9	16,60	31.447
$C28/35$	29,05	37,05	19,37	32.588
$C32/40$	33,2	41,2	22,13	33.643

Table 5. Mechanical characteristics for each concrete strength class

For the constitutive law of concrete the parabola-rectangle model has been used:

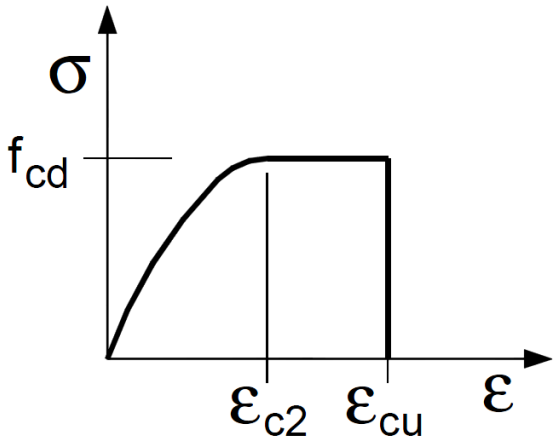

Figure 9. Constitutive law for concrete: $\sigma - \varepsilon$ diagram [5]

Chapter 5
Experimental tests

5.1 Introduction

This section deals with the experimental tests conceived and conducted in order to verify the validity of the collapse criterion, which underpins the proposed design methodology based on the new simplified mechanical model, see Chapter 3.

The overall experimental campaign has been performed on twenty-two samples, in order to study separately the shear and flexure behavior of

CSCBs at the 1st and 2nd stage and to test the behavior of the upper chord of a new model of steel structural joint at the 1st stage.
Herein will be shown and analyzed the results of shear tests on beams during the 2nd stage.

5.2 Experimental set-up

The experimentation has been conducted on 4 full scale beams, whose geometrical and mechanical characteristics are summed up in Table 1.
In the structural arrangement of the composite beam, the internal truss system can be organized in two groups of elements: those belonging to the flanges and those belonging to the web.
The flanges are the upper compressed chord made of concrete and the bottom tension chord made generally by a smooth surface steel plate.
The web is made of the following elements:
B : Steel bars, generally in tension
R : Rods made of concrete and steel, generally in compression
S : Diagonal struts made of concrete
The flanges are devoted to the flexural capacity, while the web to the shear capacity.
Technologically speaking, each diagonal truss is the result of coupling of n bent bars welded to the lower plate and to the upper longitudinal bars.
The topology of steel truss can be described referring to:

- α : the angle between the steel bars, B , and the longitudinal axis of the beam;
- θ_R : the angle between the compressive rods, R , and the longitudinal axis of the beam;
- θ_S : the angle between the concrete strut, S , and the longitudinal axis of the beam;

- γ: the angle between the steel bars and the vertical axis in the cross section;
- h: the depth of the cross section
- b_w: the width of the cross section
- L_{rs}: the length of the representative span, which, for this kind of beams, overlaps with the bar spacing s. Note that the first two representative spans have different length, L_{rs}^{*}, for constructive requirements;
- L: the span of the beam.

Moreover ϕ_B is the diameter of diagonal steel bars and ϕ_L is the diameter of the longitudinal bars.

For the purpose of analyzing the structural behavior until the shear ultimate limit state, the structural design of samples has been conceived over-sizing upper and lower longitudinal reinforcement.

ID	**Geometrical properties**						
	bxh $[m]$	span $[m]$	lower chord $\left[mm^2\right]$	upper chord	web	$\theta_R = \alpha$ [deg]	γ [deg]
C	0,3x0,4	3,50	300X6	3ϕ24	2ϕ12	53	80
D	0,3x0,4	3,50	300X6	3ϕ32	2ϕ20	53	80
E	0,3x0,4	3,50	300X6	3ϕ24	2ϕ12*	53	80
F	0,3x0,4	3,50	300X6	3ϕ32	2ϕ20*	53	80

*web: steel truss without steel compression bars

Table 1. Samples: geometrical characteristics

Concrete C32/40	f_{ck}	f_{cm}	f_{cd}	E_{cm}	**Steel S355**	f_{tk}	f_{yk}	f_{yd}	f_{ym}	E_s
	33,2	41,2	22,13	33643		510	355	338	409	210000

Table 2. Samples: materials $[N / mm^2]$

As previously stated, experimental tests have been performed on four types of beam. This section deals with the tests on samples C and D, whose web reinforcement is made of two series of bent steel bars. The results of the other two samples, E and F, in which the web reinforcement is made of only tensile bars[1], will be not illustrated in this work.

Referring to the test of sample C, the test loading condition is shown in Figure 1 and Figure 3: one concentrated force has been applied to the second upper node of the web truss by a hydraulic jack ($100t$) coupled with a loading control unit.

The constraint condition of samples, as well, is also shown in Figure 1: all the tests have been performed on simply supported beams.

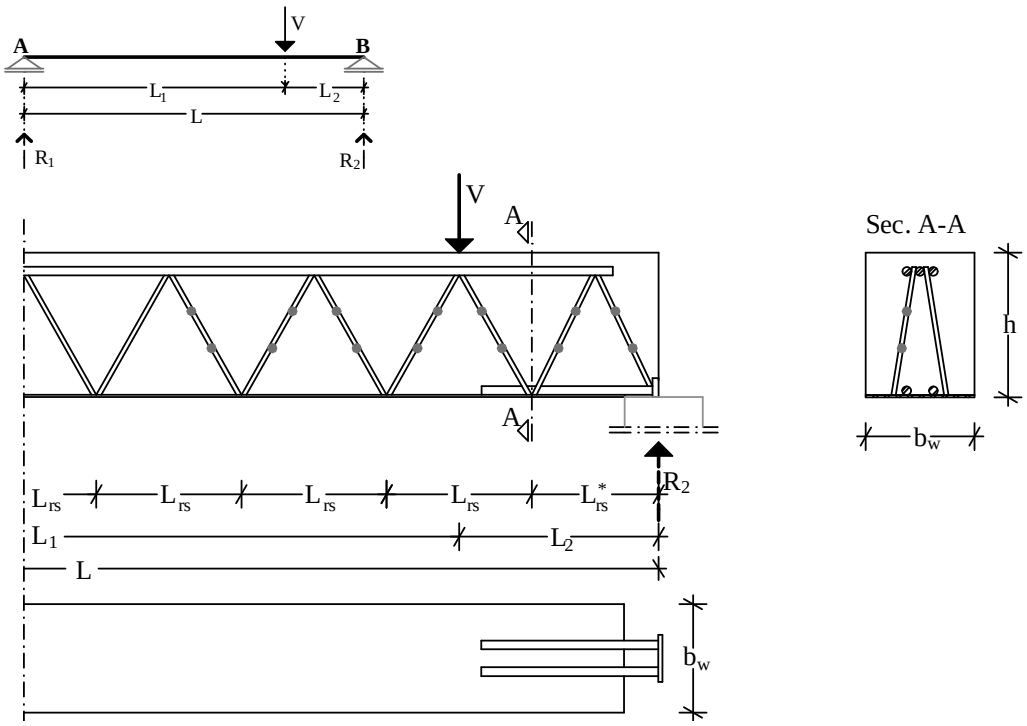

Figure 1. Sample C: experimental set-up

During all the tests, the beams have been monitored with couples of strain gauges placed on the first seven diagonal bars, see Figure 2. As explained in the following, these measurers allowed evaluating the strain of each

[1] Referring to the case of uniform load.

steel bar during the whole test duration and, by means of an acquisition software, all the data have been collected, stored and elaborated.

Moreover, before concrete filling, all the strain gauges have been tested in order to check their correct working, see Figure 2.

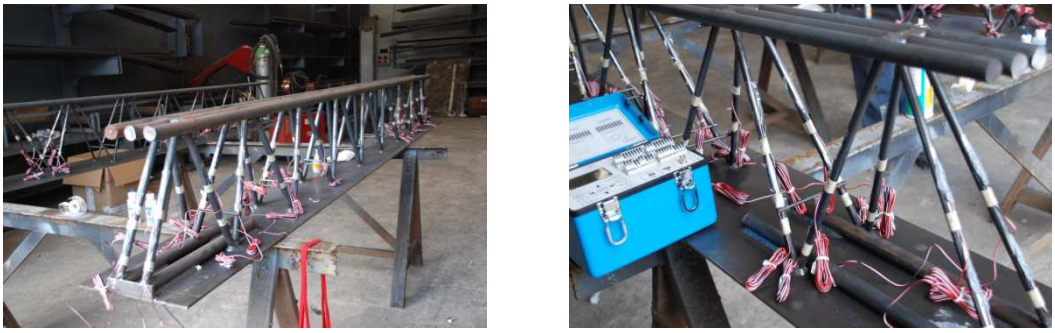

Figure 2. Sample *C* : strain gauges testing before concrete filling

Figure 3. Sample *C* before testing

5.3 Method

In order to characterize the contribution of each element to the shear capacity of CSCBs, the value of stress and strain has been evaluated by means of direct measurements for steel bars and indirect measurements for concrete elements.

In detail, starting from the values of steel bars' strain coming from the strain gauges, the constitutive law of steel allowed obtaining the value of stress and, thereby, the value of the axial load and the shear carried by

each steel bar. Therefore, by imposing the equilibrium condition on all the nodes, the values of the shear carried by the concrete element has been calculated.

In the following the method is explained in detail, referring to the set-up of the subject matter tests.

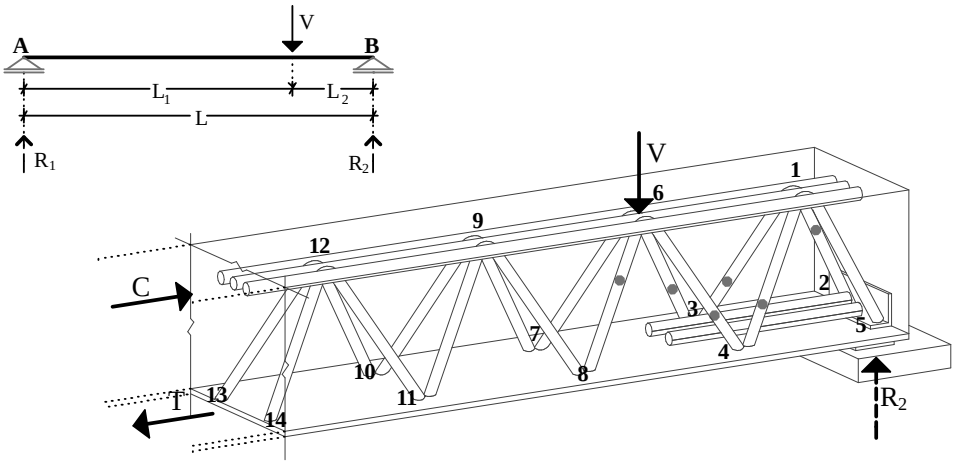

Figure 4. Strain gauges mapping

The structure is externally statically determinate in reference to vertical forces. So, the equilibrium conditions to vertical displacement and rotation of the beam, see Figure 4, allow getting the magnitude of the reaction forces at the sliding supports:

$$\begin{cases} \sum_{i=1}^{n} F_i = 0 \Rightarrow V - R_1 - R_2 = 0 \\ \sum_{i=1}^{n} M_i(O) = 0 \Rightarrow V - R_1 - R_2 = 0 \end{cases} \tag{5.1}$$

$$\begin{cases} V - R_1 - R_2 = 0 \\ \sum_{i=1}^{2} M_i(A) = 0 \Rightarrow R_2 \cdot L - V \cdot L_1 = 0 \end{cases} \Rightarrow \begin{cases} R_2 = V \cdot \dfrac{L_1}{L} \\ R_1 = V - R_2 \end{cases} \tag{5.2}$$

In the experimental tests $L_1 = \frac{5}{6} L$, so:

$$\begin{cases} R_2 = \frac{5}{6}V \\ R_1 = \frac{1}{6}V \end{cases} \tag{5.3}$$

Since the beam is internally statically indeterminate, the only equilibrium conditions do not allow evaluating the stress in each element. But, all the data collecting during the experimental tests give the value of strain in each steel element and so, as stated in the previous, through the constitutive laws, it is possible to evaluate the stress of each steel element and the relative axial force.

Moreover, since the external forces are given, see(5.3), the equilibrium condition in each node of the structure allows obtaining the value of stress in all concrete elements.

The method is briefly developed in the following: starting from the equilibrium condition above, see(5.3), the following relation holds

$$R_2 = V_{6-4-3} + V_{6-5-2} \tag{5.4}$$

In detail:

- V_{6-4-3} is the vertical force of the rod $6-4-3$, see Figure 4, and can be ideally considered equal to the sum of two quantities:

$$(V_{6-4-3})_R = (V_{6-4-3})_B + (V_{6-4-3})_C \tag{5.5}$$

  where
  - $(V_{6-4-3})_B$ is the vertical force of the two steel bars;
  - $(V_{6-4-3})_C$ is the vertical force of the concrete part of the rod.
- V_{6-5-2} is the vertical force of the concrete strut

The value of the vertical forces, V_i, can be easily obtained from the value of axial forces, N_i, see Figure 5:

$$N_i = \frac{V_i}{\sin x} \tag{5.6}$$

Referring to the term $(V_{6-4-3})_B$, since the geometrical characteristics of the steel bars are known as well as the strain of the bars, the value of the axial forces can be evaluated for each steel element:

$$\varepsilon_i \cdot E_i = \sigma_i \Rightarrow \sigma_i \cdot A_i = N_i \tag{5.7}$$

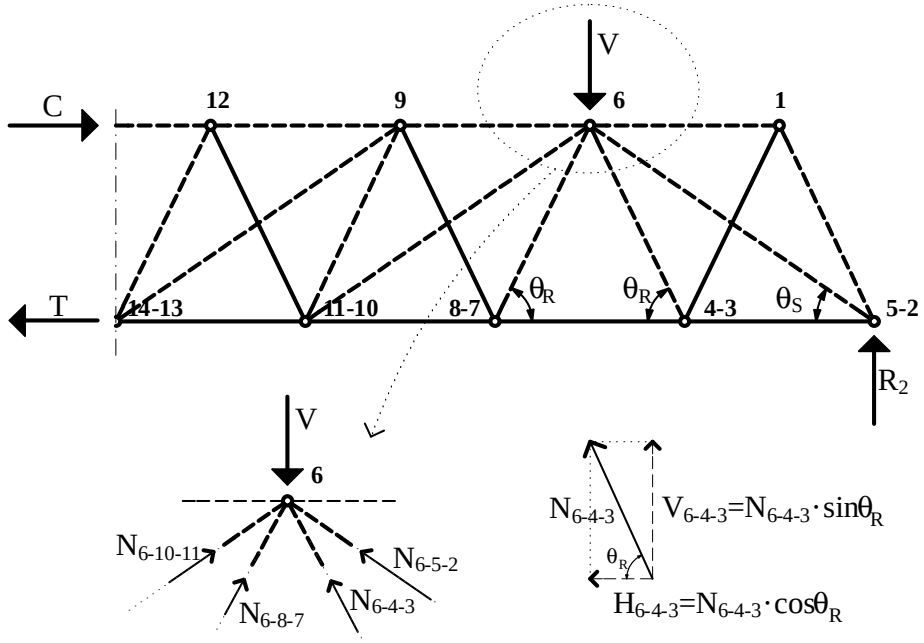

Figure 5. Node 6 : equilibrium condition

Referring to the vertical equilibrium condition of the node $4-3$, see Figure 6, the value of the term $(V_{6-4-3})_C$ can be found as:

$$(V_{6-4-3})_C = (V_{1-4-3})_B - (V_{6-4-3})_B \tag{5.8}$$

Please note that the concrete is no tensile strength, so the overall tensile stress in the element $1-4-3$ can be evaluated referring to the bars' strain.

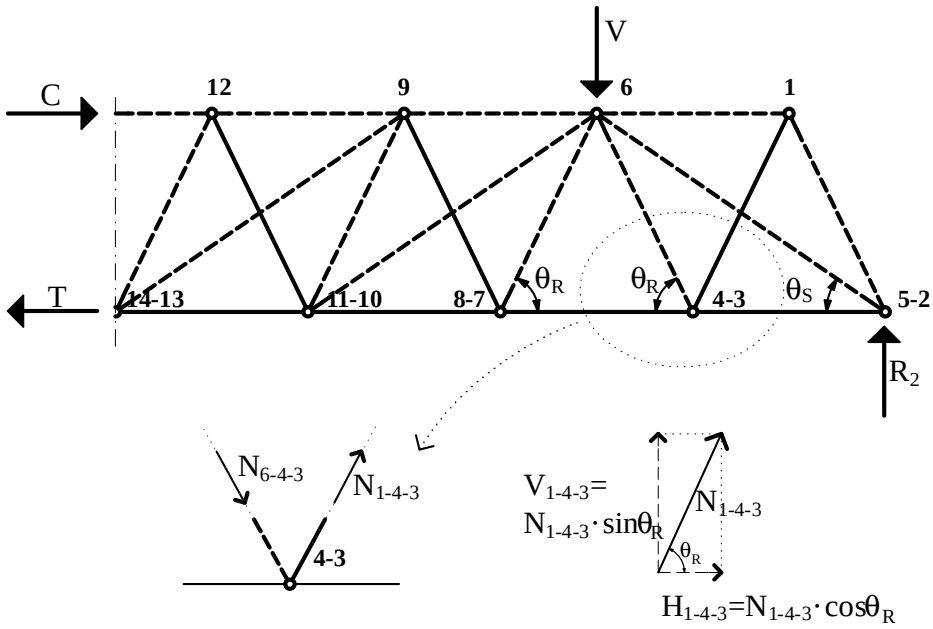

Figure 6: Node $4-3$: equilibrium condition

Starting from the(5.4), the value of V_{6-5-2} can be evaluated as the difference between the known data R_2 and V_{6-4-3}.

Please note that the same results could be reached starting the analysis from the node $5-2$.

5.4 Data analysis

5.4.1 Sample C

The strain of bars has been monitored for the whole duration of the test. The graph down below, see Figure 7, shows the deformation of the bars next to the sliding support **B**, as shown in Figure 4.

The first remark deals with the curve trend: the difference between the strain magnitudes of tensile and compressive bars hints at the contribution

of concrete to the shear strength. In fact, by drawing a vertical straight line by Load = $250kN$ e.g., it intercepts the two couples of curves, $1-4$ $1-3$ and $6-4$ $6-3$, in two couples of points, which correspond to strains that defer from one another by one order of magnitude. So the equilibrium condition, that has to be met for each node of the structure, can be satisfied only by supposing the contribution of compressive concrete elements to shear mechanical behavior.

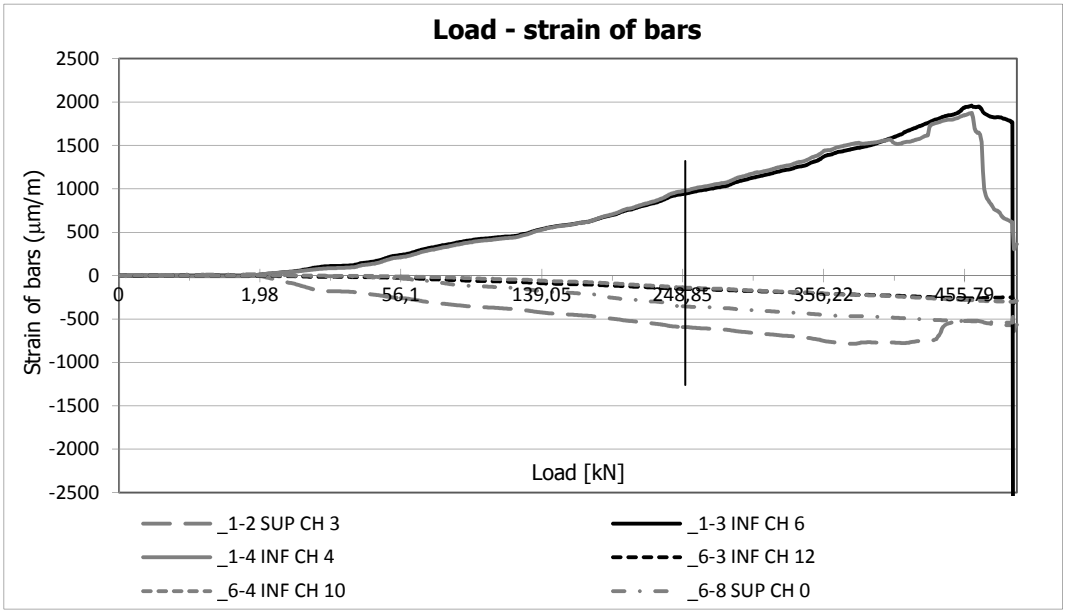

Figure 7. Sample C : Load – strain of bars.

Moreover the graph above shows that the trend is elastic until Load = $450kN$, where both the curves of tensile bars become irregular. To better understand the distribution of stresses in the structural element and to better understand the trend of tensile bars' curves, the analysis explained below has been conducted referring to 4 load-steps of the test: $V = 200kN$ $V = 400kN$ $V = 450kN$ $V = 490kN$. The tables about steel bars report the value of the strain ε , the stress σ , the ratio of stress to the yield strength of steel Δ ,the value of axial force N and vertical force V for each steel bar. The tables about concrete elements, instead, report the value of N and V obtained as explained above.

Steel bar	ε	σ [N/mm²]	Δ [%]	N [N]	V [N]
6 – 4	–0,00010	–21	5	–2.410	2.168
1 – 4	0,00077	162	40	18.278	16.439
6 – 3	–0,00013	–26	6	–2.969	2.671
1 – 3	0,00076	159	39	17.969	16.161
6 – 8	–0,00028	58	14	-6.536	5.878
1 – 2	–0,00052	–110	27	–12.388	11.142

Table 3. Direct measurements of bars' strain: $V = 200kN$

Concrete element	N [N]	V [N]
rod 6 – 3 – 4	–30.867	27.761
rod 1 – 2 – 5	–11.471	10.316
strut 6 – 5 – 2	–244.800	134.067

Table 4. Indirect evaluation of the concrete elements' forces: $V = 200kN$

Steel bar	ε	σ [N/mm²]	Δ [%]	N [N]	V [N]
6 – 4	–0,00024	–50	12	–5.684	5.112
1 – 4	0,00153	321	78	36.258	32.609
6 – 3	–0,00023	–49	12	–5.499	4.946
1 – 3	0,00160	335	82	37.914	34.098
6 – 8	–0,00049	–102	25	–11.520	10.360
1 – 2	–0,00077	–162	40	–18.338	16.493

Table 5. Direct measurements of bars' strain: $V = 400kN$

Concrete element	N [N]	V [N]
rod 6 – 3 – 4	–62.989	56.650

rod 1 – 2 – 5	–37.496	33.723
strut 6 – 5 – 2	–486.846	266.625

Table 6. Indirect evaluation of the concrete elements' forces: $V = 400kN$

Steel bar	ε	σ [N/mm²]	Δ [%]	N [N]	V [N]
6 – 4	$-0,00028$	–58	14	–6.574	5.913
1 – 4	$0,00182$	383	94	43.315	38.956
6 – 3	$-0,00026$	–54	13	–6.140	5.522
1 – 3	$0,00189$	396	97	44.770	40.265
6 – 8	$-0,00052$	–109	27	–12.356	11.112
1 – 2	$-0,00053$	–111	27	–12.540	11.278

Table 7. Direct measurements of bars' strain: $V = 450kN$

Concrete element	N [N]	V [N]
rod 6 – 3 – 4	–75.372	67.787
rod 1 – 2 – 5	–63.005	56.665
strut 6 – 5 – 2	–540.078	295.779

Table 8. Indirect evaluation of the concrete elements' forces: $V = 450kN$

Steel bar	ε	σ [N/mm²]	Δ [%]	N [N]	V [N]
6 – 4	$-0,00030$	–63	15	–7.166	6.445
1 – 4	$0,00061$	129	32	14.598	13.129
6 – 3	$-0,00025$	–53	13	–5.972	5.371
1 – 3	$0,00176$	371	91	41.909	37.692
6 – 8	$-0,00054$	–114	28	–12.888	11.591
1 – 2	$-0,00057$	–120	29	–13.593	12.225

Table 9. Direct measurements of bars' strain: $V = 490kN$

Concrete element	N [N]	V [N]
rod $6-3-4$	–43.370	39.005
rod $1-2-5$	–29.320	26.370
strut $6-5-2$	–652.801	357.513

Table 10. Indirect evaluation of the concrete elements' forces: $V = 490kN$

Referring to Table 7, the ratio of stress to the yield strength of steel is about 94% and 97% for steel bars $1-4$ and $1-3$ respectively. Moreover by increasing the load until $490kN$ the stress of tensile bars decreases, showing an irregular behavior that can be identified as the collapse of the structural element.

Figure 8 shows the crack pattern at the end of the test.

Figure 8. Sample C : cracking pattern

Starting from the collected data and the indirect evaluation of the axial forces in concrete elements, it has been possible evaluating the stress of rod and strut starting from the assumption that the relative cross sections can be defined respectively as follows:

$$A_R = n_E \cdot A_{sw} + s \cdot b_w \cdot \sin\theta_R \tag{5.9}$$

$$A_S = s \cdot b_w \cdot \sin\theta_S \tag{5.10}$$

So, for $V = 450kN$, the values of stress in each concrete element are:

Concrete element	N [N]	σ [N/mm²]	Δ [%]
rod $6-3-4$	-75.372	-0,92	3,07
rod $1-2-5$	-63.005	-0,77	2,57
strut $6-5-2$	-704.828	-19,74	65,81

Table 11. Stress in each concrete element: $V = 450kN$

5.4.2 Sample D

The same method explained above has been adopted to analyze the data of the sample D.

Referring to Figure 9, please note that the results shown and analyzed down below refer to the second test conducted on the sample D, by applying the load near to the end B, on the beam shifted of 750 cm in order to keep out the part of the beam cracked during the first test.

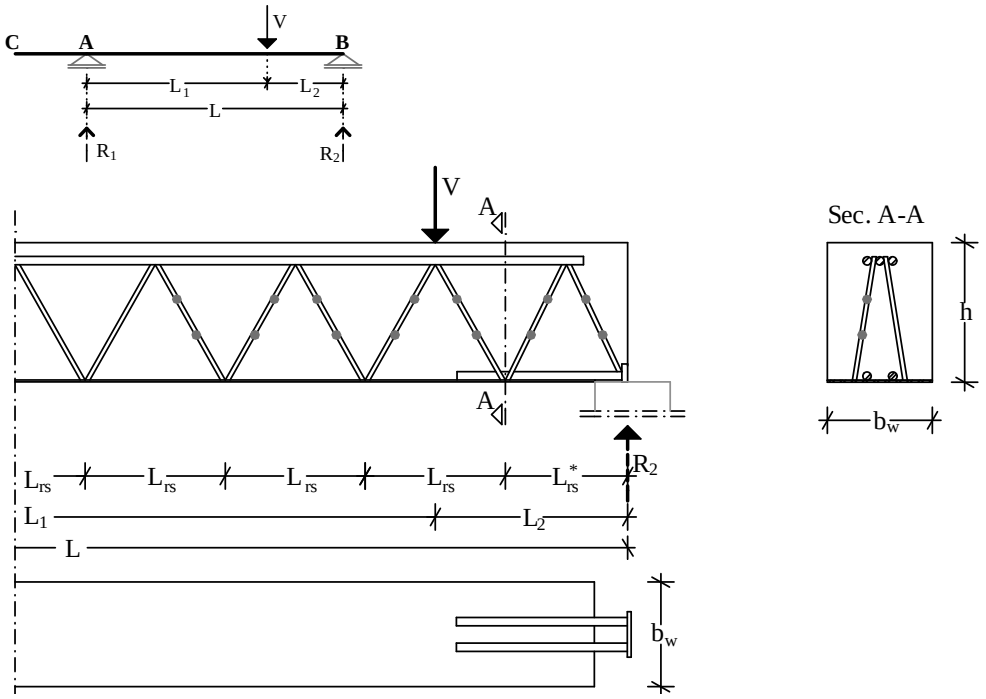

Figure 9. Sample D: Experimental set-up

The graph of Figure 10 shows the deformation of the bars $1-2$, $1-5$, $1-3$, $1-4$, $6-3$ and $6-4$, see also Figure 4: the same remarks explained for the sample C hold for the sample D. Therefore the irregular trend of the curves at $V = 670\ kN$ marks the yield of tensile steel bars and the collapse of the structure.

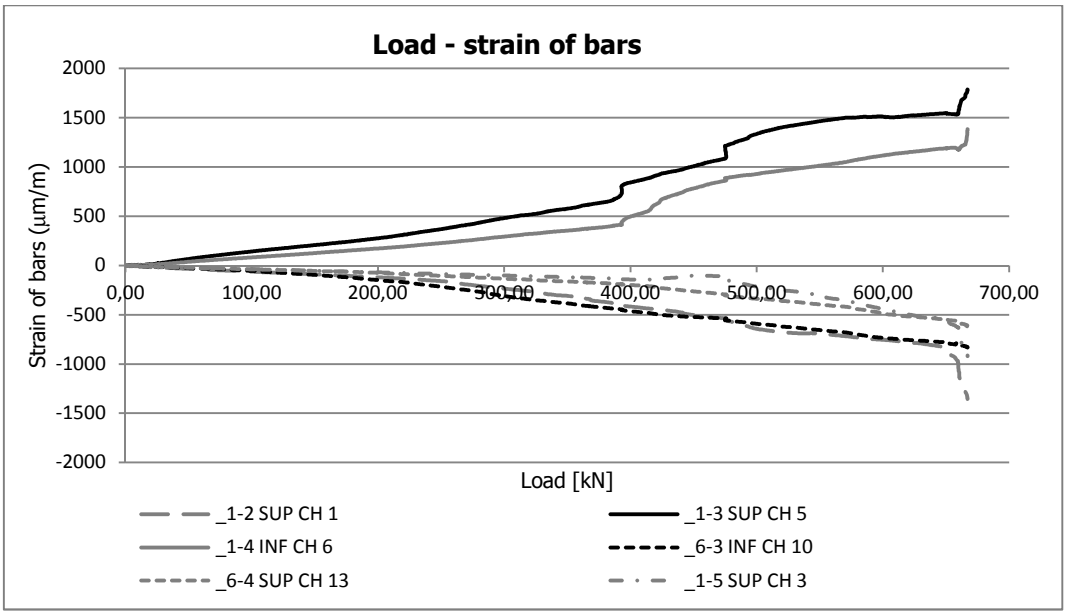

Figure 10. Sample D: Load – strain of bars

In the tables down below are shown all the data, direct and indirect ones, collected during the tests at the following steps:
$V = 200\ kN$, $V = 400\ kN$, $V = 600\ kN$ and $V = 670\ kN$.

Steel bar	ε	σ [N/mm²]	Δ [%]	N [N]	V [N]
6 – 4	–0,00007	–16	4	–4.871	4.381
1 – 4	0,00017	36	9	11.400	10.253
6 – 3	–0,00015	–31	8	–9.696	8.720
1 – 3	0,00028	58	14	18.186	16.356
1 – 5	–0,00007	–14	4	–4.539	4.082
1 – 2	–0,00012	–25	6	–7.872	7.079

Table 12. Direct measurements of bars' strain: $V = 200kN$

Concrete element	N [N]	V [N]
rod 6 – 3 – 4	–15.019	13.508
rod 1 – 2 – 5	–17.176	15.447

strut 6 – 5 – 2	–243.566	133.391

Table 13. Indirect evaluation of the concrete elements' forces: $V = 200kN$

Steel bar	ε	σ [N/mm²]	Δ [%]	N [N]	V [N]
6 – 4	–0,00020	–42	10	–13.059	11.745
1 – 4	0,00050	104	25	32.738	29.443
6 – 3	–0,00046	–97	24	–30.566	27.490
1 – 3	0,00084	177	43	55.478	49.895
1 – 5	–0,00014	–30	7	–9.334	8.395
1 – 2	–0,00042	–87	21	–27.460	24.697

Table 14. Direct measurements of bars' strain: $V = 400kN$

Concrete element	N [N]	V [N]
rod 6 – 3 – 4	–44.591	40.103
rod 1 – 2 – 5	–51.422	46.247
strut 6 – 5 – 2	–439.437	240.661

Table 15. Indirect evaluation of the concrete elements' forces: $V = 400kN$

Steel bar	ε	σ [N/mm²]	Δ [%]	N [N]	V [N]
6 – 4	–0,00049	–102	25	–32.195	28.955
1 – 4	0,00112	235	57	73.755	66.332
6 – 3	–0,00074	–154	38	–48.511	43.629
1 – 3	0,00151	317	78	99.692	89.659
1 – 5	–0,00044	–92	23	–28.953	26.039
1 – 2	–0,00075	–159	39	–49.808	44.796

Table 16. Direct measurements of bars' strain: $V = 600kN$

Concrete element	N [N]	V [N]
rod $6-3-4$	-92.740	83.407
rod $1-2-5$	-94.685	85.157
strut $6-5-2$	-591.624	324.008

Table 17. Indirect evaluation of the concrete elements' forces: $V = 600kN$

Steel bar	ε	σ [N/mm²]	Δ [%]	N [N]	V [N]
$6-4$	$-0,00063$	-133	32	-41.740	37.540
$1-4$	$0,00138$	289	71	90.719	81.590
$6-3$	$-0,00083$	-174	43	-54.739	49.231
$1-3$	$0,00178$	374	91	117.486	105.663
$1-5$	$-0,00090$	-190	46	-59.595	53.598
$1-2$	$-0,00135$	-284	69	-89.196	80.220

Table 18. Direct measurements of bars' strain: $V = 670kN$

Concrete element	N [N]	V [N]
rod $6-3-4$	-111.725	100.482
rod $1-2-5$	-59.414	53.435
strut $6-5-2$	-636.796	348.747

Table 19. Indirect evaluation of the concrete elements' forces: $V = 670kN$

Referring to Table 18, the ratio of tension to the yield strength of steel is about 91% and 71% for steel bars $1-3$ and $1-4$ respectively.

Figure 11 shows the crack pattern at the end of the test. For further analyses and the comparison between experimental results and the results of the Simplified Model and Complete Model refer to Chapter 6.

Figure 11. Sample *D* : cracking pattern

Chapter 6
Correlation studies and optimization

6.1 Introduction

This chapter deals with all the analyses carried out to verify the accuracy of the proposed mechanical model and the description of a structural optimization procedure based on it.
In order to validate the new simplified model's capability of predicting the structural behavior and the collapse load, the results obtained in the experimental tests, see Chapter 5, have been compared with those coming from both simplified and complete models.
Therefore, in the first part of the chapter the models adapted to reproduce the experimental set-up and the method adopted to predict the value of the stress in concrete elements are presented.

It is shown that the results of the analyses significantly agree with the experimental ones and have confirmed the consistency of the model with the real structure. Thus, on the basis of the new model, an optimization procedure of the beams shape is then proposed, able to ensure both a pseudo-ductile shear behavior, and the maximum contribution of concrete in the resisting system, with the minimum amount of material and labor.
Hence, the second section deals with the description of the optimization criterion and the analysis of the resulting functions that rule the variation of all the independent parameters of the optimization function as the shear demand varies.
In the next section, starting from the design method currently adopted to evaluate the shear resistance of beams, a "standard design solution" has been compared with the optimal one as obtained from the optimization function.
In the last section, as well, the proposed mechanical model, see Chapter 3, has been modified in order to adopt the same design and optimization criteria for traditional reinforced concrete structures.

6.2 Comparison: mechanical models - experimental evidence

In this section, the comparison between the results of the experimental tests with the simplified and complete model will be presented.
With reference to the simplified model, the underlying collapse criterion[1] sets the yield strength of tensile bars as the ultimate shear resistance[2]. The same model, as well, allows evaluating the magnitude of stress in all concrete elements that are part of the resisting mechanism. These values

[1] See Chapter 3.
[2] This hypothesis has been confirmed by the experimental results, see Chapter 5.

will be compared with those obtained from the experimental results, calculated as shown in Chapter 5. This analysis has been conducted in order to demonstrate, both, that the model can be adapted to different structural arrangements and that it is able to reproduce the actual behavior of the structure.

Moreover, comparisons to the complete model have been made to confirm the validity of the theoretical assumptions of the simplified model, by comparing the value of ultimate limit load and the type of collapse with the results obtained from the simplified model and, consequently, with the experimental tests.

6.2.1 Simplified mechanical model

In order to have the simplified mechanical model provide results comparable to the experimental ones, see Chapter 5, it has been modified, by neglecting the contribution of the strut, see Figure 1 and Figure 2.

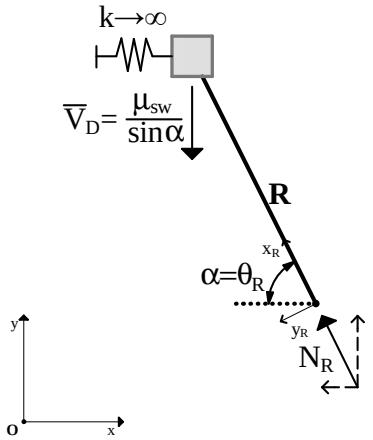

Figure 1. Simplified mechanical model.

Referring to the Figure above, the dimensionless vertical force $\overline{v}_D$ represents the collapse value for shear, since under this load the tensile bar reaches the yield stress.

The experimental tests, for the samples C and D, respectively, gave the following results:

$$\left(\mathrm{V}_D\right)_C = V_{1-4} + V_{1-3} \sim 70kN \text{ [3]} \tag{6.1}$$

$$\left(\mathrm{V}_D\right)_D = V_{1-4} + V_{1-3} \sim 187kN \tag{6.2}$$

The meaning of (6.1) and (6.2) can be verified by imposing the equilibrium condition of node 1, see Figure 2.

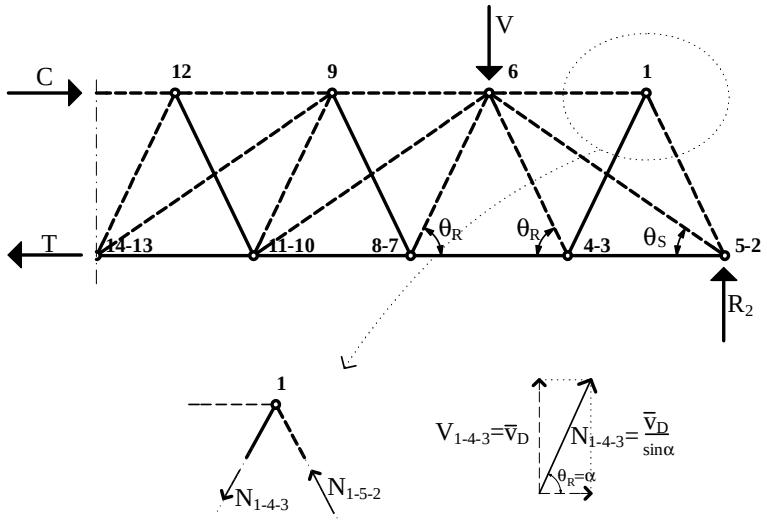

Figure 2. Node 1: equilibrium condition

So, the normalized axial forces in the rod in its local reference system can be expressed as:

$$\bar{n}_{\mathrm{R}}\left(\mu_{sw}, \alpha, \zeta\right) = \mu_{sw} \cdot \frac{1}{\sin\alpha} \cdot \frac{1}{\sin\theta_R\left(\alpha, \zeta\right)} \tag{6.3}$$

For the mechanical and geometrical properties of the beam one should refer to Table 1 and Table 2 of Chapter 5.
In the subject matter case, (6.3) gives:

[3] Note that the value of shear resistance is different from the one evaluated during the test $\bar{\mathrm{v}}_D \sim 450kN$ since the mechanical model does not take into account the contribution of the strut. Anyway, it is possible to verify that:
$R_2 - V_{6-5-2} = V_{1-4} + V_{1-3} \rightarrow 375000 - 305001 = 34421 + 35578(N)$
The same remarks hold for sample D.

$$\bar{n}_R\left(0.021,64\cdot\frac{\pi}{180},\frac{360}{550}\right)_C = 0,026 \tag{6.4}$$

$$\bar{n}_R\left(0.059,64\cdot\frac{\pi}{180},\frac{360}{550}\right)_D = 0,073 \tag{6.5}$$

The comparison between these values and the experimental ones shows that the simplified model is able to describe the mechanical behavior of the structure:

Table 1. Comparison: simplified model – experimental results

Sample		$\bar{v}_D$	$\bar{n}_R$
C (ϕ12)	Simplified model	1	0,026
	Exp. results	0,97	0,022
D (ϕ20)	Simplified model	1	0,073
	Exp. results	0,91	0,051

Note that, the value 1 of the dimensionless ultimate load $\bar{v}_D$ refers to the maximum capacity of the mechanical system, since it represents the load that causes the tensile bars to yield.

6.2.2 Complete mechanical model

The complete mechanical model, as the simplified one, has been adapted to the case study by neglecting the contribution of the concrete strut and by entering all the data, materials and geometric quantities[4], which characterized the samples.

Referring to Figure 3, a unit force, $V = 100\ kN$, has been applied to node D and then the value of the amplification factor, α, has been evaluated. The following information is obtained:

[4] See Table 1 and Table 2 of the Chapter 5

- it singles out the first element that reaches the ultimate limit state, as defined for each resisting element in Chapter 4;
- it gives the exact value of the ultimate load.

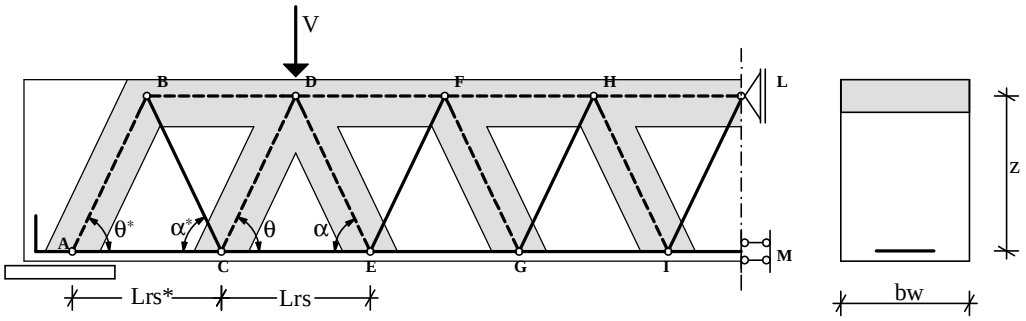

Figure 3. Complete model: experimental set up

Starting from sample C, the results of the analysis coming from the complete model are summarized in the following graphs.

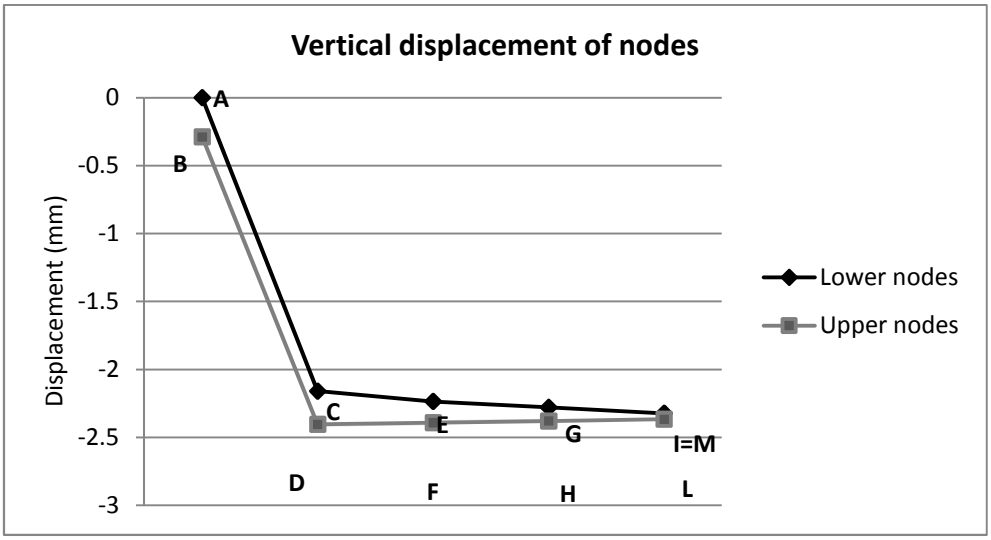

Figure 4. Sample C: vertical displacement of nodes

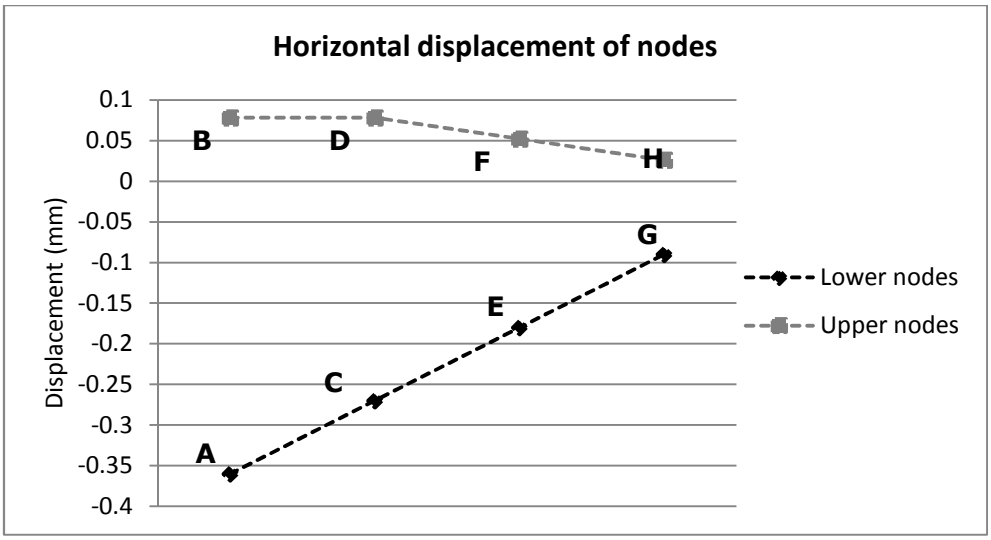

Figure 5. Sample C: horizontal displacements of nodes

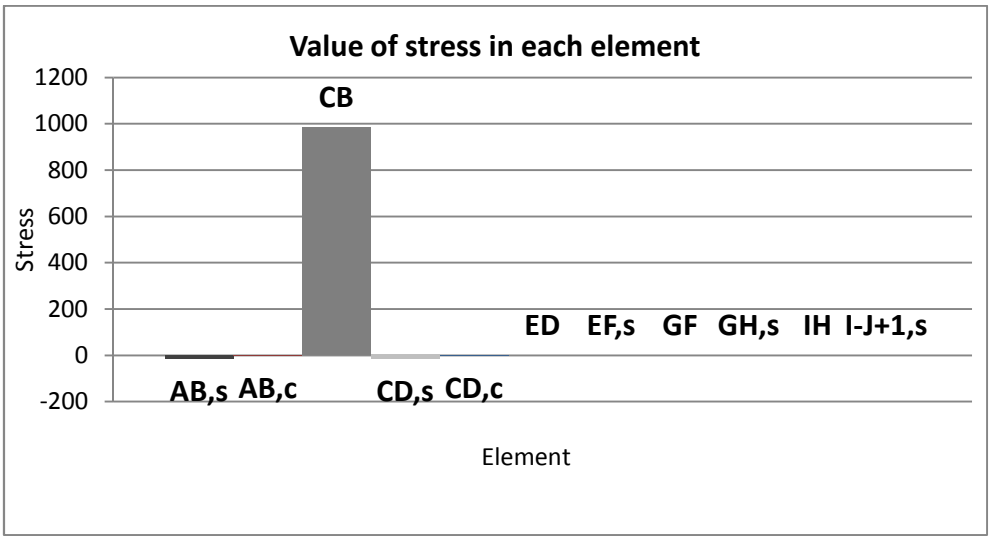

Figure 6. Sample C: value of stress in each element

The first two graphs, see Figure 4 and Figure 5, show the vertical and horizontal displacements of the nodes, see also Figure 3.

The third one, as well, see Figure 6, shows the value of stress in each element: for the loading condition of the experimental test, the maximum value of stress refers to the steel bar CB and the corresponding value of the amplification factor is:

$$\alpha_C = 0,83 \tag{6.6}$$

The product of the applied unit load by the factor (6.6) gives the ultimate limit load, which is about $83\ kN$.
Therefore, the complete model of sample C demonstrates that the yield of the steel bar CB causes the collapse of the structure under the load $V_C = 83\ kN$.

Referring to sample D, the results are summarized in the following graphs.

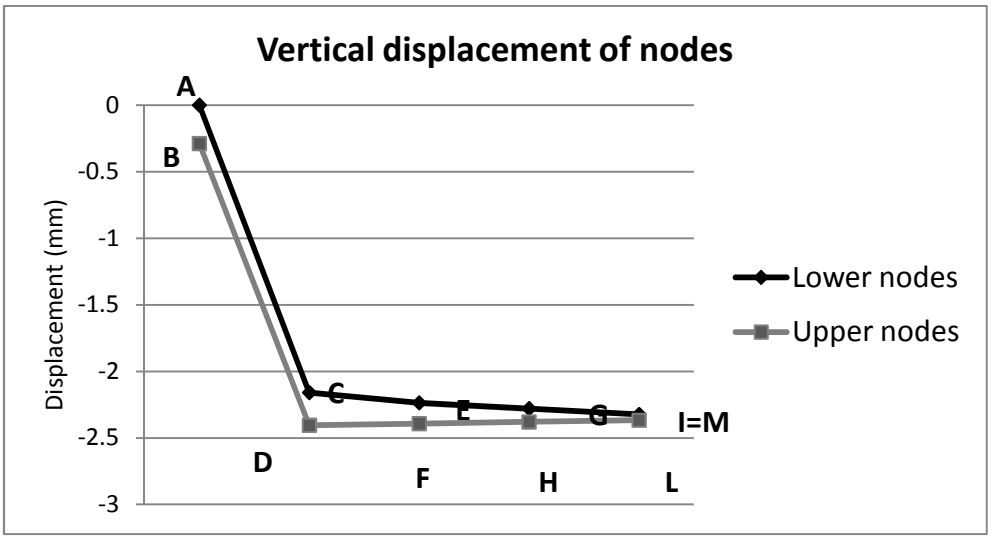

Figure 7. Sample D: vertical displacement of nodes

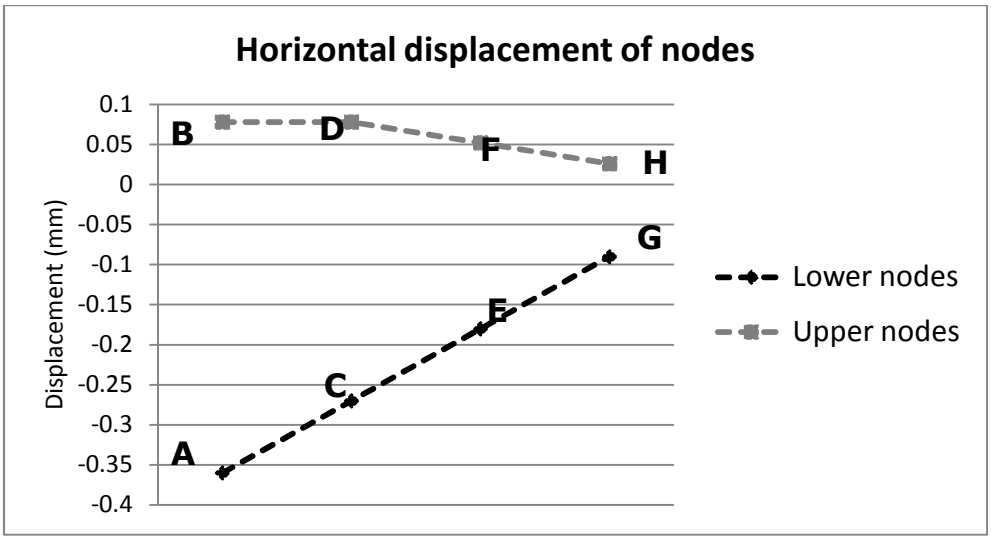

Figure 8. Sample D: horizontal displacements of nodes

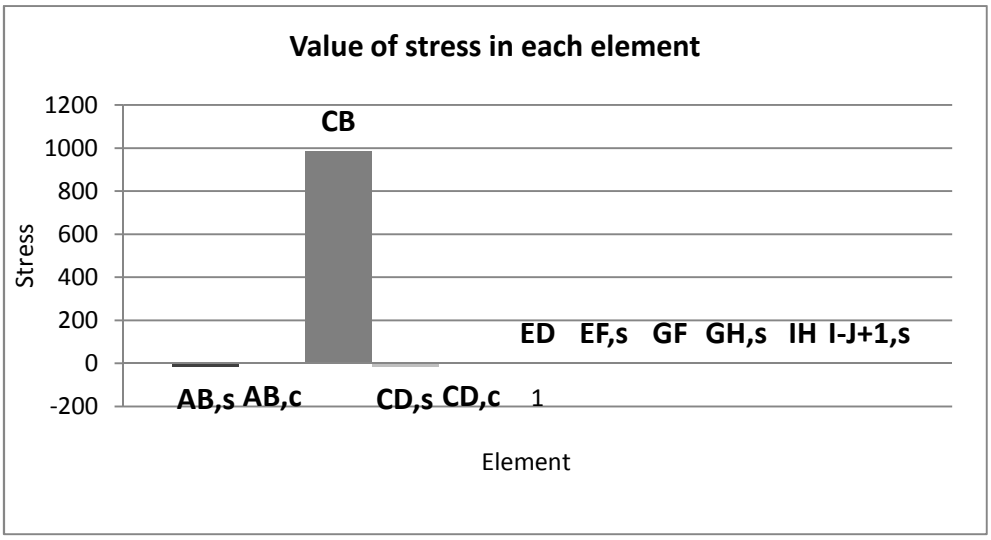

Figure 9. Sample C: value of stress in each element

The first two graphs, see Figure 7 and Figure 8, have the same meaning explained above.

The third one, see Figure 9, shows that the collapse of the structure depends on the yielding of the steel bar CB. The value of the amplification factor α is:

$$\alpha_D = 2,31 \tag{6.7}$$

Then the collapse load of the structure is $231\ kN$.

The following Table 2 summarizes the comparison between the results of the experimental tests and the complete model and shows a good agreement between the values.

In detail, the complete model allows obtaining automatically the value of the stress in each structural element: then, the values of $\bar{n}_R$ have been evaluated referring to the homogenized concrete cross-section of the structural element under analysis, steel bar AB in the subject matter case, see Figure 3, the value of concrete strength, see Chapter 4 and Chapter 5, and taking into account the amplification factor α in order to evaluate the concrete stress at the ultimate limit state.

Table 2. Comparison: complete model – experimental results

Sample		$\bar{v}_D$	$\bar{n}_R$
C (ϕ12)	Complete model	1	0,021
	Exp. results	0,84[5]	0,022
D (ϕ20)	Complete model	1	0,057
	Exp. results	0,81[6]	0,051

6.2.3 Remarks

The analyses above allow comparing and discussing the results all together and give useful information about the accuracy of the simplified model.
In detail:

- the experimental evidence confirmed the validity of the collapse criterion of the simplified model: in fact, for all tests, the ultimate limit load has been reached for tensile steel bars yielding;
- the comparison between the results of complete model and simplified model, referring to the value of $\bar{n}_R$[7], showed that the simplified model is able to predict the state of stress of the compressive elements. Therefore, the assumption of infinite stiffness of the upper chord does not affect significantly the results of the simplified model;
- the comparison between the complete model and the experimental results, as well, confirmed that the laboratory tests, even if always affected by uncertain and unpredictable variables, can be

[5] Note that this value of the load, evaluated referring to the unit one of the complete model, refers to the mean stress of tensile bars equal to $95\% f_{ym}$, see Chapter 5.

[6] This value of the load, evaluated referring to the unit one of the complete model, refers to the mean stress of tensile bars equal to $81\% f_{ym}$, see Chapter 5.

[7] For both the comparisons, see Table 1. Comparison: simplified model – experimental results, Table 1 and Table 2, the value of $\bar{v}_D$ is equal to 1, since it is the reference value for the collapse: it is the main hypothesis of the simplified model and the main evidence of the experimental results.

considered sufficiently reliable for the evaluation of the structural behavior.

6.3 Optimization of shape

The analysis of the shear behavior by means of the simplified structural model showed that the arrangement of the beam transverse reinforcement can be completely described by referring to three independent parameters:

- μ_{sw}, the mechanical transverse reinforcement ratio, see Chapter 3;
- α, the tilt angle of the tensile bars;
- ζ, the aspect ratio, see Chapter 3.

Referring to the simplified mechanical model, presented again in Figure 10, since the shear demand has been expressed as a function of μ_{sw}, the optimal solution is found by varying the values of α and ζ.

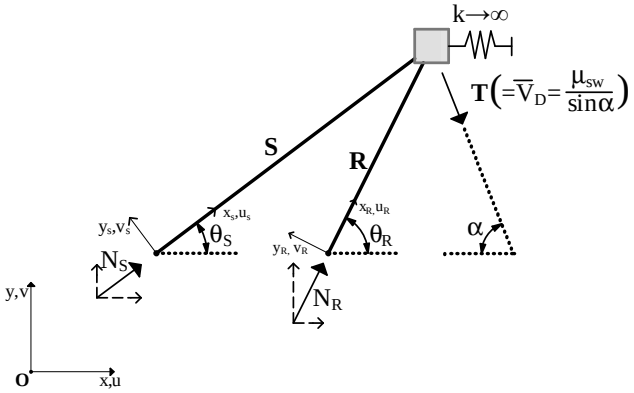

Figure 10. Simplified model

Therefore, the optimization criterion has been defined as follows:

- given the shear demand, the optimal solution, defined by α and ζ, is the one minimizing the amount and the related cost of materials and labor, where the cost of materials c_{steel} depends on the amount of shear steel and of labor c_{work} on the number of weldings and bendings.

The minimization function is defined as follows:

$$OPT\left(\mu_{sw}\right) = \text{Minimize}\left(c_{tot}, \alpha, \zeta\right) \tag{6.8}$$

$$c_{\text{tot}}\left(\mu_{sw}, \alpha, \zeta\right) = c_{\text{steel}}\left(\mu_{sw}, \alpha, \zeta\right) + c_{\text{work}}\left(\zeta\right) \tag{6.9}$$

As a result, the following formulation holds:

$$c_{\text{opt}}\left(\mu_{sw}\right) = c_{\text{tot}}\left(\mu_{sw}, \alpha_{opt}\left(\mu_{sw}\right), \zeta_{opt}\left(\mu_{sw}\right)\right) \tag{6.10}$$

Before deepening the meaning of each term of the optimization function, it is useful to underline that the adopted criterion is able to ensure that shear collapse is pseudo-ductile. In fact, the resistance of tensile bars, whose angle α is one of the outcomes of the optimization process, is laid down equal to the shear demand.

Eq. (6.9) represents the normalized cost per unit beam length, which is the goal function of the minimization.
The term c_{steel} can be expressed as follows:

$$c_{\text{steel}}\left(\mu_{sw}, \alpha, \zeta\right) = c_{\text{mat\_steel}} \mu_{sw} \frac{1}{\zeta}\left(\frac{1}{\sin\alpha} + \frac{1}{\sin\theta_R}\right) \tag{6.11}$$

where:

$$c_{\text{mat\_steel}} = c_{\text{steel\_m}^3} \cdot \frac{b_w \cdot z^2}{n_f} \tag{6.12}$$

$c_{\text{steel\_m}^3}$ represents the cost of steel per m3. All the other terms, as well, have been defined in Chapter 3 and are given data within the structural design.
By substituting Eq. (6.12) into Eq. (6.11), the following formulation holds:

$$
\begin{aligned}
c_{\text{steel}}(\mu_{sw},\alpha,\zeta) &= c_{\text{steel\_m}^3}\cdot\frac{b_w\cdot z^2}{n_f}\cdot\mu_{sw}\cdot\frac{1}{\zeta}\cdot\left(\frac{1}{\sin\alpha}+\frac{1}{\sin\theta_R}\right)= \\
&= c_{\text{steel\_m}^3}\cdot\frac{b_w\cdot s^2\zeta^2}{n_f}\cdot n_f\cdot\frac{A_{sw}}{b_w s}\cdot\frac{1}{\zeta}\cdot\left(\frac{1}{\sin\alpha}+\frac{1}{\sin\theta_R}\right)= \\
&= c_{\text{steel\_m}^3}\cdot A_{sw}\cdot z\cdot\left(\frac{1}{\sin\alpha}+\frac{1}{\sin\theta_R}\right)
\end{aligned}
\tag{6.13}
$$

Where $A_{sw}\cdot z\cdot\left(\frac{1}{\sin\alpha}+\frac{1}{\sin\theta_R}\right)$ represents the volume of tensile and compressive steel bars, per unit length of beam.

The term $c_{\text{work}}(\zeta)$ of Eq. (6.9) refers to the cost of weldings and bendings per unit length of beam, evaluated as follows:

$$
c_{\text{work}}(\zeta) = 8\cdot\zeta\cdot c_{\text{welding}} + 2\cdot\zeta\cdot c_{\text{bending}} \tag{6.14}
$$

where

- the coefficient 8 refers to the number of weldings necessary for each couple of bent bars, see Figure 11;
- the coefficient 2, instead, refers to the overall necessary bendings, one for each bar;
- $\zeta = \frac{z}{s}$ allows defining the number of weldings and bendings per unit length of beam. In fact, given the value of z, if the value of ζ decreases, the value of s will increase and the number of the overall bent bars, with relative bending and welding, will decrease within a given value of span.

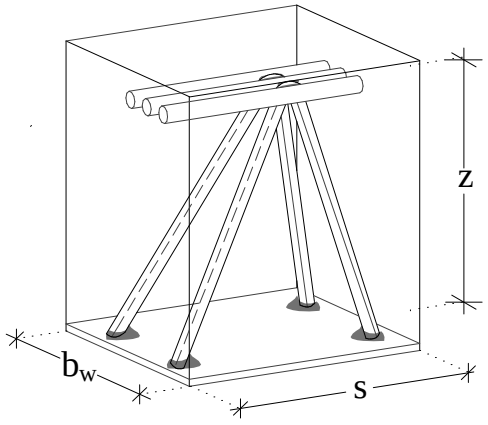

Figure 11. Weldings and bendings per z / ζ

Given the value of μ_{sw} depending on the shear demand, the function (6.9) shows the trend depicted in Figure 12.

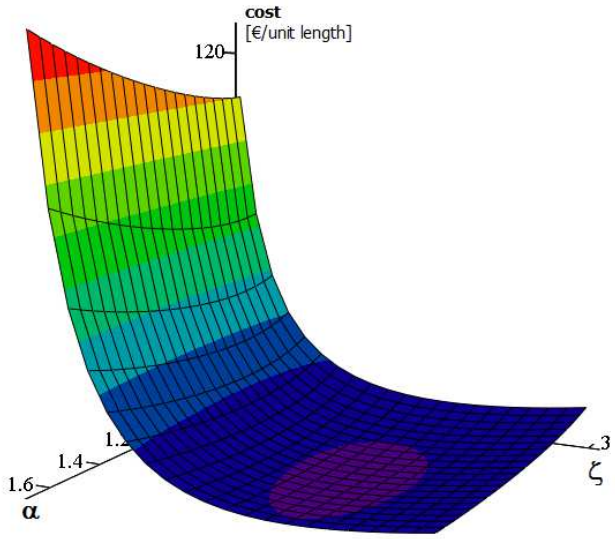

Figure 12. $c_{\text{tot}}(0.4,\alpha,\zeta) = c_{\text{steel}}(0.4,\alpha,\zeta) + c_{\text{work}}(\zeta)$

The surface shows a minimum next to the optimal values of α and ζ.

Starting from the definition of the optimization function, see (6.8), the analyses presented in the following have been carried out in order to obtain the optimal values of α and ζ, within their respective admissible range of variation, see Chapter 3, for each value of μ_{sw}.

The graph below, see Figure 13, shows the optimal values of α for each value of μ_{sw}. Note that the maximum value of α is about $70°$. In fact, even though the condition $\alpha = 90°$ maximizes the use of steel bars, since $\bar{v}_D = \mu_{sw}$, it is not able to ensure the minimum cost of the solution.

The graph of Figure 14 shows the optimal values of ζ by varying the value of shear demand: it demonstrates that as $\bar{v}_D$ increases, the aspect ratio increases, that is to say that the length of the representative span, L_{rs} becomes smaller and smaller than the depth of the beam.

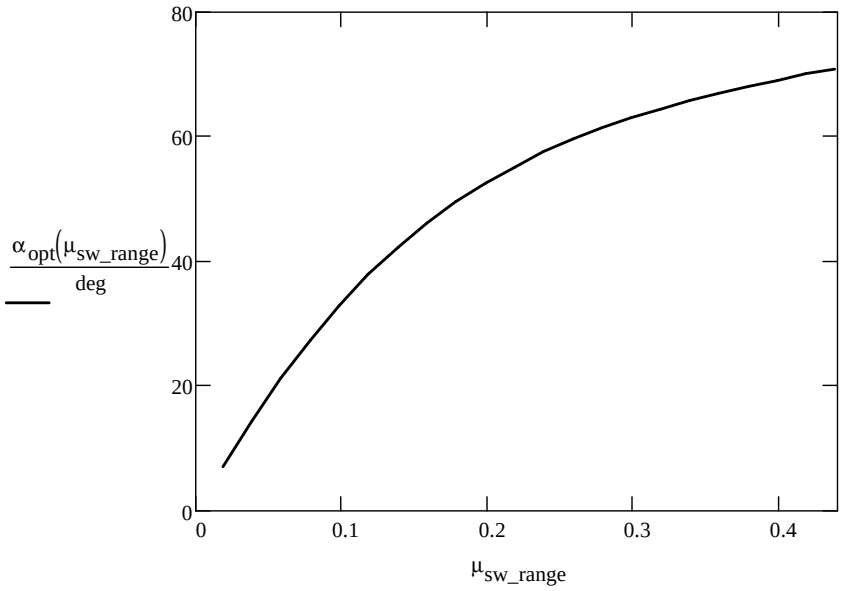

Figure 13. Optimal values of α

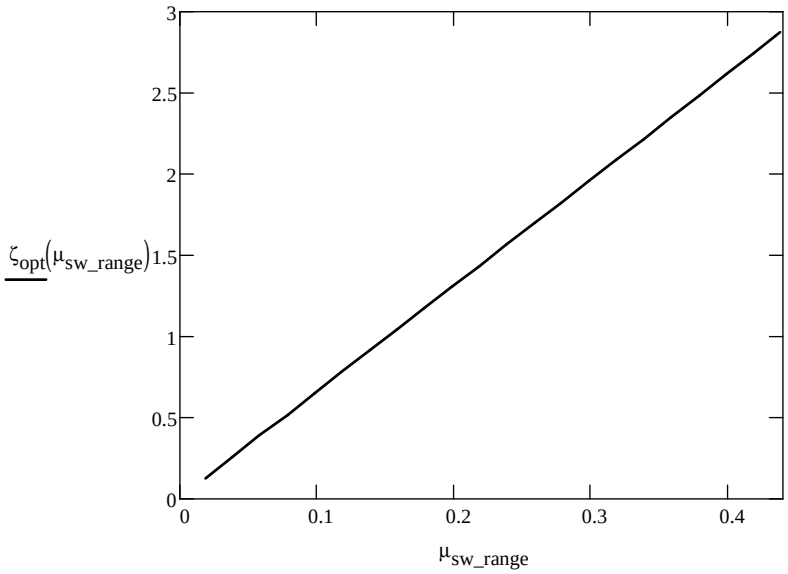

Figure 14. Optimal values of ζ

The graph below, see Figure 15, shows the trend of optimal costs. The function has a minimum for $\mu_{sw} \sim 0{,}10$. It means that, within the admissible range of variation of α and ζ, the values of shear demand included in the range $0{,}05 - 0{,}15$ allow obtaining the minimum value of costs.

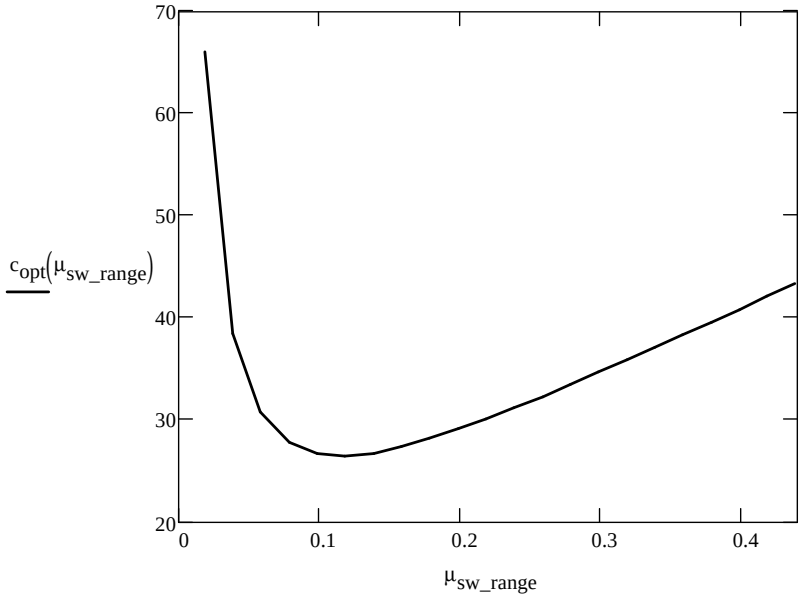

Figure 15. Range of variation of c_{opt}

After the optimization process, the value of stress in concrete elements, rod and strut, has been evaluated in order to verify the following condition:

$$\left.\begin{matrix}\overline{n_R}\left(\mu_{sw},\alpha_{opt},\zeta_{opt}\right)\\ \overline{n_S}\left(\mu_{sw},\alpha_{opt},\zeta_{opt}\right)\end{matrix}\right\}\leq\eta \tag{6.15}$$

where:

$$\eta=\frac{f_c^{'}}{f_c} \tag{6.16}$$

$$f_c^{'}=0,6\,f_c\left(1-\frac{f_c}{250}\right) \tag{6.17}$$

η is a reduction factor accounting for the biaxial stress state of concrete. The Model Code, see Regan [67], provides a formulation to evaluate the strength of concrete elements as a function of the uniaxial strength of concrete.

The values of $\overline{n_R}$ and $\overline{n_S}$ for each optimal solution have been evaluated, starting from the formulations of Chapter 3, as follows:

$$\begin{aligned}\overline{n_R}\left(\mu_{sw},\alpha_{opt},\zeta_{opt}\right)&=\frac{\mu_{sw}}{\sin\alpha_{opt}\cdot\sin\theta_R\left(\alpha_{opt},\zeta_{opt}\right)}\cdot\\&\cdot\frac{\overline{K}_R\left(\mu_{sw},\alpha_{opt},\zeta_{opt}\right)}{\left[\overline{K}_R\left(\mu_{sw},\alpha_{opt},\zeta_{opt}\right)+\overline{K}_S\left(\alpha_{opt},\zeta_{opt}\right)\right]}\\ \overline{n_S}\left(\mu_{sw},\alpha_{opt},\zeta_{opt}\right)&=\frac{\mu_{sw}}{\sin\alpha_{opt}\cdot\sin\theta_S\left(\alpha_{opt},\zeta_{opt}\right)}\cdot\\&\cdot\frac{\overline{K}_S\left(\alpha_{opt},\zeta_{opt}\right)}{\left[\overline{K}_R\left(\mu_{sw},\alpha_{opt},\zeta_{opt}\right)+\overline{K}_S\left(\alpha_{opt},\zeta_{opt}\right)\right]}\end{aligned} \tag{6.18}$$

The graph below, see Figure 16, shows that the stress of concrete elements is lower than the set value of $\eta \sim 0,5$ for all the optimal solutions.

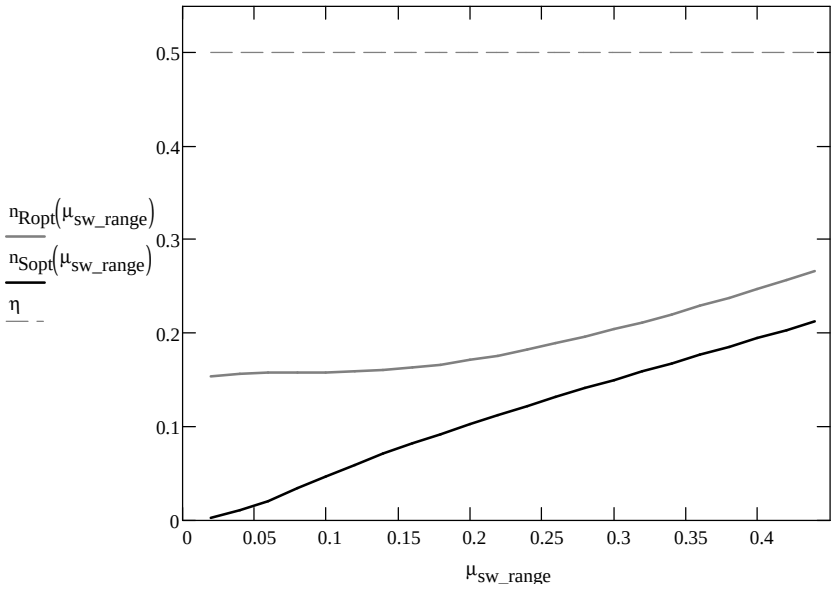

Figure 16. Value of stress in strut and rod.

6.4 Comparison: standard solution – optimum solution

This section deals, both, with the analysis of the design method currently used for CSCBs, and with the comparison between the solution deriving from this standard approach and the solution coming from the proposed mechanical model embedded in the optimization procedure.

The standard shear resistance verification for the ultimate limit state at the 2nd stage is set as follows:

- the contribution of concrete is neglected in the evaluation of shear resistance;
- the stress of shear tensile bars is compared to the yield stress of steel;
- the stress of compressive steel bars is compared to the yield stress and no lateral buckling verification is carried out[8];
- the arrangement of the shear reinforcement is set following standard shapes: the angles of truss are usually equal, $\alpha = \theta$, and the aspect ratio varies in the following range: $0,5 \leq \zeta \leq 1$.

Therefore, the shear mechanical model at the 2nd stage is a statically determinate one, made up of steel elements and the yield of steel bars is set as the collapse condition.
Following this design approach, the amount of materials depends on the span of the beam and the shear demand and does not allow controlling the value of stress in concrete elements.

Starting from a real set of data – shear demand, mechanical characteristics of materials and geometrical quantities – the design solution obtained by means of the method explained above has been compared to the solution

[8] For the evaluation of the compressive resistance the coefficient $\gamma_{M0} = 1,05$ is taken into account, according to National Code [5].

obtained by means of the proposed model and of the optimization function.

In detail, the mechanical reinforcement ratio of the "standard solution" has been evaluated as follows:

$$\mu_{sw}(\zeta) = n_f \cdot \frac{\pi}{2} \cdot \frac{\phi^2}{b_w \cdot z} \cdot \zeta \Rightarrow \mu_{sw}(1,25) = 0,108 \tag{6.19}$$

where:

- $\phi = 18\ mm$
- $b_w = 300\ mm$
- $z = 500\ mm$
- $\alpha = \theta = 54,46°$
- $L = 5850\ mm$

All the design data have been entered in the optimization code, see Eq. (6.8), and the value of the mechanical reinforcement ratio, see Eq. (6.19), has been entered in the simplified model as the value of shear demand.

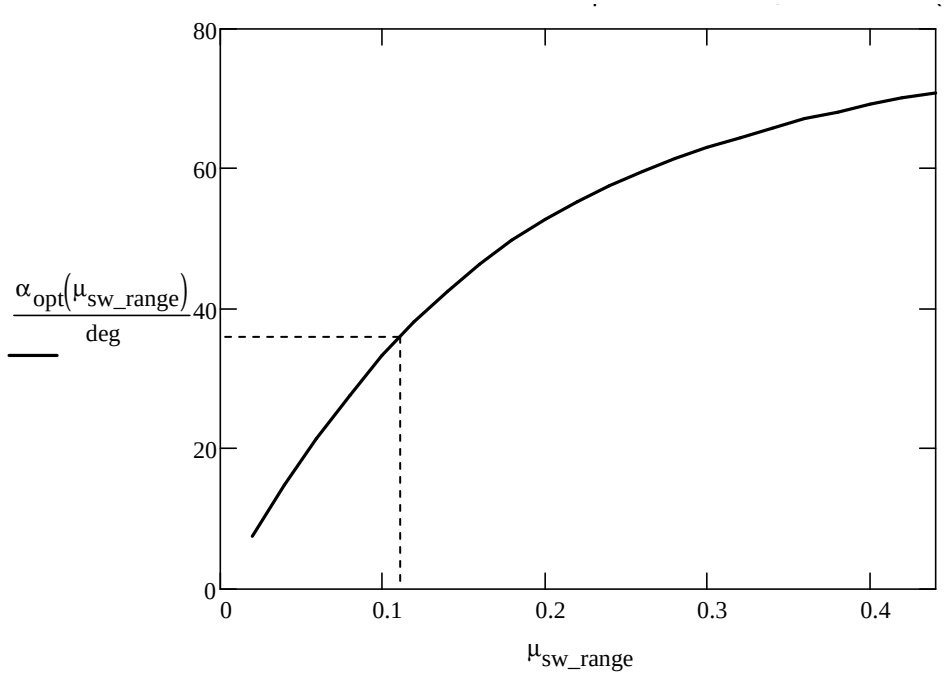

Figure 17. α_{opt}

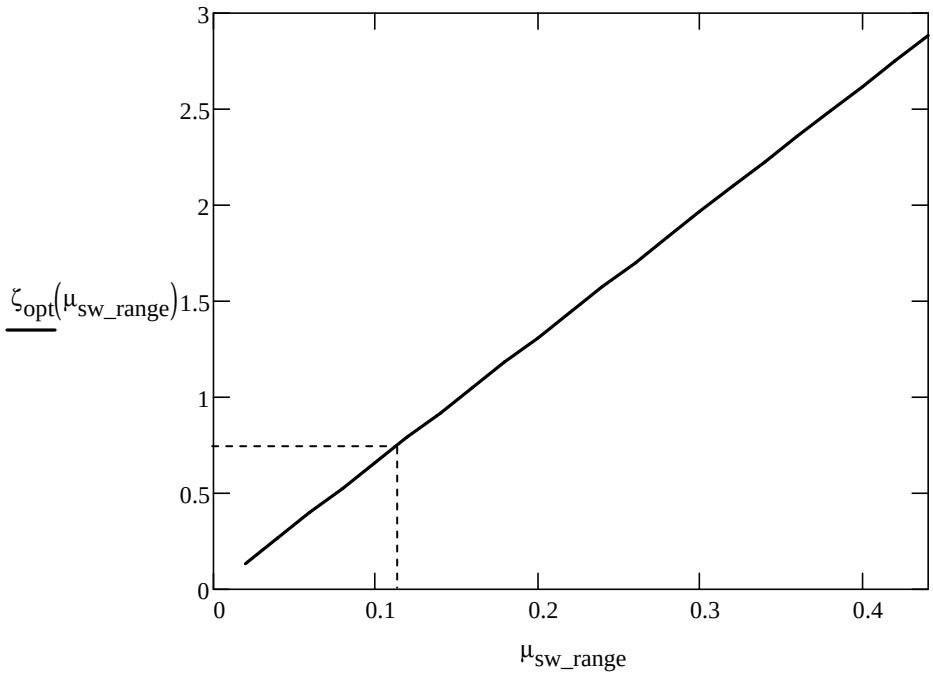

Figure 18. ζ_{opt}

The optimal arrangement of the reinforcement, see Figure 17 and Figure 18, can be described by:

- $\alpha \sim 40°$
- $\zeta \sim 0,75$

The function (6.10) gives the following value:

$$\begin{aligned} &c_{\text{opt}}\left(\mu_{sw}\right) = c_{\text{tot}}\left(\mu_{sw}, \alpha_{opt}\left(\mu_{sw}\right), \zeta_{opt}\left(\mu_{sw}\right)\right) \Rightarrow \\ &c_{\text{opt}}\left(0{,}108\right) = c_{\text{tot}}\left(\mu_{sw}, \alpha_{opt}\left(\mu_{sw}\right), \zeta_{opt}\left(\mu_{sw}\right)\right) = 26{,}9 \end{aligned} \tag{6.20}$$

for the standard solution, $c_s = 29{,}8$.

Therefore the optimal solution allows reducing the cost of the overall beam by 11%.

Moreover, as stated in the previous section, the simplified model permits to control the stress of concrete elements.

Referring to the optimum solution, see Figure 18, the value of stress is lower than the limit of the Eq. (6.16)[9].

19

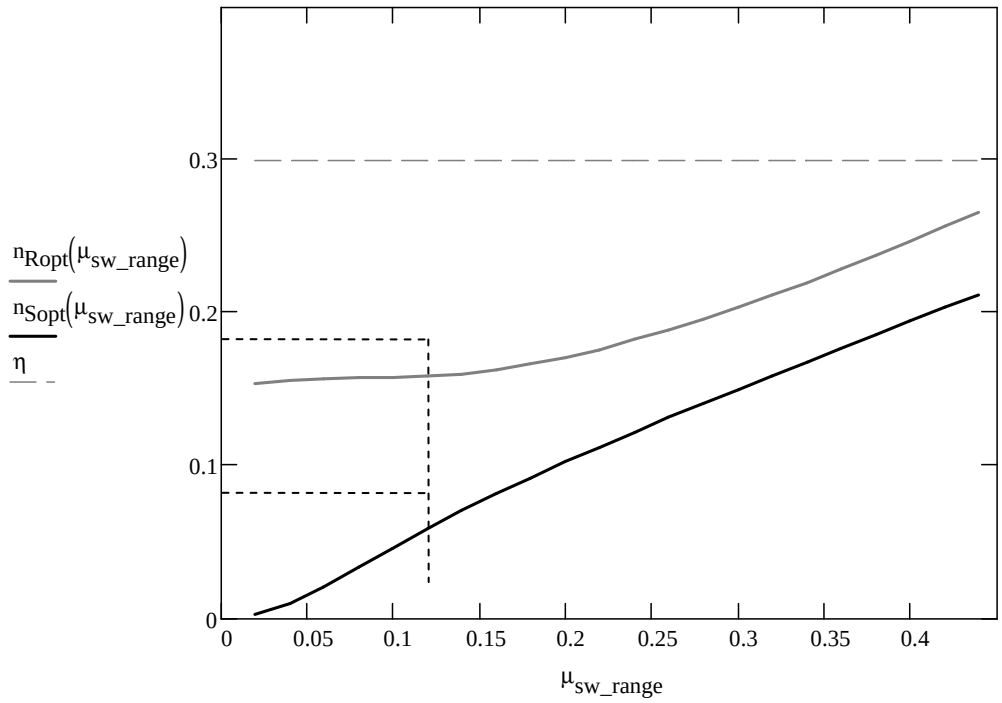

Figure 20. Control of stress in concrete elements.

[9] $C16/20 \rightarrow f_c^{'} = 16,6\ MPa$

Chapter 7
Conclusions

The developed research dealt with the study of shear resisting mechanisms in Composite Steel – Concrete Beams, in order to define a reliable mechanical model and formulations for Ultimate and Serviceability Limit State verifications.

As for today, neither National nor International Codes provide a formulation for the evaluation of shear resistance in Composite Steel-Concrete Beams (CSCB).

The Italian Code (Decreto Ministeriale of January 14th, 2008, at paragraph 4.6 [5]) numbers these structures among the constructions made of other materials, stating that for their use it is necessary to require an official

authorization to the Servizio Tecnico Centrale on the judgment of the Superior Council of Public Works.
Moreover, in spite of the wide use of these structures since about forty years, neither Codes nor a reliable bibliography provide proper mechanical models or design formulations.
Therefore, the first step of the study dealt with a comparative analysis between mechanical models and Codes' provisions of well-known structures - reinforced concrete structures and steel and concrete composite structures - and the CSCBs in order to find similarities and differences.

The deepening of the theory behind the formulations provided by Codes clarified that none of the existing models is able to reproduce the mechanical behavior of CSCBs. Moreover, the analysis of the theoretical approach of the National Code for reinforced concrete structures, based on the Lower bound Theorem within the framework of Plasticity Theory, brought out some critical aspects mainly related to the non-fulfillment of the "equilibrium condition" and of the requirement of pseudo-ductile shear behavior.

This led to the development of a new simplified mechanical model, capable of predicting the yield of shear steel bars and the corresponding stress in concrete elements.
Since unlike the variable angle model for reinforced concrete structures, the mechanical model of a CSCB is fixed by the topology of steel truss, the tensile and compressive shear resistance depends on the mechanical characteristics of the beam and the geometrical arrangement of the steel truss. This allowed considering a "representative substructure" for the definition of the shear model and the resistance of the overall CSCB.
The proposed model stems for a variational approach (Principle of Minimum Potential Energy), able to meet both the compatibility and the equilibrium conditions and it is capable of:

- describing the shear behavior of CSCB;

- setting the pseudo-ductile shear behavior;
- allowing cracking control (SLS) of compressive elements and lateral buckling verification;

Starting from this substructure, a design procedure, based on the capacity design criterion, has been defined, which seeks the equality between shear demand and tensile shear capacity, while verifying crushing of concrete compressive elements and lateral buckling of compressive steel bars.
In the application of the capacity design criterion, this setting of the model allows considering the capacity of the tensile elements as the externally acting force that must be equilibrated by the compressive elements.

The next step of the work dealt with the development of a parametric stiffness matrix of a CSCB, embedded in a worksheet able to evaluate stresses and strains of each element of beam, the collapse load and the pseudo-ductile or brittle behavior of the structural element.
This model allowed verifying the reliability of the results coming from the simplified model: the correlation studies showed a significant agreement between the results coming from the simplified and the complete models, since the simplified one is able to predict the state of stress of the compressive elements: therefore the assumption of infinite stiffness of the upper chord does not significantly affect the results of the simplified model.

Afterwards, experimental tests on full-scale beams have been conceived and conducted in order to verify the validity of the collapse criterion, which underpins the proposed design methodology.
The comparison between the experimental evidence and the results of the simplified mechanical model confirmed the validity of the collapse criterion, since, for all tests, the ultimate limit load has been reached for tensile steel bars yielding. Moreover, the comparison between the value of

stress of compressive elements coming from the model and the tests confirmed the reliability of the simplified model.

Starting from the validation of the simplified model, an optimization procedure of beams' shape has been proposed able to guarantee a pseudo-ductile shear behavior, the maximum contribution of concrete in the resistance system and the minimum amount of material.
In detail, the analysis of the shear behavior by means of the structural simplified model showed that the arrangement of the reinforcement of the beam can be completely described referring to three independent parameters: μ_{sw}, α and ζ. Therefore, the optimization criterion has been defined as follows:
given the shear demand, expressed as a function of the shear demand $\overline{V}_D$, the optimal solution, defined by α and ζ, is the one minimizing the amount and the related cost of materials and labor, where the cost of materials c_{steel} depends on the amount of shear steel and of labor c_{work} on the number of weldings and bendings.

The further step of the work dealt with the comparison between the solution deriving from the design method nowadays adopted and the solution coming from the proposed mechanical model embedded in the optimization procedure. The analyses of the results showed that the optimal solution allows reducing the cost of the overall beam by 11%.
Moreover, since the simplified model permits controlling the stress of concrete elements, it has been possible to verify also the increase of stress in concrete elements for optimal solutions.

Therefore, the developed research brought to the development of mechanical models and design procedure that are much more reliable than the ones proposed by Codes: they are able to always guarantee the pseudo-ductile shear behavior of structures since the yield of steel becomes the

base condition of design and optimization and to allow controlling of stress and strain in compressive elements.

As for future scenarios, this work can be the basis for the development of an optimization procedure of the overall beam: shear and flexure reinforcement.

Bibliography

[1] Fenwick R.C. and Paulay T., “Mechanisms of Shear Resistance of Concrete Beams”, Journal of the Structural Division, ASCE, Vol. 94, ST10, October 1968, pp. 2235-2350;

[2] Hibbeler, R.C., “Structural analysis” sixth edition, Pearson Prentice Hall, Singapore, 2006;

[3] Park R., Paulay. T., “Reinforced concrete structures”, John Wiley & Sons, New York, 1975;

[4] Beeby A. W., Narayanan R. S., “Designers' Guide to EN 1992-1-1 and EN 1992-1-2. Eurocode 2: Design of concrete structures. Genera rules and rules for buildings and structural fire design” Thomas Telford Publishing, Londra;

[5] Ministero delle Infrastrutture, D.M. 14.01.2008, Norme tecniche per le costruzioni;

[6] Legge 05.11.1971 n. 1086, Norme per la disciplina delle opere di conglomerato cementizio armato, normale e precompresso ed a struttura metallica;

[7] Legge 02.02.1974 n. 64, Provvedimenti per le costruzioni con particolari prescrizioni per le zone sismiche;

[8] Circolare del Ministero delle Infrastrutture e dei Trasporti 2 febbraio 2009 n. 617, Istruzioni per l’applicazione delle “Nuove Norme tecniche per le Costruzioni” di cui al Decreto Ministeriale 14 gennaio 2008;

[9] UNI EN 1990 -1 -1, EUROCODE 0 – Basis of structural design;

[10] UNI EN 1992 -1 -1, EUROCODE 2 – Progettazione delle strutture in calcestruzzo – Parte 1-1: Regole generali e regole per gli edifici. Novembre 2005;

[11] UNI EN 1993 1-1-EUROCODE 3 - Progettazione delle strutture di acciaio - Parte 1-1: Regole generali e regole per gli edifici. Agosto 2005;

[12] UNI EN 1994 1-1-EUROCODE 4 - Progettazione delle strutture composte acciaio-calcestruzzo - Parte 1-1: Regole generali e regole per gli edifici. Agosto 2005;

[13] Mezzina M., Raffaele D., Vitone A., "Teoria e Pratica delle costruzioni in cemento armato" Vols. 1 and 2, CittàStudiEdizioni, Torino, 2007;

[14] Ang A. H-S, Tang W.H. "Probability concepts in Engineering Planning and design" Volume I, Basic Principles, JOHN WILEY & SONS, Canada, 1975;

[15] Southwell R. V. Castigliano's "Principle of Minimum Strain-Energy", Proceedings of the Royal Society of London. Series A, Mathematical and Physical Sciences Vol. 154, No. 881 (Mar. 2, 1936), pp. 4-21;

[16] Dentamaro C., Uva G., Vitone V., "L'analisi elastica degli elementi in cemento armato normale" in "Costruire con il cemento armato" a cura di M. Mezzina, Utet, Torino, 2001, ISBN 88-7750-658-X;

[17] Connor J. J., "Analysis of structural member systems", The Ronald Press Company, New York, 1976;

[18] Leonhardt F., Mönnig E., "C.a. & c.a.p. calcolo di progetto e tecniche costruttive", Voll. 1-2-3, Edizioni Tecniche ET, Milano, 1977;

[19] Regan P., "Ultimate limit state principles", in "Fib Bullettin n.2: Structural concrete volume 2", Sprint-Druck, Stuttgart, 1999;

[20] Leonhardt F, "Reducing the shear reinforcement in reinforced concrete beams and slabs", Magazine of concrete research, Vol.17, n.53, December 1965, pp.187-198;

[21] Wong M.Bill, "Plastic analysis and design of steel structures" Elsevier, United States of America, 2009, ISBN: 978-0-7506-8298-5;

[22] Nielsen, M. P. "Limit Analysis and Concrete Plasticity" (2nd ed.), Boca Raton, Florida: CRC Press, 1998;

[23] Brenni P., "Il comportamento al taglio di una struttura a sezione mista in calcestruzzo a getti successivi" Istituto d'Ingegneria Strutturale Politecnico Federale Zurigo, Zurigo, 1995;

[24] E. Mörsch, "Teoria e pratica del cemento armato", a cura di L. Santarella, Milano, Hoepli, 1923;

[25] Sadd Martin H., "Elasticity. Theory, Applications, and Numerics" (2nd edition), Academic press, Burlington USA, 2009;

[26] Petrone F., Liotta M., Marano G.C., Trentadue F., Monti G., "Studio sperimentale per la valutazione del contributo del calcestruzzo nella resistenza a taglio delle travi reticolari miste" XIV Convegno di Ingegneria Sismica - ANIDIS, Bari, 2011;

[27] Duthinh Dat, Carino Nicholas J., "Shear design of high-strength concrete beams: a review of the state of art", Building and Fire Research Laboratory National Institute of Standards and Technology, Gaithersburg, 1996;

[28] Collins Michael P., Mitchell Denis, Adebar Perry, Vecchio Frank J., "A general shear design method", ACI Structural Journal, Michigan, USA, January-February 1996, pp 36-60;

[29] Ramirez Julio A., Breen John E., "Evaluation of a modified truss-model approach for beams in shear", ACI Structural Journal, Michigan, USA, September-October 1991, pp. 562-571;

[30] Vecchio Frank J., Collins Michael P., "Predicting the response of reinforced concrete beams subjected to shear using modified compression field theory", ACI Structural Journal, Michigan, USA, May-June 1988, 258-268;

[31] Bentz Evan C., Vecchio Frank J., Collins Michael P., "Simplified modified compression field theory for calculating shear strength of reinforced concrete elements", ACI Structural Journal, Michigan, USA, July-August 2006, 614-624;

[32] Kaufmann Walter, Marti Peter, "Structural concrete: cracked membrane model", ASCE;

[33] Kaufmann Walter, “Strength and deformation of structural concrete subjected to in-plane shear and normal forces” Institute of Structural Engineering Swiss Federal Institute of Technology Zurich, Zurich, July 1998;

[34] Prager, W., “Limit Analysis: the Development of a Concept” Problems of Plasticity, edited by A. Sawczuk, Nordhoff International, Leyden, The Netherlands, 1974, pp. 3-24;

[35] Chen, W.F., “Limit Analysis and Soil Plasticity”, Developments in Geotechnical Engineering, Vol. 7, Elsevier, Amsterdam, 1975, 638 pp.;

[36] Hsu Thomas T. C. and Mo Y. L., “UNIFIED THEORY OF CONCRETE STRUCTURES” WILEY, A John Wiley and Sons, Ltd., Publication University of Houston, USA, 2010;

[37] Schlaich J., Schäfer K., Jennewin M., “Toward a consistent design for structural concrete”, PCI Journal, Vol. 32, n.3, 1987, pp.75-150;

[38] Schlaich J., Schäfer K., “Desaign and Detailing using Strut and Tie Models, Workshop, Tainan 1996, Strut and Tie Models for the Design of Structural Concrete, Report;

[39] Kupfer H. and Baumann T., “Staffelung der Biegezugbewehrung bei hohen Schubspannungen in Schlanken Stahlbetontragern mit I – Querschnitt”, Beton-und Stahlbetonbau, Vol.64, December 1969, pp.278-283;

[40] William K., Hansen E. and Kang H.D. “Performance evaluation of damage and plasticity formulations for concrete” Modeling of inelastic behavior of RC structures under seismic loads, edited by P. Benson Shing and Tada-Aki Tanabe, ASCE, SEI, USA, 2001;

[41] Rose B.D., Shing P.B., Spacone E. and William K.J., “A reinforced concrete model for analyzing inelastic behavior of RC members” Modeling of inelastic behavior of RC structures under seismic loads, edited by P. Benson Shing and Tada-Aki Tanabe, ASCE, SEI, USA, 2001;

[42] Sotelino E. D. and Chen Wai-Fah., “Modeling and simulation of concrete materials” Modeling of inelastic behavior of RC structures

under seismic loads, edited by P. Benson Shing and Tada-Aki Tanabe, ASCE, SEI, USA, 2001;

[43] Jirásek Milan, Bažant Zdeněk P., "Inelastic analysis of structures", JOHN WILEY & SONS, LTD, England, 2001;

[44] Cook W.D. and Mitchell D., "Studies of disturbed regions near discontinuities in reinforced concrete members", ACI Structural Journal, V.85, No. 2, Mar. – Apr. 1988, pp. 206-2016;

[45] Adebar P. and Collins M.P., "Shear strength of members without transverse reinforcement", Canadian Journal of Civil Engineering, V.23, No.1, Feb. 1996, pp. 30-41;

[46] Roller J. J. and Russel H. G., "Shear strength of high-strength concrete beams with web reinforcement" ACI Structural Journal, V.87, No.2, Mar.-Apr. 1990, pp. 191-198;

[47] Thurlimann B., "Shear strength of reinforced and prestressed concrete beams CEB approach", Technical report, ACI Symposium 1976, Feb. 1977, Revised copy, 33 pp.;

[48] Nielsen M. P. and Braestrup N. W., "Plastic shear strength of reinforced concrete beams", Technical report No.3, Bygningsstatiske Meddelelser, 1975, V. 46;

[49] Leonhardt F. and Walther R., "Tests on T-Beams under severe shear load conditions", Bullettin No. 156, Deutscher Ausschuss fur Stahlbeton, Berlin, 1962, 71 pp.;

[50] Leonhardt F. and Walther R., "Shear tests on T-Beam with varying shear reinforcement", Bullettin No.156, Deutscher Ausschuss fur Stahlbeton, Berlin, 1962, 84 pp.;

[51] Mattock A.H., "Diagonal tension cracking in concrete beams with axial forces", Journal of the structural division, Proceedings ASCE, V. 95, No. ST9, Sept. 1969, pp. 1887-1990;

[52] Vecchio F.J. and Collins M.P., "The Modified Compression-Field Theory of reinforced concrete elements subjected to shear", ACI Jurnal, Proceedings V. 83, No.2, Mar.-Apr. 1986, pp.219-231;

[53] Wong P.S.-L., "User Facilities for Two-Dimensional Nonlinear Finite Element Analysis of Reinforced Concrete", MASc thesis, Department of Civil Engineering, University of Toronto, Toronto, Ontario, Canada, 2002, 213 pp;

[54] ACI Committee 318 (2008) 'Building Code Requirements for Reinforced Concrete (ACI 318-08),' American Concrete Institute, Detroit, MI;

[55] Colajanni P., La Mendola L., Monaco A., "Modelli per l'interpretazione dei risultati di prove di push-out su travi reticolari miste", XIV Convegno di Ingegneria Sismica - ANIDIS, Bari, 2011;

[56] Desiderio G., Latour M., Rizzano G., "Modellazione Analitica e FEM del Meccanismo di trasferimento degli sforzi tra Fondello in Acciaio e Calcestruzzo nelle Travi Tralicciate Miste", XIV Convegno di Ingegneria Sismica - ANIDIS, Bari, 2011;

[57] Brunesi E., Bellotti D., Bolognini D., Nascimbene R. "Sviluppo di modelli per la definizione della rigidezza equivalente di differenti configurazioni di travi tralicciate", XIV Convegno di Ingegneria Sismica - ANIDIS, Bari, 2011;

[58] Cancelli A. N., Aiello M., "Connessione Acciaio – Calcestruzzo nelle Travi Reticolari Miste: Prove di Push-Out", XIV Convegno di Ingegneria Sismica - ANIDIS, Bari, 2011;

[59] "Shar and Diagonal Tension", pt.2, ACI-ASCE Committee 326, J. ACI, vol. 59, no. 2, 1962, pp. 277-333;

[60] Bresler B. and MacGregor J.G. "Review of Concrete Beams Failing in Shear", J. Struct. Div., ASCE, vol. 93, no. ST1, 1967, pp. 343-372;

[61] "The Shear Strength of Reinforced Concrete Members", ASCE-ACI Committee 426, Proc. ASCE, vol. 99, no. ST6, 1973, pp. 1091-1187;

[62] Collins M.P., "Toward a Rational Theory for RC Members in Shear", J. Struct. Div., ASCE, vol. 104, no. ST4, April 1978, pp. 649-666

[63] Nilson H. Arthur, Darwin David, Dolan Charles W., "Design of Concrete Structures" 13th edition, Mc Graw Hill, New York, NY, 2004;

[64] Reddy J. N., "Energy principles and variational methods in applied mechanics", John Wiley & Sons, inc., USA, 2002;

[65] UNI EN 1998 1-1-EUROCODE 8 - Progettazione delle strutture per la resistenza sismica. Parte 1: Regole generali, azioni sismiche e regole per gli edifici. Marzo 2005;

[66] Rabbat Basile G. and Collins Michael P. , "A Variable Angle Space Truss Model for Structural Concrete Members Subjected to Complex Loading", ACI Structural Jurnal, Michigan, USA, August , 1978;

[67] Regan P. E., "Research on shear: a benefit to humanity or a waste of time?" The Structural Engineer, Volume 71, No 19, 5 October 1993;

[68] Consiglio Superiore dei Lavori Pubblici "Procedure per il rilascio dell'autorizzazione all'impiego di travi tralicciate in acciaio conglobate nel getto di calcestruzzo collaborante (punto 4.6 DM 14/01/2008)" 2009;

[69] Taylor H. P. J., "Investigation of the Dowel Shear Forces Carried by the Tensile Steel in Reinforced Concrete Beams", Cement and Concrete Association, London, TRA 431, 1969, 24 pp.;

[70] H. P. J. Taylor, "Investigation of the Forces Carried Across Cracks in Reinforced Concrete Beams in Shear by Interlock of Aggregate", Cement and Concrete Association, London, TRA 42.447, 1970, 22 pp.;

[71] Paulay T. and Loeber P. J., "Shear Transfer by Aggregate Interlock", Shear in Reinforced Concrete, ACI Special Publication 42, Vol. 1, Detroit, 1974, pp. 1-15;

C) 1 CAMPIONE (2 prove)

MATERIALI		
Acciaio S355	F_{yk} = 355 N/mm²	F_{tk} = 510 N/mm²
Calcestruzzo	C32/40	

STRUTTURA TRALICCIO	
PIATTO INFERIORE	300x6 L=3500
CORRENTI SUPERIORI TRAVE	3ϕ24 L=3400
ANIME TRAVE	**2ϕ12** 7x400 + 2x350
TERMINALE	2 ϕ 24 L=500
BARROTTO TRASVERSALE	1 ϕ 20 L=400

*Barrotto trasversale saldato inferiormente al piatto di acciaio, utilizzato per il sollevamento della trave

D) 1 CAMPIONE (2 prove)

MATERIALI		
Acciaio S355	F_{yk} = 355 N/mm²	F_{tk} = 510 N/mm²
Calcestruzzo	C32/40	

STRUTTURA TRALICCIO	
PIATTO INFERIORE	300x6 L=3500
CORRENTI SUPERIORI TRAVE	3ϕ32 L=3400
ANIME TRAVE	2ϕ20 7x400 + 2x350
TERMINALE	2ϕ32 L=500
BARROTTO TRASVERSALE	1 ϕ 20 L=400

*Barrotto trasversale saldato inferiormente al piatto di acciaio, utilizzato per il sollevamento della trave

Prove di comportamento a taglio - TRALICCIO GETTATO

C) 1 CAMPIONE (2 prove)

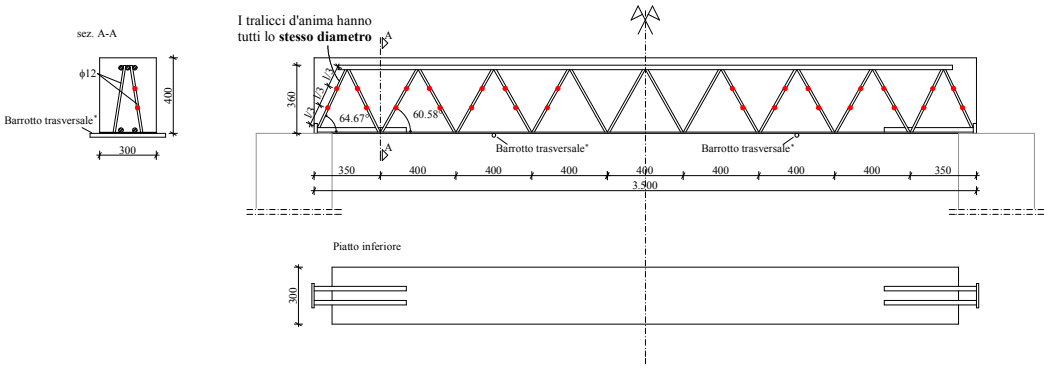

• **posizione singolo strain gauge**

D) 1 CAMPIONE (2 prove)

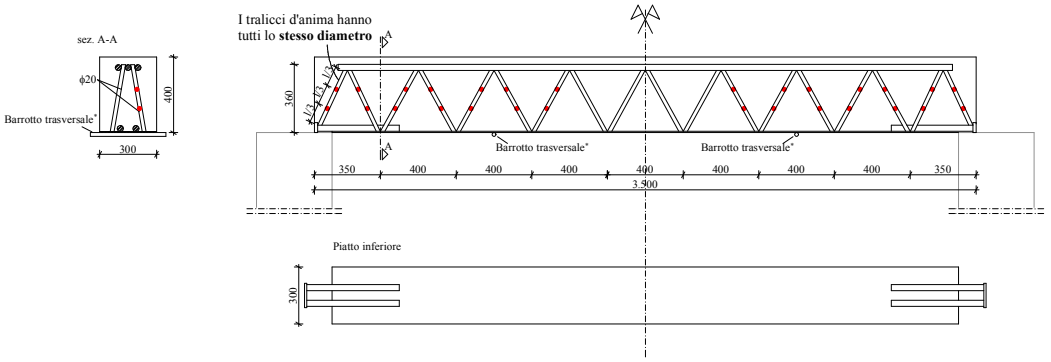

• **posizione singolo strain gauge**

Scala 1:20

1. Sample C

1-5 INF CH 0	1-4 INF CH 2	6-4 SUP CH 5	6-8 INF CH 6	9-8 INF CH 10	9-11 INF CH 12	12-11 INF CH 14	1-2 INF CH 16	6-3 INF CH 20	6-7 INF CH 21	TEMP CH 22	CELLA 500 KN CH 23	50 MM CH 24	100 MM CH 25
µm/m	µm/m	µm/m	µm/m	µm/m	µm/m	µm/m	µm/m	µm/m	µm/m	µm/m	kN	mm	mm
0	0	0	1	0	0	0	0	0	0	0,5	0	0	0
-6	13	-1	0	2	0	0	-3	-1	-1	-0,7	4,89	-0,03	-0,03
-9	18	-2	0	3	0	1	-4	-1	-1	-0,7	6,48	-0,06	-0,04
-10	19	-1	0	3	0	1	-4	-2	-1	-0,7	6,78	-0,06	-0,04
-48	160	-6	2	42	-5	9	-26	-8	-7	-1,4	29,22	-0,41	-0,34
-51	176	-6	3	45	-6	11	-28	-9	-8	-1,4	31,41	-0,44	-0,38
-56	197	-6	3	50	-7	13	-31	-10	-9	-1,1	34,56	-0,49	-0,42
-68	242	-7	6	60	-9	22	-40	-12	-11	-1,4	42,81	-0,62	-0,54
-71	251	-8	7	62	-10	24	-43	-12	-11	-1,4	44,55	-0,64	-0,57
-75	265	-8	8	66	-11	28	-46	-13	-12	-1,4	47,49	-0,69	-0,62
-79	279	-8	8	69	-11	32	-50	-13	-12	-1,6	50,13	-0,73	-0,66
-87	307	-9	11	75	-12	40	-58	-15	-13	-1,1	55,95	-0,82	-0,75
-94	333	-9	13	80	-13	47	-65	-15	-14	-1,1	60,48	-0,88	-0,82
-96	342	-9	14	82	-13	50	-68	-16	-14	-1,1	62,22	-0,91	-0,83
-156	579	-16	38	125	-20	129	-159	-27	-21	-0,5	116,58	-1,63	-1,53
-157	585	-16	39	126	-20	131	-162	-27	-21	-0,7	118,08	-1,65	-1,56
-159	592	-16	40	128	-21	134	-165	-27	-22	-0,5	119,94	-1,67	-1,58
-160	600	-16	40	129	-21	137	-168	-28	-22	-0,5	121,98	-1,69	-1,61
-162	607	-16	41	130	-21	139	-171	-28	-22	-0,5	123,72	-1,72	-1,64
-163	613	-17	42	131	-21	141	-174	-29	-22	-0,7	125,43	-1,73	-1,66
-165	619	-17	42	132	-21	144	-177	-29	-22	-0,7	127,14	-1,75	-1,69
-166	626	-17	43	133	-21	145	-180	-29	-22	-0,7	128,7	-1,78	-1,71
-167	632	-17	44	134	-21	147	-183	-29	-23	-0,7	130,38	-1,79	-1,74
-168	637	-17	44	135	-22	149	-185	-30	-23	-0,5	131,61	-1,81	-1,75
-170	645	-18	45	137	-22	152	-188	-30	-23	-0,7	133,71	-1,83	-1,78
-172	650	-18	45	138	-22	154	-191	-30	-23	-0,7	135,18	-1,85	-1,81

-174	662	-18	47	139	-22	158	-195	-31	-24	-0,7	138,33	-1,88	-1,84
-179	685	-19	49	143	-23	166	-205	-32	-24	-0,9	144,78	-1,96	-1,94
-183	705	-19	51	147	-24	173	-213	-33	-24	-0,7	150,03	-2,02	-2,01
-186	721	-20	52	149	-24	179	-219	-34	-25	-0,7	154,41	-2,07	-2,08
-190	741	-20	54	152	-25	186	-227	-35	-25	-0,5	159,96	-2,13	-2,16
-195	762	-21	55	156	-25	194	-235	-36	-26	-0,7	165,72	-2,20	-2,24
-325	1344	-37	78	275	-43	415	-400	-68	-37	-0,7	330,06	-3,97	-4,51
-326	1345	-37	78	276	-43	416	-400	-68	-37	-0,9	330,51	-3,97	-4,51
-327	1352	-37	78	278	-43	417	-402	-68	-37	-0,9	331,89	-3,99	-4,53
-328	1353	-37	78	278	-43	417	-402	-68	-37	-0,9	331,98	-4,00	-4,53
-331	1362	-37	77	280	-43	419	-405	-69	-37	-1,4	333,81	-4,02	-4,56
-333	1375	-37	78	285	-43	425	-407	-70	-37	-1,4	337,86	-4,05	-4,61
-336	1391	-38	80	289	-44	432	-410	-71	-38	-2,1	342,51	-4,10	-4,66
-338	1393	-38	79	289	-44	433	-412	-71	-38	-2,3	343,08	-4,11	-4,68
-350	1462	-40	83	308	-46	467	-426	-75	-38	-3,4	364,32	-4,30	-4,94
-353	1479	-40	84	312	-46	475	-429	-75	-39	-3,4	369,24	-4,35	-5,01
-361	1512	-41	87	320	-47	491	-438	-77	-40	-3,4	378,87	-4,46	-5,14
-362	1515	-41	87	321	-47	491	-439	-77	-40	-3,4	379,08	-4,46	-5,14
-372	1560	-43	89	335	-48	511	-449	-80	-40	-3,9	391,14	-4,58	-5,31
-380	1607	-44	92	348	-49	533	-458	-83	-41	-3,4	404,28	-4,71	-5,47
-388	1638	-45	94	355	-50	545	-467	-84	-41	-3,0	411,63	-4,80	-5,59
-398	1681	-46	97	368	-51	565	-477	-86	-41	-2,3	423,27	-4,92	-5,74
-404	1710	-47	100	376	-52	582	-484	-88	-41	-2,3	432,81	-5,03	-5,87
-560	1773	-60	181	481	-58	745	-595	-195	15	-2,1	505,89	-6,31	-7,26
-577	1745	-60	184	485	-58	750	-601	-197	17	-1,6	507,6	-6,36	-7,31
-626	1696	-62	192	496	-59	764	-626	-200	24	-1,8	514,5	-6,53	-7,47
-657	1672	-62	197	502	-59	771	-653	-202	29	-1,4	517,47	-6,63	-7,56
-766	1785	-64	206	503	-60	776	-767	-207	45	-2,5	518,46	-6,93	-7,76
-779	1784	-64	208	507	-60	780	-764	-208	48	-2,5	520,35	-7,01	-7,82
-797	1749	-64	210	493	-60	765	-785	-208	53	-1,8	511,95	-7,08	-7,83
-798	1755	-64	210	494	-59	766	-789	-208	54	-2,1	512,16	-7,08	-7,83
-801	1757	-64	210	494	-59	766	-792	-209	54	-2,3	511,86	-7,08	-7,83

-802	1756	-64	210	494	-59	766	-793	-209	54	-2,3	511,86	-7,08	-7,83
-806	1757	-64	209	501	-60	773	-809	-211	56	-2,3	514,53	-7,14	-7,88
-802	1748	-64	210	497	-60	770	-814	-210	57	-2,7	512,28	-7,16	-7,86
-806	1757	-64	209	497	-60	770	-822	-211	57	-3,0	511,47	-7,17	-7,88
-808	1762	-64	209	497	-60	770	-824	-211	57	-3,0	511,53	-7,18	-7,89
-811	1788	-65	209	507	-60	777	-834	-213	58	-2,3	516	-7,25	-7,96
-811	1774	-64	209	501	-60	771	-841	-212	60	-4,3	512,43	-7,27	-7,97
-811	1774	-64	209	501	-60	771	-841	-212	60	-4,3	512,37	-7,27	-7,97
-811	1773	-64	209	501	-60	771	-841	-212	60	-4,3	512,34	-7,27	-7,97
-811	1773	-64	209	501	-60	771	-842	-212	60	-4,3	512,28	-7,27	-7,97
-825	1818	-65	213	513	-61	780	-889	-215	66	-3,4	517,29	-7,51	-8,15
-827	1831	-66	212	516	-61	784	-892	-216	65	-3,4	519,3	-7,51	-8,16
-828	1801	-64	213	500	-60	767	-894	-213	67	-5,3	510,27	-7,51	-8,10
-837	1918	-67	212	503	-64	771	-911	-221	80	-4,8	507,66	-7,64	-8,13
-755	1386	-48	176	183	-52	481	-817	-195	87	-7,8	358,29	-6,56	-6,53
-747	1364	-47	174	174	-52	473	-809	-194	87	-7,5	352,92	-6,50	-6,45
-741	1356	-47	173	172	-51	470	-804	-194	87	-7,5	351,15	-6,48	-6,43
-11	-285	3	141	36	-2	85	-44	-96	118	-7,8	29,01	-2,33	-1,67
24	-321	4	141	34	0	81	-26	-89	124	-7,8	24,39	-2,22	-1,57
53	-349	5	141	32	2	77	-11	-82	128	-7,8	20,97	-2,13	-1,50
67	-362	5	141	32	2	76	-3	-80	131	-7,8	19,5	-2,09	-1,47
80	-373	6	141	31	3	74	5	-77	132	-7,8	18,33	-2,05	-1,44
89	-381	6	141	31	3	74	10	-76	133	-7,5	17,49	-2,03	-1,41
101	-392	6	141	30	3	72	17	-73	135	-7,5	16,35	-1,99	-1,39
112	-403	7	141	29	4	71	24	-71	136	-7,8	15,18	-1,96	-1,36
118	-408	7	142	29	4	71	27	-70	137	-7,8	14,67	-1,95	-1,35
122	-412	7	142	29	4	70	30	-68	137	-7,8	14,28	-1,94	-1,34
127	-416	7	142	29	4	70	33	-65	138	-7,5	13,98	-1,93	-1,33
177	-468	9	141	25	6	67	58	-57	142	-8,0	7,38	-1,74	-1,18
189	-479	9	141	25	7	65	64	-55	142	-8,2	6,03	-1,70	-1,14
197	-488	9	141	24	7	64	70	-53	143	-8,0	5,04	-1,67	-1,12
205	-495	10	141	24	8	64	74	-52	144	-8,0	4,26	-1,64	-1,09

212	-501	10	141	24	8	63	78	-51	144	-8,2	3,72	-1,62	-1,08
216	-504	10	141	24	8	63	80	-50	145	-8,2	3,39	-1,61	-1,08
284	-549	12	142	22	10	58	127	-36	153	-8,2	0,21	-1,46	-0,95
285	-550	12	142	22	10	58	128	-36	153	-8,2	0,18	-1,46	-0,94
288	-551	12	142	22	10	58	130	-35	153	-8,2	0,12	-1,46	-0,94
291	-553	12	142	21	10	58	133	-35	154	-8,5	0,03	-1,45	-0,94
295	-555	13	143	22	11	58	136	-33	154	-8,7	-0,06	-1,45	-0,94
296	-555	13	143	22	11	58	137	-33	154	-8,5	-0,09	-1,45	-0,94
296	-555	13	143	22	11	58	137	-33	155	-8,7	-0,09	-1,45	-0,94
301	-558	13	143	22	11	58	142	-32	155	-8,2	-0,18	-1,44	-0,94
302	-559	13	143	21	11	58	143	-31	155	-7,8	-0,21	-1,44	-0,93
304	-560	13	143	21	11	58	144	-31	155	-7,8	-0,24	-1,43	-0,92
310	-565	12	143	21	11	57	149	-29	156	-9,4	-0,24	-1,42	-0,91
310	-566	12	143	21	11	57	150	-29	156	-9,4	-0,24	-1,42	-0,91
312	-581	3	135	13	2	41	149	-40	147	-9,1	-0,24	-1,41	-0,90
324	-579	11	143	19	11	55	163	-24	157	-11,0	-0,21	-1,40	-0,89
325	-579	11	144	19	11	54	164	-24	157	-10,5	-0,21	-1,40	-0,88
327	-583	11	145	18	11	54	168	-24	157	-9,8	-0,21	-1,39	-0,86
328	-583	11	144	18	11	53	168	-24	157	-9,8	-0,21	-1,39	-0,87
329	-584	10	144	18	10	49	169	-23	155	-7,8	-0,21	-1,38	-0,87
329	-584	10	144	18	11	49	169	-24	155	-8,0	-0,21	-1,38	-0,87
331	-587	9	144	18	10	49	171	-23	155	-11,2	-0,18	-1,38	-0,97
332	-589	9	143	17	10	48	173	-23	153	-15,3	-0,18	-1,38	-0,99

2. Sample D

_1-2 INF CH 0	_1-5 INF CH 2	_1-3 INF CH 4	_1-4 INF CH 6	_6-3 INF CH 10	_6-4 INF CH 12	_9-7 INF CH 16	_50 MM CH 24	_100 MM CH 25	CARICO TOTALE CH 24
µm/m	µm/m	µm/m	µm/m	µm/m	µm/m	µm/m	mm	mm	KN
29.07.11 11.58.52	29.07.11 11.58.52	29.07.11 11.58.52	29.07.11 11.58.52	29.07.11 11.58.52	29.07.11 11.58.52	29.07.11 11.58.52	29.07.11 11.58.52	29.07.11 11.58.52	29.07.11 11.58.52
-28	-3	19	5	-8	8	-3	-0,30	-0,79	13,83
-29	-3	19	5	-8	9	-3	-0,31	-0,81	14,10
-29	-4	20	5	-9	9	-3	-0,32	-0,83	14,52
-30	-4	21	5	-9	10	-4	-0,35	-0,86	15,03
-32	-4	23	6	-9	10	-4	-0,39	-0,89	15,75
-33	-4	23	7	-9	10	-4	-0,42	-0,91	16,17
-33	-4	24	6	-9	9	-4	-0,43	-0,93	16,32
-33	-4	24	6	-9	10	-4	-0,44	-0,93	16,32
-34	-4	24	6	-10	11	-4	-0,45	-0,93	16,44
-34	-4	24	6	-10	12	-4	-0,45	-0,95	16,74
-35	-4	25	7	-10	12	-4	-0,46	-0,97	17,25
-36	-5	26	7	-11	13	-4	-0,47	-0,99	17,70
-37	-5	27	7	-11	13	-5	-0,49	-1,01	18,18
-38	-4	27	7	-11	13	-5	-0,51	-1,03	18,45
-38	-4	28	8	-11	13	-5	-0,53	-1,03	18,48
-38	-5	28	7	-11	13	-4	-0,54	-1,04	18,36
-37	-5	27	7	-11	13	-5	-0,55	-1,04	18,33
-38	-4	28	7	-11	14	-4	-0,55	-1,04	18,36
-39	-5	28	8	-11	14	-4	-0,55	-1,05	18,90
-40	-5	29	8	-11	15	-5	-0,56	-1,07	19,44
-41	-5	30	8	-12	15	-5	-0,57	-1,09	19,92
-42	-5	31	8	-12	15	-5	-0,58	-1,11	20,28

-42	-5	32	8	-12	15	-5	-0,59	-1,13	20,55
-43	-5	32	9	-12	15	-5	-0,61	-1,14	20,82
-272	-118	242	157	-127	41	110	-2,98	-3,40	182,82
-273	-119	243	158	-128	41	110	-2,99	-3,41	183,72
-274	-120	244	159	-129	41	111	-3,00	-3,43	184,56
-275	-120	245	159	-130	41	112	-3,01	-3,43	185,10
-275	-120	245	160	-130	41	112	-3,02	-3,44	185,43
-276	-120	245	160	-131	41	112	-3,03	-3,44	185,67
-276	-120	245	160	-131	41	112	-3,03	-3,44	185,82
-277	-120	245	161	-131	41	112	-3,03	-3,45	185,97
-277	-121	245	160	-132	40	113	-3,04	-3,45	186,24
-277	-121	246	161	-132	41	113	-3,04	-3,46	186,54
-278	-121	246	161	-133	41	114	-3,05	-3,47	186,66
-278	-121	246	162	-133	41	115	-3,05	-3,48	187,14
-279	-122	247	162	-134	41	114	-3,06	-3,48	187,80
-280	-122	248	163	-134	41	114	-3,06	-3,49	188,43
-280	-122	249	163	-135	40	114	-3,07	-3,50	189,00
-281	-123	250	164	-135	41	115	-3,08	-3,51	189,48
-282	-123	250	164	-136	40	115	-3,08	-3,51	189,93
-282	-123	251	165	-137	40	115	-3,08	-3,52	190,41
-283	-123	251	165	-137	41	115	-3,08	-3,53	190,86
-283	-124	251	165	-138	41	115	-3,09	-3,53	191,16
-284	-124	252	165	-138	41	115	-3,09	-3,54	191,43
-284	-124	252	165	-139	41	115	-3,09	-3,54	191,70
-284	-124	252	165	-139	41	115	-3,10	-3,54	192,03
-285	-124	253	166	-140	41	116	-3,10	-3,55	192,36
-285	-125	253	167	-140	40	116	-3,11	-3,56	192,87
-286	-125	254	167	-141	40	116	-3,12	-3,56	193,38
-287	-125	255	168	-141	40	116	-3,13	-3,57	194,16
-288	-126	256	168	-142	40	117	-3,14	-3,58	195,00
-311	-136	277	186	-162	38	125	-3,35	-3,81	213,12
-312	-136	279	187	-163	38	123	-3,37	-3,83	213,87

-313	-136	280	187	-163	38	121	-3,38	-3,83	214,53
-315	-137	281	188	-164	38	119	-3,38	-3,84	215,55
-316	-138	283	190	-166	38	119	-3,40	-3,86	216,96
-318	-139	285	192	-167	38	117	-3,42	-3,88	218,58
-320	-139	287	193	-168	39	117	-3,43	-3,90	220,11
-322	-140	288	194	-170	39	115	-3,45	-3,92	221,46
-323	-140	290	196	-171	38	115	-3,47	-3,93	222,54
-325	-141	291	197	-173	38	114	-3,47	-3,94	223,62
-326	-141	292	198	-174	38	112	-3,49	-3,96	224,55
-328	-142	293	199	-176	38	112	-3,50	-3,97	225,42
-329	-143	294	200	-177	38	111	-3,51	-3,98	226,23
-330	-143	295	201	-179	38	110	-3,53	-3,99	226,98
-331	-143	296	202	-180	37	109	-3,54	-4,00	227,70
-332	-144	297	203	-181	37	109	-3,55	-4,01	228,45
-345	-148	308	213	-195	34	104	-3,66	-4,12	237,00
-345	-148	308	214	-195	34	104	-3,66	-4,13	237,36
-345	-149	308	214	-197	34	104	-3,66	-4,13	237,66
-346	-149	308	215	-197	34	104	-3,67	-4,14	238,20
-347	-149	309	215	-198	34	104	-3,67	-4,14	238,83
-347	-149	310	216	-200	34	104	-3,68	-4,15	239,40
-348	-150	311	217	-200	34	104	-3,68	-4,16	240,03
-349	-150	311	217	-201	34	104	-3,69	-4,16	240,69
-350	-150	312	218	-202	34	104	-3,69	-4,17	241,35
-351	-151	313	219	-203	33	103	-3,70	-4,18	242,04
-352	-151	313	220	-204	34	104	-3,71	-4,19	242,88
-353	-152	315	221	-205	34	103	-3,72	-4,19	243,75
-354	-152	316	222	-206	34	103	-3,73	-4,21	244,65
-355	-152	317	223	-208	34	103	-3,74	-4,22	245,46
-356	-153	318	223	-209	34	103	-3,75	-4,23	246,24
-365	-156	325	231	-219	31	100	-3,84	-4,31	252,84
-365	-157	326	232	-220	31	99	-3,85	-4,32	253,41
-366	-157	326	232	-221	31	99	-3,86	-4,33	254,04

-367	-157	327	233	-223	31	99	-3,87	-4,33	254,70
-378	-164	355	252	-247	28	100	-4,03	-4,51	268,92
-392	-172	387	277	-280	30	102	-4,19	-4,71	286,83
-392	-173	389	277	-283	29	103	-4,20	-4,73	287,58
-392	-173	391	279	-284	29	103	-4,20	-4,73	288,33
-393	-173	392	280	-286	29	103	-4,21	-4,74	289,05
-393	-174	394	281	-288	29	103	-4,22	-4,75	289,74
-394	-174	395	282	-290	29	103	-4,22	-4,76	290,40
-395	-174	397	283	-291	29	103	-4,23	-4,76	291,03
-421	-188	443	324	-352	24	113	-4,58	-5,14	324,42
-435	-206	524	382	-419	21	111	-5,08	-5,72	371,85
-379	-77	685	696	-507	-87	110	-5,72	-6,43	429,63
-379	-74	686	701	-507	-89	109	-5,74	-6,44	430,80
-379	-69	688	706	-508	-91	109	-5,76	-6,46	431,88
-379	-67	689	710	-509	-93	109	-5,77	-6,46	432,69
-379	-65	688	714	-509	-94	109	-5,78	-6,48	433,62
-379	-63	689	717	-510	-96	109	-5,79	-6,49	434,58
-380	-61	690	720	-511	-97	109	-5,80	-6,49	435,48
-380	-59	692	723	-512	-98	109	-5,80	-6,51	436,26
-380	-57	693	725	-512	-99	108	-5,82	-6,52	436,92
-380	-56	694	728	-513	-100	108	-5,82	-6,53	437,55
-380	-54	695	731	-514	-101	108	-5,83	-6,54	438,18
-380	-53	695	733	-514	-102	108	-5,84	-6,54	438,69
-381	-52	695	735	-515	-103	108	-5,84	-6,55	439,11
-381	-51	696	737	-515	-104	107	-5,84	-6,56	439,50
-381	-49	696	738	-515	-105	107	-5,85	-6,56	439,80
-381	-48	696	740	-515	-105	107	-5,85	-6,57	440,22
-365	0	798	907	-569	-188	95	-6,31	-7,13	484,71
-365	0	799	909	-570	-189	95	-6,31	-7,14	485,22
-634	-106	730	1126	-739	-498	23	-9,25	-10,09	604,62
-634	-107	725	1128	-740	-499	21	-9,30	-10,12	605,37
338	193	222	1238	-821	-816	-43	-12,87	-13,12	665,31

413	216	216	1248	-822	-817	-41	-12,97	-13,16	665,64
484	241	211	1266	-824	-817	-40	-13,09	-13,19	666,00
562	270	208	1291	-825	-823	-39	-13,13	-13,23	666,39
648	315	202	1316	-825	-836	-38	-13,16	-13,25	666,63
740	358	194	1339	-825	-859	-37	-13,21	-13,28	666,75
853	410	189	1353	-827	-874	-36	-13,27	-13,31	666,72
966	484	184	1369	-828	-891	-33	-13,36	-13,36	666,87
1072	570	181	1375	-830	-901	-31	-13,43	-13,39	667,02
1162	665	177	1385	-832	-912	-28	-13,49	-13,43	666,99
-4411	-2954	-807	-190	-2325	-1043	-17	-21,38	-15,51	249,96
-4411	-2954	-257	-372	-1787	-829	-50	-18,88	-13,06	91,77
-4411	-2954	-142	-353	-1371	-768	-58	-17,03	-11,53	29,64
-4411	-2954	-129	-239	-1707	-990	-22	-18,21	-13,21	138,24
-4411	-2954	-126	-239	-1713	-991	-22	-18,23	-13,24	139,47
-4411	-2954	-125	-239	-1718	-993	-21	-18,26	-13,26	140,49
-4411	-2954	-124	-239	-1724	-995	-21	-18,28	-13,28	141,66
-4411	-2954	-122	-239	-1729	-997	-21	-18,31	-13,29	143,04
-4411	-2954	-121	-238	-1736	-999	-21	-18,35	-13,33	144,57
-4411	-2954	-119	-239	-1743	-1001	-20	-18,40	-13,35	146,22
-4411	-2954	-119	-238	-1750	-1002	-20	-18,43	-13,37	147,84